

**THE INFLUENCE OF TURBINE GEOMETRY ON  
THE PERFORMANCE OF C-SECTION VERTICAL  
AXIS WIND TURBINE**

**A THESIS SUBMITTED TO THE GRADUATE  
SCHOOL OF APPLIED SCIENCES**

**OF**

**NEAR EAST UNIVERSITY**

**By**

**Abdalla El-Ghazali**

**In Partial Fulfillment of the Requirements for  
the Degree of Master of Science  
in  
Mechanical Engineering**

**NICOSIA, 2016**

**Abdalla El-Ghazali: THE INFLUENCE OF TURBINE GEOMETRY ON THE  
PERFORMANCE OF C-SECTION VERTICAL AXIS WIND TURBINE**

**Approval of Director of Graduate School of  
Applied Sciences**

**Prof. Dr. İlkay SALIHOĞLU**

**We certify that this thesis is satisfactory for the award of the degree of Masters of  
Science in Mechanical Engineering**

**Examining Committee in Charge:**

I hereby declare that all information in this document has been obtained and presented in accordance with academic rules and ethical conduct. I also declare that, as required by these rules and conduct, I have fully cited and referenced all material and results that are not original to this work.

Name, Last name:

Signature:

Date:

## **ACKNOWLEDGEMENT**

I would like to thank my professors and staff of the Department of Mechanical engineering for their encouragement, guidance, and assistance throughout my university years.

I would like to specially thank my supervisor Assist. Prof. Dr. Hüseyin Çamur for helping me all these years and for encouraging his students to give the best of them.

I would like to thank Mr. Youssef Kassem for being there from the first day I came to the university, and all the assistance and help he have provided me throughout the time. I also would like to thank every member in my family, dad, mom and my wife for their support and care through the duration of my time in graduate school.

I am very grateful for my friends and colleagues because their advice, support and knowledge contributed throughout the development of the thesis.

**To my parents.....**

## ABSTRACT

Wind energy systems have been utilized for centuries as a source of energy for mankind. Using vertical axis wind turbines at buildings seems favorable due to the fact that they do not suffer from frequent wind direction changes, have a design simply integrate with building architecture and they have a better response in turbulent wind flow which is common in urban areas. This study proposes a design for C-section vertical axis wind turbine. This thesis presents a theoretical and experimental study into the aerodynamics and performance of small scale C-section vertical axis wind turbine and describes the effect of some design parameters including number of blades, blade size and rotor diameter on the performance of the C-section rotor. The theoretical study conducted in this thesis aims to predict and investigate the aerodynamic effects on by means of velocity analysis on the performance of C-section rotor turbine by converting the wind energy to mechanical energy to overcome load applied to the rotating main shaft. The comparison between theoretical prediction based on theoretical analysis of C-section rotor and experimental results obtained from literature allowed a thorough understanding of the main configuration of mechanical power on C-section vertical axis wind turbine. The results of this study show that the increasing wind speed, blade number, blade size, and rotor diameter lead to increase the mechanical power of the turbine. Also, it shows that 3 blades with diameter 10 cm gives better mechanical power than the other blades. And the effect of the blade size and number blade of a C-section blade of 10 cm on the mechanical power of the C - section rotor is greater than other blade of 7cm and 15 cm respectively. This study proves the feasibility of the proposed system through a sample design for a wind turbine that produces a power of 10 W per hour.

**Keywords:** Vertical axis; wind turbine; velocity analysis; mechanical power, blade size; blade number

## ÖZET

Rüzgar enerji sistemleri yüzyıllardır insanlar için bir enerji kaynağı olarak kullanılmıştır. Binalardaki dikey eksen rüzgar türbinleri, sık rüzgar yönü değişikliklerine maruz kalmadığı, bina mimarisiyle basit şekilde bütünleşen bir yapıya sahip olduğu ve kentsel alanlarda yaygın olan çalkantılı rüzgar akışında daha iyi bir tepki verebilmesinden dolayı daha elverişli görünmektedir. Bu çalışma C-kesit dikey eksen rüzgar türbini için bir tasarım önermektedir. Bu tez, aerodinamik ve C-kesit dikey eksen rüzgar türbininin performansı üzerine teorik ve deneysel bir çalışma sunar ve kanatların sayısı, kanatların boyutu ve rotor çapı dahil olmak üzere bazı tasarım parametrelerinin C-kesit rotorun performansı üzerindeki etkisini anlatmaktadır. Bu tezde yapılan teorik çalışmaların amacı, dönen ana şaftına uygulanan yükün üstesinden gelmek için rüzgar enerjisi mekanik enerjiye dönüştürerek C-kesit rotor türbininin performansı üzerindeki hızı analiz vasıtasıyla aerodinamik etkilerinin tahmini ve araştırılmasıdır. C-kesit rotorun teorik analizine dayanan teorik tahminler ile alanyazından elde edilen deneysel sonuçlar arasındaki karşılaştırma, C-kesit dikey eksen rüzgar türbini üzerindeki mekanik enerjinin ana yapılandırması hakkında kapsamlı bir anlayış geliştirdi. Bu çalışmanın sonuçları artan rüzgar hızı, kanat sayısı, kanat boyutu ve rotor çapı türbinin mekanik enerjisinde artışa neden oldu. Ayrıca, 10 cm çaplı 3 kanadın diğer kanatlara göre daha iyi mekanik güç ürettiği gösterildi. Buna ek olarak, 10 cm'lik bir C-kesit kanadın kanat boyutu ve sayısının etkisinin sırasıyla 7 cm'lik ve 15 cm'lik diğer iki kanattan daha yüksekti. Bu çalışma, saatte 10 W'lık bir güç üreten bir rüzgar türbini için örnek bir tasarım ile önerilen sistemin uygulanabilirliğini kanıtlamaktadır.

**Anahtar Kelimeler:** Dikey eksen; rüzgar türbini; hız analizi; mekanik enerji; kanat Büyüklüğü; kanat sayısı

## TABLE OF CONTENTS

<b>ACKNOWLEDGEMENT</b> .....	ii
<b>ABSTRACT</b> .....	iv
<b>ÖZET</b> .....	v
<b>TABLE OF CONTENTS</b> .....	vi
<b>LIST OF TABLES</b> .....	x
<b>LIST O FIGURES</b> .....	xi
<b>LIST OF SYMBOLS AND ABBREVIATIONS USED</b> .....	xvi
<b>CHAPTER 1: INTRODUCTION</b> .....	1
1.1 Background .....	1
1.2 Aim of Thesis .....	2
1.3 Outline of Thesis .....	2
<b>CHAPTER 2: WIND TURBINES</b> .....	3
2.1 Brief History of Wind Power .....	3
2.2 Horizontal-Axis and Vertical-Axis Wind Turbines .....	7
2.2.1 Vertical Axis Wind Turbines (VAWT) .....	8
2.2.1.1 Advantages and Disadvantages of Vertical Axis Wind Turbine .....	13
2.2.2 Horizontal Axis Wind Turbine (HAWT) .....	14
2.2.2.1 Types of HAWT .....	15
2.2.2.2 Advantages and Disadvantages of Horizontal Axis Wind Turbine .....	15
2.3 Modern Wind Turbine Design .....	16
<b>CHAPTER 3: VERTICAL AXIS WIND TURBINE AND AERODYNAMIC FORCE</b> .....	19
3.1 Capturing the Wind .....	19
3.1.1 Aerodynamic Forces .....	20
3.2 Drag Devices .....	20
3.3 Drag Force .....	22



3.3.1 Types of Drag .....	22
3.3.1.1 Friction Drag .....	23
3.3.1.2 Pressure Drag .....	23
3.3.2 Drag Coefficient .....	24
3.2.3 Friction Coefficient.....	26
3.4 Wind Turbine Types.....	27
3.4.1 Rotor Axis Orientation.....	27
3.4.2 Lift or Drag Type.....	28
3.5 Reviews on Three Blade Wind Turbine.....	28
3.6 Vertical Axis Wind Turbine (VAWT).....	30
3.6.1 Working Principle of VAWT.....	33
3.7 Estimate the Torque and Mechanical Power Output.....	35
3.8 Rotational Speed.....	38
<b>CHAPTER 4: METHODOLOGY OF RESEARCH .....</b>	<b>39</b>
4.1 Vertical axis C-Section Wind Turbine.....	40
4.2 Measuring Wind Speed Experimentally.....	41
4.3 Worm Gear.....	42
4.4 Measuring the Torque of Vertical Axis Wind Turbine Experimentally.....	43
4.5 Theoretical Procedures for Calculating the Mechanical Power.....	44
<b>CHAPTER 5: RESULTS AND DISCUSSIONS .....</b>	<b>46</b>
5.1 Comparison of Theoretical Study and Experimental Torque of Three Blade C-section Savonius Wind Turbine Rotor.....	46
5.2 Theoretical Results of Torque of C-section Rotor.....	48
5.3 Relationship Between Rotor Speed and Wind Speed with Variable Blade Size and Rotor Diameter.....	53
5.4 Relationship Between Torque and Wind Speed with Variable Blade Size and Rotor Diameter.....	60

5.5 Relationship Between Torque and Rotor Speed with Variable Blade Size and Rotor Diameter.....	67
5.6 Relationship Between Torque and Blade Diameter with Variable Blade Height, Wind Speed and Rotor Diameter .....	74
5.7 Comparison of Theoretical Study and Experimental Torque of C-section Wind Turbine rotor.....	81
5.8 Comparison of Theoretical Study and Experimental Power of C-section Wind Turbine Rotor.....	88
<b>CHAPTER 6: CONCLUSIONS AND FUTURE WORKS .....</b>	<b>95</b>
6.1 Conclusions.....	95
6.2 Future Works.....	96
<b>REFERENCES .....</b>	<b>97</b>

## LIST OF TABLES

<b>Table 3.1:</b>	Drag Coefficient Data .....	27
<b>Table 4.1:</b>	Different Fixed and Variable Parameters Considered in the Design Analyses.....	41
<b>Table 5.1:</b>	Theoretical and Experimental Values of Torque and Torque Coefficient of Savonius (C-section blade) Wind Turbine .....	47

## LIST OF FIGURES

<b>Figure 2.1:</b>	Persian Windmills .....	3
<b>Figure 2.2:</b>	Dutch Windmill .....	4
<b>Figure 2.3:</b>	American Multi Blade Windmill .....	5
<b>Figure 2.4:</b>	Darrieus wind Turbine .....	6
<b>Figure 2.5:</b>	Wind Turbine Types .....	8
<b>Figure 2.6:</b>	Darrieus Rotor with Nomenclature .....	10
<b>Figure 2.7:</b>	Darrieus Configurations .....	11
<b>Figure 2.8:</b>	Novel Darrieus .....	11
<b>Figure 2.9:</b>	Household-Size Darrieus .....	12
<b>Figure 2.10:</b>	HAWT Rotor Configurations .....	16
<b>Figure 2.11:</b>	Major Components of A Horizontal Axis Wind Turbine .....	17
<b>Figure 3.1:</b>	Three Pitch Scenarios .....	19
<b>Figure 3.2:</b>	Flow Conditions and Aerodynamic Force with a Drag Device.....	21
<b>Figure 3.3:</b>	Wake Behind Stationary Bodies .....	24
<b>Figure 3.4:</b>	Drag Breakdowns on non-Lifting and Lifting Bodies .....	25
<b>Figure 3.5:</b>	Bird’s eye View of a Vertical Axis Turbine .....	31
<b>Figure 3.6:</b>	Geometry of Vertical Axis Wind Turbine Designs as Viewed From Above the Turbines .....	32
<b>Figure 3.7:</b>	Lift principle of Three-Bladed VAWT Rotor: The Aerofoil of the Blades are Adjusted .....	34
<b>Figure 3.8:</b>	Simplified Model of C-section Wind Turbine .....	35
<b>Figure 3.9:</b>	Vector Components of the Wind Speed of C-section Rotor.....	37
<b>Figure 3.10:</b>	Scheme of a C-section rotor Showing the Velocity of the Rotor and Wind Speed .....	37
<b>Figure 4.1:</b>	Schematic of the Experimental Setup Used to Measure Torque and Rotational Speed of the Shaft (Front View) .....	40
<b>Figure 4.2:</b>	Three Dimensional Views of Experimental Setup Used to Measure Torque and Rotational Speed of the C-section Rotor Wind Turbine...	40

<b>Figure 4.3:</b>	Design Parameter of C-section Wind Turbine .....	41
<b>Figure 4.4:</b>	Anemometry Device .....	42
<b>Figure 4.5:</b>	The Cut Section of a Worm Gearbox .....	42
<b>Figure 4.6:</b>	Scheme of Electromechanical Dynamometer (Front and Right Views) showing the Components of Electromechanical Dynamometer .....	44
<b>Figure 4.7:</b>	The Procedure for Calculating Mechanical Power of the C - section Rotor .....	45
<b>Figure 5.1:</b>	Scheme of a Savonius Rotor with $L=0$ mm .....	46
<b>Figure 5.2:</b>	Theoretical Predictions and Experimental Torque of Savonius Wind Turbine Rotor .....	47
<b>Figure 5.3:</b>	Theoretical Predictions and Experimental Torque Coefficient of Savonius Wind Turbine Rotor .....	48
<b>Figure 5.4:</b>	Torque Versus Angle of Rotation for Different Diameter with Fixed $V = 4\text{m/s}$ , $H = 40$ cm and $R= 28\text{cm}$ .....	49
<b>Figure 5.5:</b>	Torque Versus Angle of Rotation for Different Diameter with Fixed $V = 6\text{m/s}$ , $H = 40$ cm and $R= 28\text{cm}$ .....	50
<b>Figure 5.6:</b>	Torque Versus Angle of Rotation for Different Diameter with Fixed $V = 10\text{m/s}$ , $H = 40$ cm and $R= 28\text{cm}$ .....	51
<b>Figure 5.7:</b>	Torque Versus Angle of Rotation for Different Wind Speed with Fixed $D =10\text{cm}$ , $H = 40$ cm and $R= 28\text{cm}$ .....	52
<b>Figure 5.8:</b>	Torque Versus Angle of Rotation for Different Rotor Radius with a Fixed $d = 7\text{cm}$ , $H = 40\text{cm}$ and $V = 4\text{m/s}$ .....	53
<b>Figure 5.9:</b>	RPM Versus Wind Speed for Different Rotor Radius and Blade Diameter with a fixed $H = 30\text{cm}$ and $N = 2$ Blades .....	54
<b>Figure 5.10:</b>	RPM Versus Wind Speed for Different Rotor Radius and Blade Diameter with a Fixed $H = 30\text{cm}$ and $N = 3$ Blades .....	55
<b>Figure 5.11:</b>	RPM Versus Wind Speed for Different Rotor Radius and Blade Diameter with a Fixed $H = 30\text{cm}$ and $N = 4$ Blades .....	56
<b>Figure 5.12:</b>	RPM Versus Wind Speed for Different Rotor Radius and Blade Diameter with a Fixed $H = 40\text{cm}$ and $N = 2$ Blades.....	57

<b>Figure 5.13:</b>	RPM Versus Wind Speed for Different Rotor Radius and Blade Diameter with a Fixed $H = 40\text{cm}$ and $N = 3$ Blades .....	58
<b>Figure 5.14:</b>	RPM Versus Wind Speed for Different Rotor Radius and Blade Diameter with a Fixed $H = 40\text{cm}$ and $N = 4$ Blades .....	59
<b>Figure 5.15:</b>	Torque Versus Wind Speed for Different Rotor Radius and Blade Diameter with a Fixed $H = 30\text{cm}$ and $N = 2$ Blades .....	61
<b>Figure 5.16:</b>	Torque Versus Wind Speed for Different Rotor Radius and Blade Diameter with a Fixed $H = 30\text{cm}$ and $N = 3$ Blades .....	62
<b>Figure 5.17:</b>	Torque Versus Wind Speed for Different Rotor Radius and Blade Diameter with a Fixed $H = 30\text{cm}$ and $N = 4$ Blades .....	63
<b>Figure 5.18:</b>	Torque Versus Wind Speed for Different Rotor Radius and Blade Diameter with a Fixed $H = 40\text{cm}$ and $N = 2$ Blades .....	64
<b>Figure 5.19:</b>	Torque Versus Wind Speed for Different Rotor Radius and Blade Diameter with a Fixed $H = 40\text{cm}$ and $N = 3$ Blades .....	65
<b>Figure 5.20:</b>	Torque Versus Wind Speed for Different Rotor Radius and Blade Diameter with a Fixed $H = 40\text{cm}$ and $N = 4$ Blades .....	66
<b>Figure 5.21:</b>	Torque Versus Rotor Speed, RPM, for Different Rotor Radius and Blade Diameter with $H = 30\text{cm}$ and $N = 2$ Blades .....	68
<b>Figure 5.22:</b>	Torque Versus Rotor Speed, RPM, for Different Rotor Radius and Blade Diameter with $H = 30\text{cm}$ and $N = 3$ Blades .....	69
<b>Figure 5.23:</b>	Torque Versus Rotor Speed, RPM, for Different Rotor Radius and Blade Diameter with $H = 30\text{cm}$ and $N = 4$ Blades .....	70
<b>Figure 5.24:</b>	Torque Versus Rotor Speed, RPM, for Different Rotor Radius and Blade Diameter with $H = 40\text{cm}$ and $N = 2$ Blades .....	71
<b>Figure 5.25:</b>	Torque Versus Rotor Speed, RPM, for Different Rotor Radius and Blade Diameter with $H = 40\text{cm}$ and $N = 3$ Blades .....	72
<b>Figure 5.26:</b>	Torque Versus Rotor Speed, RPM, for Different Rotor Radius and Blade Diameter with $H = 40\text{cm}$ and $N = 4$ Blades .....	73
<b>Figure 5.27:</b>	Torque Versus Blade Diameter for Different Rotor Radius with Fixed $H = 30\text{ cm}$ and $N = 2$ Blades .....	75
<b>Figure 5.28:</b>	Torque Versus Blade Diameter for Different Rotor Radius with Fixed $H = 30\text{ cm}$ and $N = 3$ Blades .....	76

<b>Figure 5.29:</b>	Torque Versus Blade Diameter for Different Rotor Radius with Fixed H = 30 cm and N = 4 Blades .....	77
<b>Figure 5.30:</b>	Torque Versus Blade Diameter for Different Rotor Radius with Fixed H = 40 cm and N = 2 Blades .....	78
<b>Figure 5.31:</b>	Torque Versus Blade Diameter for Different Rotor Radius with Fixed H = 40 cm and N = 3 Blades .....	79
<b>Figure 5.32:</b>	Torque Versus Blade Diameter for Different Rotor Radius with Fixed H = 40 cm and N = 4 Blades .....	80
<b>Figure 5.33:</b>	The Theoretical Result and Experimental Torque of C-section Wind Turbine Rotor Versus Wind Speed for Different Rotor Radius and Blade Diameter with a Fixed H= 30cm and N=2 Blades .....	82
<b>Figure 5.34:</b>	The Theoretical Result and Experimental Torque of C-section Wind Turbine Rotor Versus Wind Speed for Different Rotor Radius and Blade Diameter with a Fixed H= 30cm and N=3 Blades .....	83
<b>Figure 5.35:</b>	The Theoretical Result and Experimental Torque of C-section Wind Turbine Rotor Versus Wind Speed for Different Rotor Radius and Blade Diameter with a Fixed H= 30cm and N=4 Blades .....	84
<b>Figure 5.36:</b>	The Theoretical Result and Experimental Torque of C-section Wind Turbine Rotor Versus Wind Speed for Different Rotor Radius and Blade Diameter with a Fixed H= 40cm and N=2 Blades .....	85
<b>Figure 5.37:</b>	The Theoretical Result and Experimental Torque of C-section Wind Turbine Rotor Versus Wind Speed for Different Rotor Radius and Blade Diameter with a Fixed H= 40cm and N=3 Blades .....	86
<b>Figure 5.38:</b>	The Theoretical Result and Experimental Torque of C-section Wind Turbine Rotor Versus Wind Speed for Different Rotor Radius and Blade Diameter with a Fixed H= 40cm and N=4 Blades .....	87
<b>Figure 5.39:</b>	The Theoretical Result and Experimental Torque of C-section Wind Turbine Rotor Versus Wind Speed for Different Rotor Radius and Blade Diameter with a Fixed H= 30cm and N= 2 Blades .....	88
<b>Figure 5.40:</b>	The Theoretical Result and Experimental Torque of C-section Wind Turbine Rotor Versus Wind Speed for Different Rotor Radius and Blade Diameter with a Fixed H= 30cm and N=3 Blades.....	90

<b>Figure 5.41:</b>	The Theoretical Result and Experimental Torque of C-section Wind Turbine Rotor Versus Wind Speed for Different Rotor Radius and Blade Diameter with a Fixed H= 30cm and N=4 Blades .....	91
<b>Figure 5.42:</b>	The Theoretical Result and Experimental Torque of C-section Wind Turbine Rotor Versus Wind Speed for Different Rotor Radius and Blade Diameter with a Fixed H= 40cm and N=2 Blades .....	92
<b>Figure 5.43:</b>	The Theoretical Result and Experimental Torque of C-section Wind Turbine Rotor Versus Wind Speed for Different Rotor Radius and Blade Diameter with a Fixed H= 40cm and N=3 Blades.....	93
<b>Figure 5.43:</b>	The Theoretical Result and Experimental Torque of C-section Wind Turbine Rotor Versus Wind Speed for Different Rotor Radius and Blade Diameter with a Fixed H= 40cm and N=4 Blades .....	94



## LIST OF SYMBOLS AND ABBREVIATIONS USED

<b><i>A</i></b>	Area [m <sup>2</sup> ]
<b><i>ar</i></b>	Aspect Ratio
<b><i>A<sub>p</sub></i></b>	Planform Area
<b><i>B</i></b>	Wingspan is the Distance from one Wingtip to the Other Wingtip of the Airplane
<b><i>C</i></b>	Chord Length
<b><i>D</i></b>	Aerodynamic Drag Force [N]
<b><i>C<sub>D</sub></i></b>	Drag Coefficient
<b><i>C<sub>D,0</sub></i></b>	Drag Coefficient at Zero Lift
<b><i>C<sub>D,i</sub></i></b>	Induced Drag Coefficient
<b><i>C<sub>f</sub></i></b>	Friction Coefficient
<b><i>C<sub>p</sub></i></b>	Power Coefficient
<b><i>V</i></b>	Wind Velocity [m/s]
<b><i>V<sub>∞</sub></i></b>	Speed of the Object Relative to the Fluid
<b><i>v<sub>r</sub></i></b>	Air Velocity [m/s]
<b><i>v<sub>res</sub></i></b>	Relative Velocity [m/s]
<b><i>P</i></b>	Power Capture [W]
<b><i>P<sub>A</sub></i></b>	Aerodynamic Pressure [Pa]
<b><i>Re</i></b>	Reynolds Number
<b><i>ρ</i></b>	Air Density [kg/m <sup>3</sup> ]

# CHAPTER 1

## INTRODUCTION

### 1.1 Background

Wind is called a renewable energy source because the wind will blow as long as the sun shines. It has been harnessed for thousands of years. The wind's kinetic energy can be converted into other forms of energy, either electrical energy or mechanical energy. One of the oldest uses of wind energy is transportation, people use it to sail ships, and farmers also have been using wind energy to pump water, grind grain. More recently, it has been widely used for special purposes in the world, such as generating electricity, and modern wind turbines are the machines which are extremely efficient converting the wind energy into electricity. The existing technology can offer different power ratings from a few kilowatts to several megawatts.

The wind turbine is one the oldest know the method used to extract energy from the natural sources (wind in this case). With the changing weather and wind speed, it is not possible to produce high constant power from the wind turbine, but a small scale wind turbine can use for small appliance at home.

A wind turbine is a device that extracts kinetic energy from the wind and converts it into mechanical energy. Therefore wind turbine power production depends on the interaction between the rotor and the wind. So the major aspects of wind turbine performance like power output and loads are determined by the aerodynamic forces generated by the wind.

There are two types of wind turbines, namely horizontal-axis wind turbine (and vertical-axis wind turbine. The vertical axis wind turbine has many advantages, such as low cost, simple-structured blades, convenient installation and maintenance, and the ability to utilize wind from all directions without the need of a steering mechanism.

The main aim of the research is to design a small C-section vertical axis wind turbine that can generate electricity for home appliances. The thought of designing directs us to look into the various aspects such as manufacturing, noise, and cost.

This research presents a theoretical and experimental study into the aerodynamics and performance of small scale C-section vertical axis wind turbines and describes the effect of some design parameters including wind speed, number of blades, and blade size and rotor diameter on the performance of them. Considerable improvements in the understanding of vertical axis wind turbine can be achieved through the use of theoretical study based on velocity analysis and experimental measurements.

## **1.2 Aim of Thesis**

The main aims of the research are outlined below:

1. To investigate the aerodynamic effects on the performance of C-section blade wind turbine converting the wind energy to mechanical energy to overcome load applied to the rotating main shaft.
2. To examine the effect of blade size and blade number of C-section on the rotational speed, torque or mechanical power.
3. To compare the theoretical results based on the velocity analysis with experimental data to obtain the absolute error between them.

## **1.3 Outline of Thesis**

In chapter 2, briefly the types of wind turbines and characteristics of them are discussed in details. A literature review of the performance of vertical turbine is presented in chapter 3 including previous attempts to improve the performance of the turbine. The methodology and all the results of the experiments are presented in chapter 4 and 5 for vertical axis C-section blade wind turbine, followed by a comparison between the theoretical data with experimental data of vertical axis C-section blade wind turbine. The thesis ends with conclusions and suggestions for future work in chapter 6.

## CHAPTER 2

### WIND TURBINES

The wind turbine can be classified according to the turbine generator configuration, airflow path relative to the turbine rotor, turbine capacity, the generator-driving pattern, the power supply mode and the location of turbine installation.

#### **2.1 Brief History of Wind Power**

The first known use of wind power is placed, according to various sources, in the area between today's Iran and Afghanistan in the period from 7th to 10th century (D'Ambrosio & Medaglia, 2010) These windmills were mainly used to pump water or to grind wheat. They had vertical axis and used the drag component of wind power: this is one of the reason for their low efficiency. Moreover, to work properly, the part rotating in the opposite direction compared to the wind, had to be protected by a wall (see Figure 2.1).



**Figure 2.1:** Persian Windmills

Obviously, devices of this type can be used only in places with a main wind direction, because there is no way to follow the variations.

The first windmills built in Europe and inspired by the Middle Eastern ones had the same problem, but they used a horizontal axis. So they substitute the drag with the lift force, making their inventors also the unaware discoverer of aerodynamics.

During the following centuries, many modifies were applied for the use in areas where the wind direction varies a lot: the best examples are of course the Dutch windmills, used to drain the water in the lands taken from the sea with the dams, could be oriented in wind direction in order to increase the efficiency as shown in Figure 2.2.



**Figure 2.2:** Dutch Windmill

The wind turbines used in the USA during the 19th century and until the '30 of the 20th century were mainly used for irrigation. They had a high number of steel-made blades and

represented a huge economic potential because of their large quantity: about 8 million were built all over the country (see Figure 2.3).



**Figure 2.3:** American multi blades Windmill

The first attempt to generate electricity was made at the end of the 19th century, and they become more and more frequent in the first half of the following century. Almost all those models had a horizontal axis, but in the same period (1931) Georges Jean Marie Darrieus designed one of the most famous and common type of VAWT (see Figure 2.4), that still bears his name.



**Figure 2.4:** Darrieus wind Turbine

The recent development led to the realization of a great variety of types and models, both with vertical and horizontal axis, with a rated power from the few kW of the beginning to the 6 MW and more for the latest constructions. In the electricity generation market the HAWT type has currently a large predominance (D'Ambrosio & Medaglia, 2010).

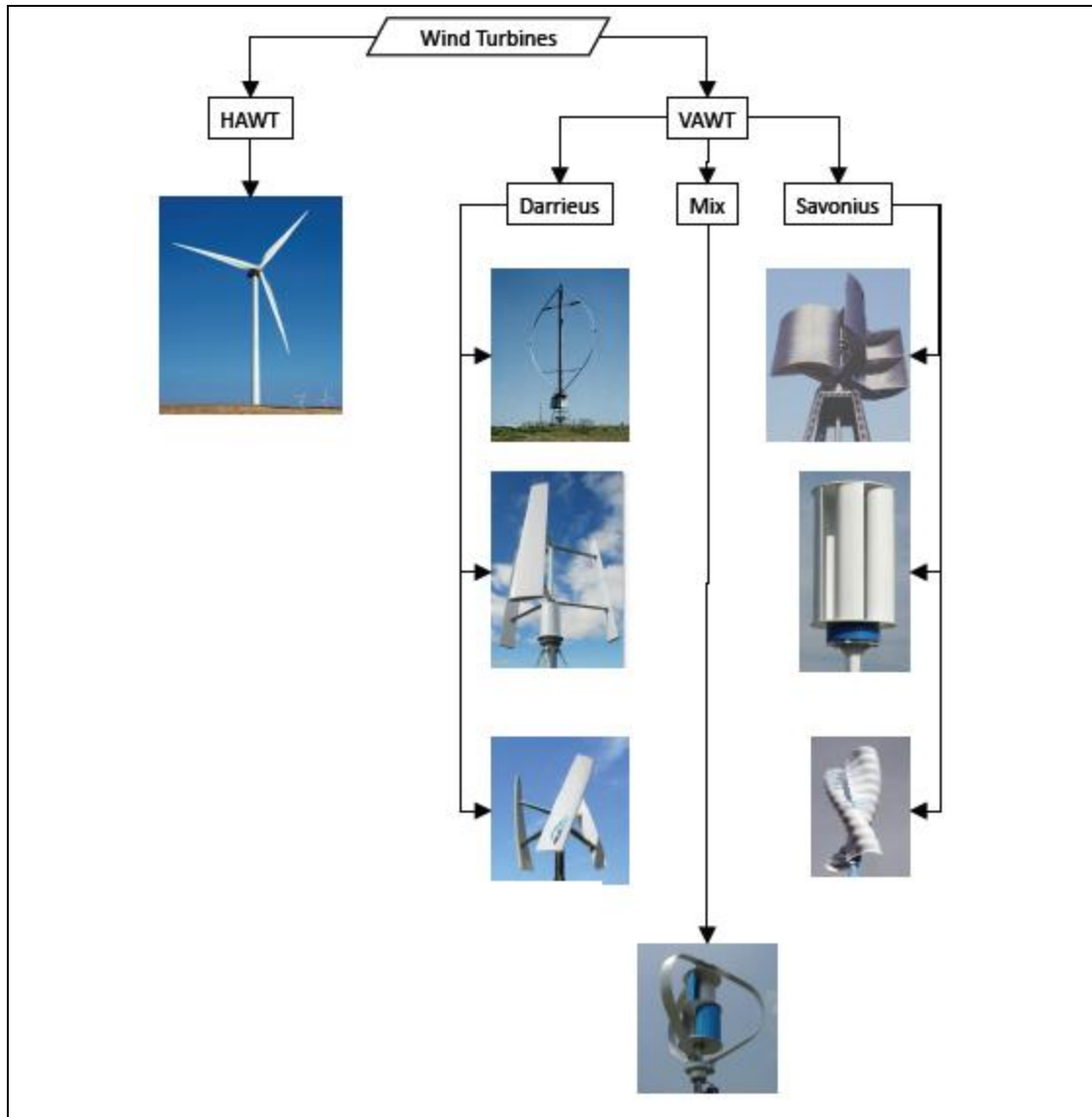
## **2.2 Horizontal-Axis and Vertical-Axis Wind Turbines**

When considering the configuration of the rotating axis of rotor blades, modern wind turbines can be classified into horizontal-axis and vertical axis turbines.

Most commercial wind turbines today belong to the horizontal-axis type, in which the rotating axes of the blades are parallel to the wind stream. The advantages of this type of wind turbines include the high turbine efficiency, high power density, low cut-in wind speed and low cost per unit power output.

Several typical vertical-axis wind turbines are shown in Figure 2.5. The blades of vertical – axis wind turbines rotate with respect to their vertical axes that are perpendicular to the ground. A significant advantage of vertical-axis wind turbines is that the turbine can accept wind from any direction and thus no yaw control is needed. Since the wind generator, gearbox, and other main turbine components can be set up on the ground, it greatly simplifies the wind tower design and construction, and consequently reduces the turbine cost. However, the vertical axis wind turbines must use an external energy source to rotate the blades during initialization (Rivkin & Silk, 2013). Because the axis of the wind turbine is supported only on one end at ground, its maximum practical height is thus limited. Due to the lower wind power efficiency, vertical-axis wind turbines today make up only a small percentage of wind turbines (Hemami, 2012).





**Figure 2.5:** Wind turbine types

### 2.2.1 Vertical Axis Wind Turbines (VAWT)

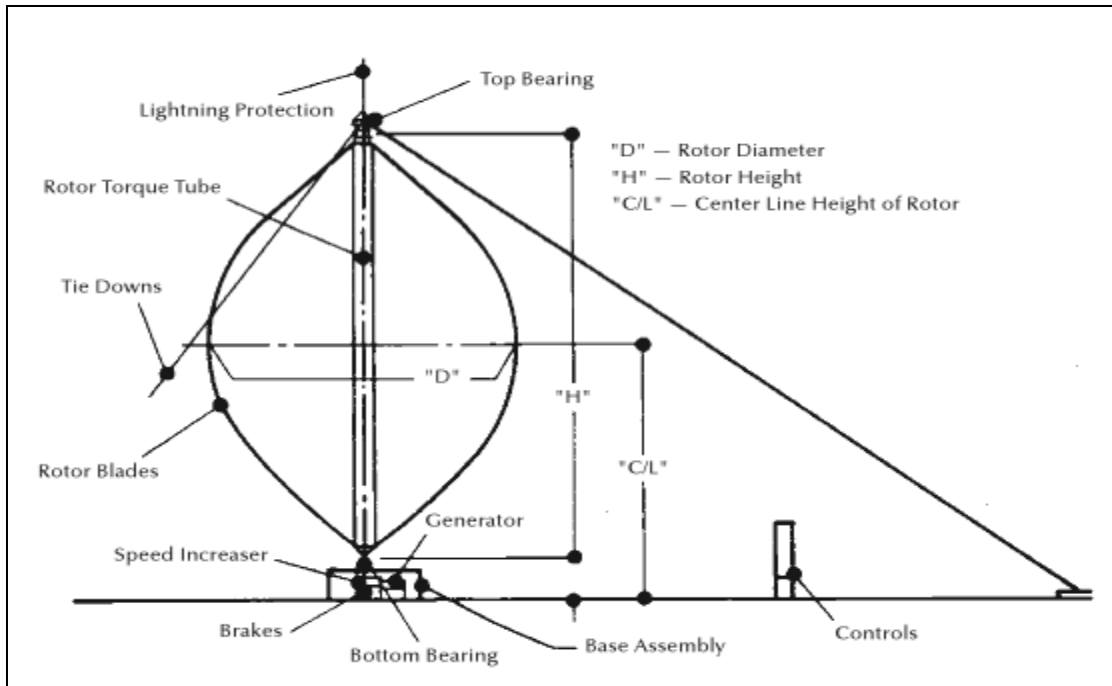
The principle advantage of modern vertical axis wind machine over their conventional counterpart is that VAWT are omnidirectional. They accept the wind from any direction. This simplifies their design and eliminates the problem imposed by gyroscopic forces on the rotor of conventional machine as the turbine tracks the wind. The vertical axis of rotation also permits mounting the generator and drive train at ground level as shown in Figure 2.5.

Vertical-axis turbines can be divided into two major groups:

- Those that use aerodynamic drag to extract power from wind.
- Those that use the lift.

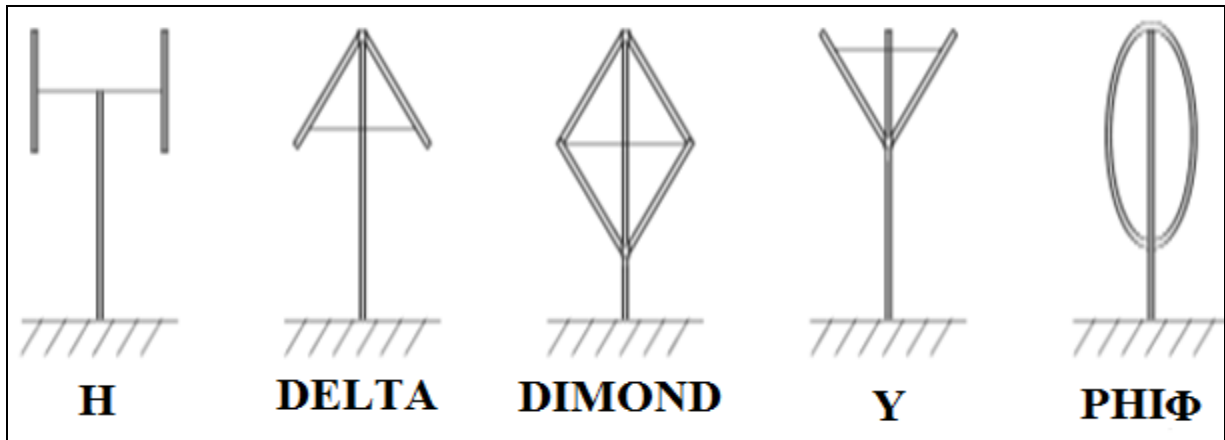
The simplest configuration uses two or more straight blades attached to the ends of the horizontal cross-arm. This gives the rotor the shape of the large H (see Figure 2.7). Unfortunately, this configuration permits centrifugal forces induce server bending stress on the blades at their point of attachment.

During the 1920s French inventor D.G.M. Darrieus patented a wind machine that cleverly dealt with this limitation. Instead of using straight blades, he attached curved blades to the rotor. When the turbine was operating, the curved blades would take on the form of a spinning rope held at both ends. This troposkein shape directs centrifugal forces through the blade's length toward the points of attachment, thus creating tension, rather than bending, in the blades. Because materials are stronger in tension than in bending, the blades can be lighter for the same overall strength and operate at higher speeds than straight blades. Although the phi ( $\Phi$ ) or Eggbeater configuration is the most common, Darrieus conceived several other versions, including Delta, Diamond, and Y as shown in Figure 2.7. All have been tried at one time or another (see Figure 2.6, Darrieus configurations). Some have linked the phi-configuration about a vertical axis.

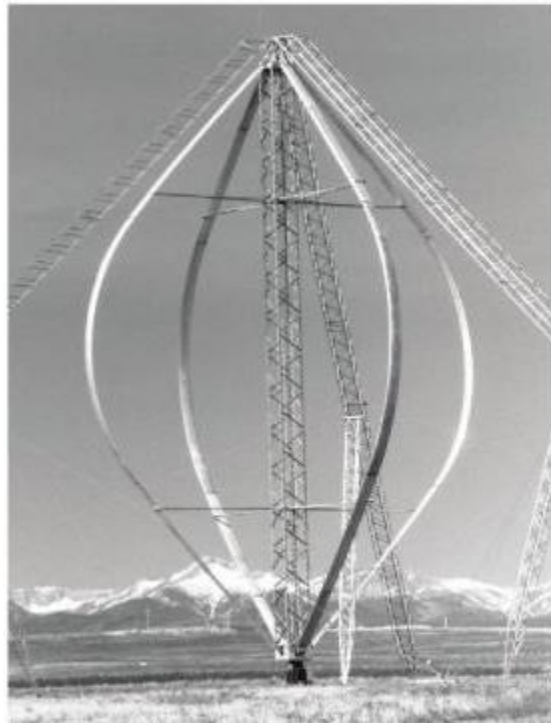


**Figure 2.6:** Darrieus rotor with nomenclature

The Darrieus's concept eventually faded into obscurity. Canada's National Research Council reinvented the design in the mid-1960s, and subsequently Canadian wind research focused on Darrieus turbines (see Figure 2.8). In the United States, Sandia National Laboratories have also pursued the technology. Several terms in Europe and North America attempted to commercialize Darrieus technology, but had little lasting success as shown in Figure 2.9. Work on the technology has practically ceased, and there are few Darrieus turbines still in service. Carl Brothers operate one of the last of the breed in Canada's Atlantic, Wind Test Site on Prince Edward Island. The test site has operated at 35 kW DAF-Indal.



**Figure 2.7:** Darrieus configurations



**Figure 2.8:** Novel Darrieus



**Figure 2.9:** Household-size Darrieus

Design for more than 15 years, probably a world record for Darrieus turbine. With the exception of some very small Savonius rotors, there are no VAWTs in widespread use. Darrieus turbines were bedeviled by poor performance and poor reliability. The aluminum blades often fatigued and sometimes failed catastrophically. This was in part because the lift forces, which propel the blades, reverse direction every revolution, flexing their attachment to the torque tube or central mast. Another source of frequent flexing of the blades is inherent in the rotor's eggbeater shape. When the rotor is at rest, the blades sag due to their own weight, stressing the connection to the torque tube. Moreover, the presumed advantage of the housing the drive train at ground level was offset by the large bearing and guy cables at the top of the rotor (Gipe, 2009).

### **2.2.1.1 Advantages and Disadvantages of Vertical Axis Wind Turbine**

#### **A. Advantages:**

1. The generator, gearbox and other components may be placed on the ground, so the tower doesn't need to support it, and it is more accessible for maintenance.
2. Relative cost of production, installation and transport compared to horizontal axis turbines.
3. The turbine doesn't need to be pointed into the wind to be effective. This is an advantage on sites where the wind direction is highly variable.
4. Hilltops, ridge lines and passes can have higher and more powerful winds near the ground than higher up because due to the speed up the effect of winds moving up a slope. In these places, vertical axis turbines are suitable.
5. The blades spin at slower speeds than the horizontal turbines, decreasing the risk of injuring birds.
6. It is significantly quieter than the horizontal axis wind turbine. As a result, vertical axis wind turbines work well on rooftops, making them particularly useful in residential and urban environments. They may also be built in locations where taller structures are prohibited by law.
7. They are particularly suitable for areas with extreme weather conditions, like in the mountains where they can supply electricity to mountain huts.

#### **B. Disadvantages**

1. They are less efficient than horizontal axis wind turbines. Most of them are only half as efficient as the horizontal ones because of the additional drag that they have as their blades rotate into the wind.
2. Airflow near the ground and other objects can create turbulent flow, which can introduce issues of vibration. This can include noise and bearing wear which may increase the maintenance or shorten the service life.
3. The machine may need guy wires to hold it up. Guy wires are impractical in heavily farmed areas (Rivkin et al., 2014).

### **2.2.2 Horizontal Axis Wind Turbine (HAWT)**

Horizontal axis wind turbines usually have three blades that operate upwind (toward the wind). The main rotor shaft and electrical generator are located at the top of the tower and face upwind. Many small HAWTs use a wind vane (weather vane) and large turbines use wind sensors (with a servo motor). Most horizontal axis turbines have a gearbox to increase the rotational speed of the generator well above the rotational speed of the blades. The turbine must point upwind because the structure, it produces turbulence behind it. To prevent damage, the turbine blades of a HAWT are usually very sturdy and positioned as far away from the tower as possible (sometimes tilted forward at the lower arc).

Though usually able to produce more energy than their counterparts (VAWT), horizontal axis wind turbines employ automated systems that readjust the orientation of the nacelle such that the rotor remain perpendicular to oncoming wind. Downwind HAWTs have been manufactured to reduce wind realignment and decrees blade damage. These HAWTs have flexible blades, because there is no risk of tower interference, but the flexible blades can reduce the swept area. Wind turbulence causes fatigue failure is most downwind turbines. Thus, to reap the most benefits, most horizontal axis wind turbines tend to be upwind rather than downwind.

Most modern wind turbines on wind farm are horizontal axis with three blades and face upwind. These highly efficient and highly reliable (low torque ripple) commercial turbines reach a high top speed of over 320km/h. Blades the range from 20 to 40 plus meters rotate at 10-22 revolutions per minutes. Knowing this information is helpful for finding tip-speed ratio (TSR). TSR is the ratio between the blade tip speed and the current wind speed in a given moment. If the tip speed is exactly the same as the wind speed, TSR is 1. TSR is related to efficiency. Higher tip speeds result in higher noise levels and due to large centripetal forces (it is a force that makes a body follows a curved path. Its direction is always orthogonal to the motion of the body and towards the fixed point of the instantaneous center of curvature of the path), the need for stronger blades. The tubular steel towers of these turbines vary in height from 60 to 90 meters. Gearboxes are usually used to adjust the speed of the generator; otherwise annular generators (direct drive) are used, which negates the necessity of the gearbox. Most of these turbines are variable speed types that use solid-state electronic power converters to more efficiently collect energy from the wind (Rivkin et al., 2014).

### **2.2.2.1 Types of HAWT**

There are two types of horizontal axis wind turbines

- A. Horizontal upwind: the generator shaft is positioned horizontally and the wind hits the blade before the tower. Turbine blades are made stiff to prevent the blades from being pushed into the tower by high winds, and the blades are placed at a considerable distance in front of the tower and are sometimes tilted up a small amount.

Horizontal downwind: the generator shaft is positioned horizontally and the wind hits the tower first and then the blade. Horizontal downwind does not need an additional mechanism for keeping it in line with the end, and in high winds the blades can be allowed to bend, which reduces their swept area and thus their wind resistance. The horizontal downwind turbine is also free of turbulence problems.

### **2.2.2.2 Advantages and Disadvantages of Horizontal Axis Wind Turbine**

#### **A. Horizontal Axis Wind Turbine Advantages:**

The advantages of using this type of turbine are following

- Their tall towers allow wind turbine blades to access strong wind. If we increase the height of wind turbine blades to every 10 meters, we will get 20% more speed and 34% more power output.
- The efficiency of this type of wind turbine is more as compare to vertical axis wind turbine because blades are perpendicular to wind. With this direction, they have more capability to receive wind impact.
- These turbines have variable blade pitch. By this behavior, blades get the optimum angle of attack which allows the blades to adjust it for greater control to get maximum wind energy.

#### **B. Horizontal Axis Wind Turbine Disadvantages:**

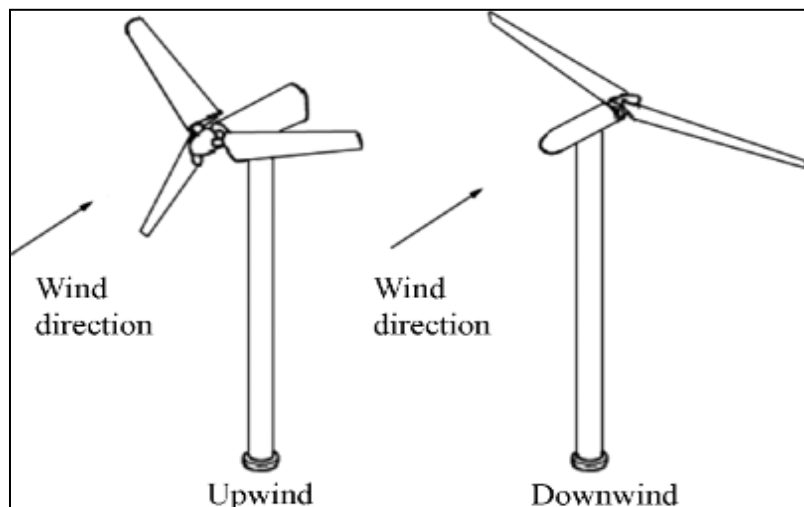
Because of getting high attitude, tower needs massive construction to support heavy blades and its other components like gearbox and electricity. Tower height makes wind turbine visible across many areas which will create disturbance to view the landscape. Horizontal axis wind turbines designed on downwind failed due to fatigue and failure when turbine blades pass through the shadow of tower. Horizontal axis wind turbines need yaw control mechanism for turning their blades to get maximum wind energy.



Horizontal axis wind turbines need yawing or braking devices when the speed of wind is enough. If such type of situations where we don't stop wind turbines it can destroy itself also. Due to the movements of turbine blades, cyclic stresses generate because one of the blades of turbine faces minimum wind energy and other at the same time faces maximum which will create twists and crack the blade quickly (Casper, 2007).

### 3.2 Modern Wind Turbine Design

Today, the most common design of wind turbine is the horizontal axis wind turbine (HAWT). That is, the axis of rotation is parallel to the ground. HAWT rotors are usually classified according to the rotor orientation (upwind or downwind of the tower), hub design (rigid or teetering), rotor control (pitch vs. stall), number of blades (usually two or three blades), and how they align with the wind (free yaw or active yaw). Figure 2.10 shows the upwind and downwind configurations.



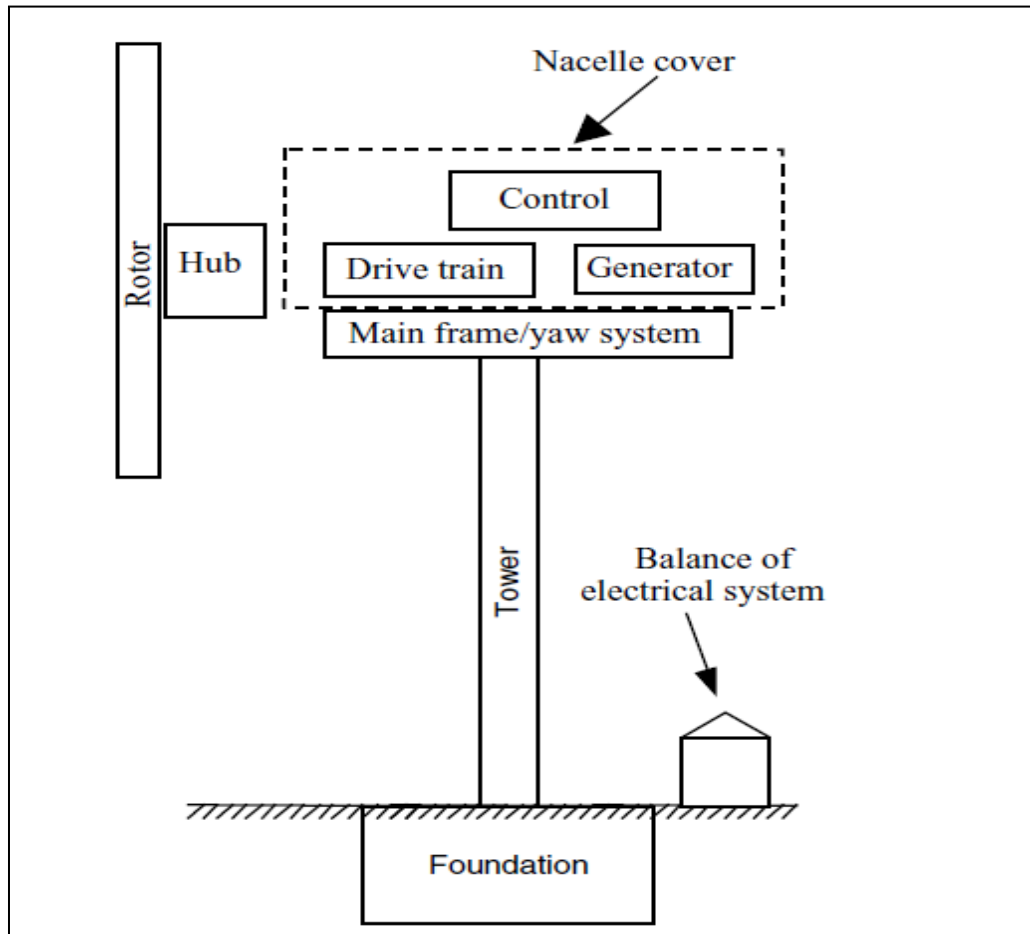
**Figure 2.10:** HAWT rotor configurations

The principal subsystems of a typical horizontal axis wind turbine are shown in Figure 2.11.

These include:

- The rotor, consisting of the blades and the supporting hub.
- The drive train, which includes the rotating parts of the wind turbine (exclusive of the rotor); it usually consists of shafts, gearbox, coupling, a mechanical brake, and the generator.

- The nacelle and main frame, including wind turbine housing, bedplate, and the yaw system the tower and the foundation.
- The machine controls the balance of the electrical system, including cables, switchgear, transformers, and possibly electronic power converters (Manwell et al., 2014).



**Figure 2.11:** Major components of a horizontal axis wind turbine

The picture above shows the various components of a Horizontal Axis Wind Turbine (HAWT). The three most important parts are the rotor, the gear box, and the generator.

- Rotor blades: The blades are basically the sails of the system; in their simplest form, they act as barriers to the wind (more modern blade designs go beyond the barrier method). When the wind forces the blades to move, it has transferred some of its energy to the rotor.

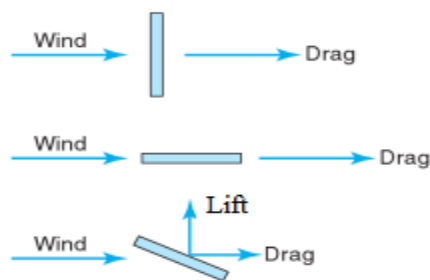
- Shaft: The wind-turbine shaft is connected to the center of the rotor. When the rotor spins, the shaft spins as well. In this way, the rotor transfers its mechanical, rotational energy to the shaft, which enters an electrical generator on the other end.
- Generator: At its most basic, a generator is a pretty simple device. It uses the properties of electromagnetic induction to produce an electrical voltage - a difference in electrical charge. Voltage is essentially electrical pressure - it is the force that moves electricity, or electrical current, from one point to another. So generating voltage is in effect generating current. A simple generator consists of magnets and a conductor. The conductor is typically a coiled wire. Inside the generator, the shaft connects to an assembly of permanent magnets that surrounds the coil of wire. In electromagnetic induction, if you have a conductor surrounded by magnets, and one of those parts is rotated relative to the other, it induces a voltage in the conductor. When the rotor spins the shaft, the shaft spins the assembly of magnets, generating voltage in the coil of wire. That voltage drives, electrical current (typically alternating current, or AC power) out through power lines for distribution (Hau, 2006).

## CHAPTER 3

### VERTICAL AXIS WIND TURBINE AND AERODYNAMIC FORCE

#### 3.1. Capturing The Wind

The wind turbine rotor assembly is designed to convert mechanical power from the wind into an electrical output. The rotor assembly includes the hub, spinner, blades and all the enclosed systems used to control blade pitch. The electric output process will remain efficient only through diligence, proactive service and a maintenance plan. A good rotor assembly, maintenance plan should include inspections to ensure blade structural integrity along with activities to maintain clean, smooth exterior surfaces and the aerodynamic profile. Wind turbine blades are designed to enable the airflow around them to create reaction forces perpendicular and parallel to the oncoming wind. The reaction force perpendicular to oncoming wind is considered drag. The amount of lift and drag created by an object are function of shape, surface area and wind velocity. A thin flat panel positioned or pitched perpendicular to the wind will create drag without any lift force. The same flat panel pitched parallel to the wind will create a small amount of the drag but no lift. To create both lift and drag, the panel must be pitched at an angle to the oncoming wind. Figure 3.1 shows examples of these pitch scenarios. Because these forces result from the interaction of an object within a moving fluid (wind), they are considered aerodynamic forces (Kilcollins, 2013).



**Figure 3.1:** Three pitch scenarios

### 3.1.1 Aerodynamic Forces

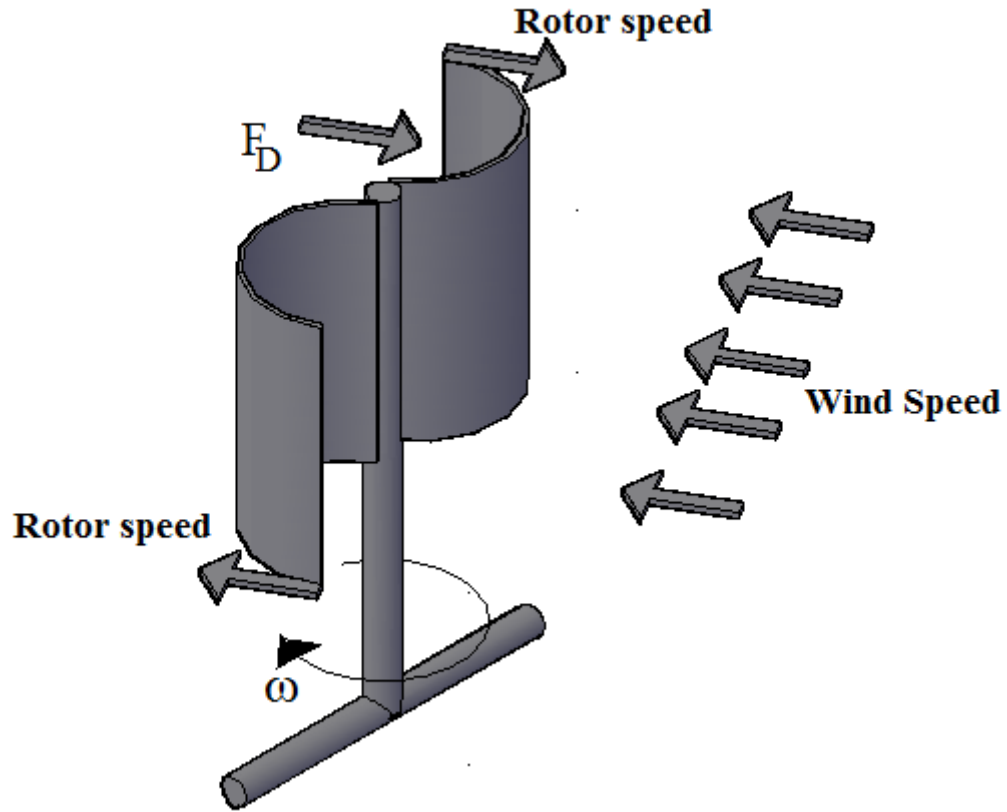
The force from the wind on a plate is called aerodynamic force. We referred to the two aerodynamic force component as lift and drag; any force can be broken into two components. Here the lift force and drag force are the two components of the aerodynamic force on the plate under consideration. These two components are perpendicular to each other; that is, they make an angle of  $90^\circ$  with each other as shown in Figure 3.1. Recall that the force exerted on a surface (the plate surface) is always the product of the area and pressure on the surface (Hemami, 2012).

Aerodynamic force is a function of aerodynamic pressure created by wind impacting the surface of the object. This force may be calculated using the aerodynamic pressure caused by wind impacting the blade and the blade exposed surface area. Aerodynamic pressure ( $P_A$ ) is a function of the adjusted air density and the wind velocity squared ( $P_A = (1/2)\rho V^2$ ). Adjusted air density refers to the change in density because of elevation and temperature. Increasing elevation from sea level and ambient temperature, above or below the standard temperature will change the air density and so will an increase the temperature. Decreasing the air temperature will increase the air density value. This is why cold air blowing in the winter will have more available power than the same velocity wind on a hot summer day (Kilcollins, 2013).

### 3.2. Drag Devices

The simplest type of wind energy conversion can be achieved by means of pure drag surface (Figure 3.2). The air impinges on the surface  $A$  with wind velocity,  $v_w$ , the power capture,  $P$ , of which can be calculated from the aerodynamic drag,  $F_D$ , the area  $A$  and the rotor velocity or rotor speed,  $v_r$  with which it moves

$$P = F_D v_r \tag{3.1}$$



**Figure 3.2:** Flow conditions and aerodynamic force with a drag device

The relative velocity  $v_{rel} = v_w - v_r$ , which effectively impinges on the drag area, is decisive from its aerodynamic drag, using common aerodynamic drag coefficient,  $C_D$ , the aerodynamic drag can be expressed as :

$$F_D = \frac{1}{2} \rho C_D (v_w - v_r)^2 A \quad (3.2)$$

The resultant power is

$$P = \frac{1}{2} \rho C_D (v_w - v_r)^2 A v_r \quad (3.3)$$

If the power is expressed again in terms of the power contained in the free stream airflow, the following power coefficient is obtained (Hau, 2006):.

$$C_p = \frac{P}{P_0} = \frac{\frac{1}{2} \rho C_D (v_w - v_r)^2 A v_r}{\frac{1}{2} \rho v_w^3 A} \quad (3.4)$$

Drag force can be defined as in fluid mechanics, the force which exerted on the solid object in the upstream direction of the relative flow velocity (Hutchinson, 2016).

Drag force depends on flow velocity and it decreases the fluid velocity (French & Ebison, 1986). Therefore, drag force also called air resistance or fluid resistance.

### **3.3. Drag Force**

Drag is the force experienced by an object that is in line with the flow of any fluid such as the air stream. The drag force is developed by obstructing the flowing wind and creating a turbulence. Drag devices are simple wind machines that use flat or curved blades to catch the wind in the enclosed area to turn the rotor. Drag force depends on exposing a flat or curved area on one side of a rotor to the wind while shielding the other, the resulting differential drag force turns the rotor (Earnest, 2015).

The drag on an object in the wind, whether it is a tall building, tower or wind turbine is a function of air density, the area intercepting the wind, the speed of the wind and dimensionless coefficient that represents the object's shape and its angle to the wind.

$$F_D = \frac{1}{2}\rho AV^2 C_D \quad (3.5)$$

where  $F_D$  is drag force,  $\rho$  air density,  $A$  is the area intercepting the wind,  $V$  is the wind speed and  $C_D$  is the coefficient of the drag.

#### **3.3.1 Types of Drag**

As already mentioned, the drag is the resistive force encountered by body when it is moving through a fluid or when the fluid flows past a solid body. In both cases, in order to maintain steady motion, a force in the direction of relative motion has to be exerted. Thus, when the submarine moves through water or an aero-plane flies through atmosphere, the vehicle has to exert a forward force sufficient enough to balance the drag force. Drag force may be related to the effect of boundary layer, flow separation and wake. The existence of viscosity for the fluid is mainly responsible for causing drag on bodies.

The total drag may be separated into a number of items each contributing to the total. As first step, it is divided into friction drag and pressure drag.

### **3.3.1.1 Friction Drag**

Due to the viscous nature of fluid, the fluid motion tends to be rotational which gives rise to velocity gradient in the thin boundary layer region. In the laminar boundary, since the adjacent fluid layers move with different velocities, tangential shear stress is set up. In the turbulent layer, since there is velocity fluctuation, additional shear stress is set up. These shear stresses leads to the shear drag or friction drag, friction drag does not exist in a flow assumed to be inviscide.

### **3.3.1.2 Pressure Drag**

The drag force arising from the resolved components of the pressure on the boundary is the pressure drag. The pressure drag may itself be considered as sum of the several distinct items.

#### **i. Form Drag**

Form drag is mainly due to the wake formed behind anybody having relative motion with the fluid. When the surface of the body is not parallel to the flowing stream, the flow pattern gets considerably modified due to boundary layer growth and separations from the surface of the body. The separated flow gives rise to a low pressure region called wake on the rear side of the body. The pressure difference between the two sides of the body gives rise to pressure drag, which is referred to as form drag. Figure 3.3 (a), (b) and (c) gives an indication of the comparative width of the wake behind a few bodies. Its magnitude depends on the size of the wake which depends on the position of separation points

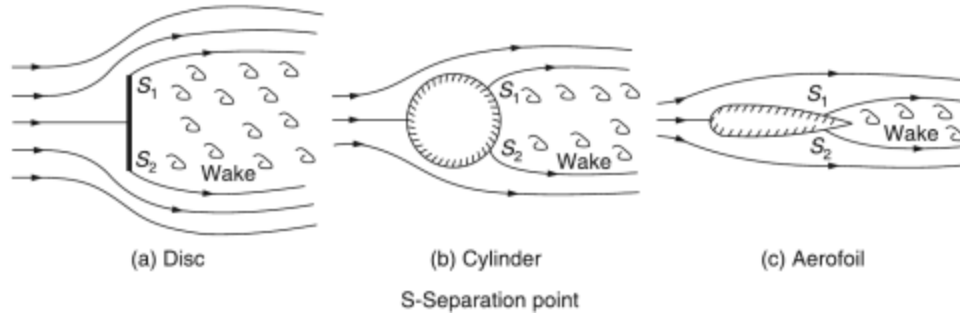
#### **ii. Wave Drag**

The wave drag is due the waves formed in the flow, incompressible flow, it is due to the formation of the compression shock wave.

#### **iii. Induced drag**

The induced drag is due to the trailing vortex formed due to the flow past the body, it depends on the lift force.





**Figure 3.3:** Wake behind stationary bodies

If the wave drag and induced drag are neglected, then the total drag is essentially the skin friction drag and the form drag (Balachandran, n.d.).

### 3.3.2 Drag Coefficient

In fluid dynamic, the drag coefficient (commonly denoted as:  $C_D$  or  $C_w$ ) is a dimensionless that is used to quantify the drag or resistance of an object in a fluid environment such as air or water. It is used in the drag equation, where a lower drag coefficient indicates the object will have less aerodynamic drag. The drag coefficient is always associated with a particular surface area. The drag coefficient of any object comprises the effects of the two basic contributors to fluid drag: skin friction and form drag. The drag coefficient of a lifting airfoil also includes the effects of lift-induced drag. The drag coefficient of a complete structure such as an aircraft also includes the effects of interference drag. The drag coefficient  $C_D$  is defined as:

$$C_D = \frac{2F_D}{\rho V_\infty^2 A} \quad (3.6)$$

Where,

$F_D$  is the drag force, which is by definition the force component in the direction of the flow velocity,

$\rho$  is the mass density of the fluid,

$V_\infty$  is the speed of the object relative to the fluid, and

$A$  is the reference area.

Drag on airfoils arises from viscous and pressure forces. Viscous drag or Skin friction changes with Reynolds number and arises from the interaction between the fluid and the skin of the body but only slightly with angle of attack. These relationships and some commonly used terminology are illustrated in Figure 3.4.

A useful approximation to drag polar for complete aircraft may be obtained by adding the induced drag or vortex drag, or sometimes drag due to lift, is a drag force that occurs whenever a moving object redirects the airflow coming at it to the drag at zero lift. The drag at any lift coefficient is obtained from

$$C_D = C_{D,0} + C_{D,i} = C_{D,0} + \frac{C_L^2}{\pi ar} \quad , \quad ar = \frac{b^2}{A_p} \quad (3.7)$$

Where,

$C_{D,0}$ : drag coefficient at zero lift

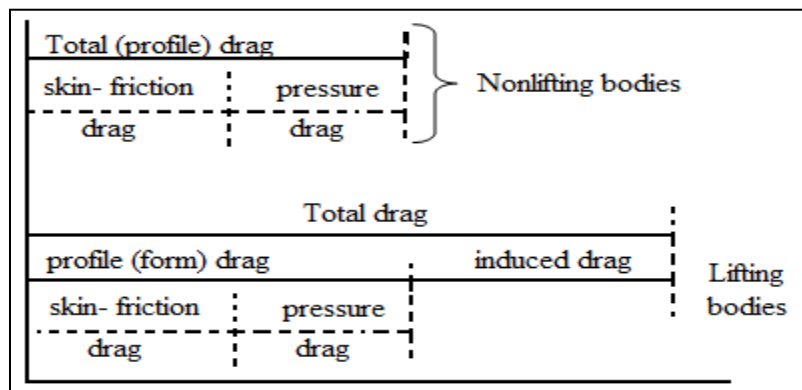
$C_{D,i}$ : induced drag coefficient

ar: Aspect ratio

b: wingspan or is the distance from one wingtip to the other wingtip of the airplane

$A_p$ : Planform area

c: chord length.



**Figure 3.4:** Drag breakdowns on nonlifting and lifting bodies

The drag coefficient for all objects with sharp edge is essentially independent of Reynolds number (for  $Re \geq 10000$ ) because the separation points and therefore the size of the wake are

fixed by the geometry of the object. Drag coefficients for selected objects are given in table 3.1

### 3.2.3. Friction Coefficient

The friction coefficient for laminar flow over a flat plate can be determined theoretically by solving the conservation of mass and momentum equations numerically. For turbulent flow, however, it must be determined experimentally and expressed by empirical correlation. The local friction coefficient varies along the surface of the flat plate as a result of the changes in the velocity boundary layer in flow direction. We are usually interested in drag force on the entire surface, which can be determined using average friction coefficient. But sometimes we are also interested in the drag force at a certain location, and in such cases, we need to know the local value of the friction coefficient. With this in mind, we present correlations for both local (identified with the subscript  $x$ ) and average friction coefficients over a flat plate for laminar, turbulent, and combined laminar and turbulent flow conditions. Once the local values are available, the average friction coefficient for the entire plate can be determined by integration from

$$C_f = \frac{1}{L} \int_0^L C_{f,x} dx \quad (3.8)$$

Based on the analysis, the boundary layer thickness and the local friction coefficient at location  $x$  for laminar flow over a flat plate were determined by

$$\text{Laminar: } \delta = \frac{4.91x}{Re_x^{0.5}} \quad \text{and } C_{f,x} = \frac{0.664}{Re_x^{0.5}} \quad ; \quad Re_x < 5 \times 10^5 \quad (3.9)$$

$$\text{Turbulent: } \delta = \frac{0.38x}{Re_x^{1/5}} \quad \text{and } C_{f,x} = \frac{0.059}{Re_x^{1/5}} \quad ; \quad 5 \times 10^5 \leq Re_x \leq 10^7 \quad (3.10)$$

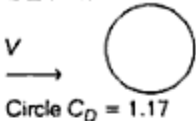
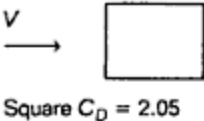

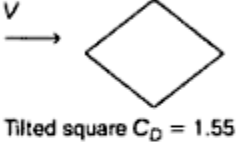
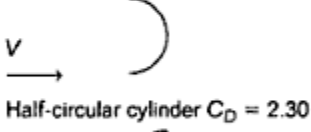

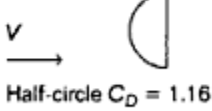

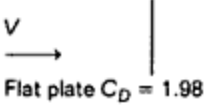
where  $x$  is the distance from the leading edge of the plate and  $Re_x = Vx/\nu$  is the Reynolds number at location  $x$ . Note that  $C_{f,x}$  is proportional to  $1/Re_x^{0.5}$  and thus to  $x^{-1/2}$  for laminar flow and it is proportional to  $x^{1/5}$  for turbulent flow. In either case,  $C_{f,x}$  is infinite at the leading edge ( $x = 0$ ), and therefore Eqs. 3.9 and 3.10 are not valid close to the leading edge. The local friction coefficients are higher in turbulent flow than they are in laminar flow because of the intense mixing that occurs in the turbulent boundary layer. Note that  $C_{f,x}$  reaches its

highest values when the flow becomes fully turbulent, and then decreases by a factor of  $x^{-1/5}$  in the flow direction. The average friction coefficient over the entire plate is determined by

$$\text{Laminar, } C_f = \frac{1.33}{Re_L^{1/2}} \quad Re < 5 \times 10^5 \quad ,$$

$$\text{turbulent, } C_f = \frac{0.074}{Re_L^{1/5}} \quad ; \quad 5 \times 10^5 < Re < 10^7 \quad (3.11)$$

**Table 3.1:** Drag coefficient data for selected

### 3.4. Wind Turbine Types

Wind turbines can be classified in a first approximation according to its rotor axis orientation and the type of aerodynamic forces used to take energy from wind.

#### 3.4.1 Rotor Axis Orientation

The major classification of wind turbines is related to the rotating axis position in respect to the wind; care should be taken to avoid confusion with the plane of rotation:

- Horizontal Axis Wind Turbines (HAWT): the rotational axis of this turbine must be oriented parallel to the wind in order to produce power. Numerous sources claim a major efficiency per same swept area and the majority of wind turbines are of this type.
- Vertical Axis Wind Turbines (VAWT): the rotational axis is perpendicular to the wind direction or the mounting surface. The main advantage is that the generator is on ground level so they are more accessible and they don't need a yaw system. Because of its proximity to the ground, wind speeds available are lower. One interesting advantage of VAWTs is that the blades can have a constant shape along their length and, unlike HAWTs, there is no need in twisting the blade as every section of the blade is subjected to the same wind speed. This allows an easier design, fabrication and replication of the blade which can influence in a cost reduction and is one of the main reasons to design the wind turbine with this rotor configuration (Graebel, 2001).

### **3.4.2. Lift or Drag Type**

There are two ways of extracting the energy from the wind depending on the main aerodynamic forces used:

- The drag type takes less energy from the wind, but has a higher torque and is used for mechanical applications as pumping water. The most representative models of drag-type VAWTs is the Savonius.
- The lift type uses an aerodynamic airfoil to create a lift force, they can move quicker than the wind flow. This kind of windmills is used for the generation of electricity. The most representative models of a lift-type VAWT is the Darrieus turbine; its blades have a troposkien shape which is appropriate for standing high centrifugal forces.

### **3.5. Reviews on Three Blade Wind Turbine**

Mohammed, 2013, carried out an experimental study using subsonic wind tunnel under low wind speed. Also, he compared and investigated the performance of two and three blades of Savonius wind turbine rotor. He concluded that increasing the number of blades will increase

the drag surfaces against the windair flow and causes it to increase the reverse torque and leads to a decrease in the net torque working on the blades of a Savonius wind turbine.

Mashhadet al., 2013, studied experimentally and computationally the feasibility of improving the performance of the three blades vertical-axis Savonius wind turbine with different overlap ratios and without overlap under low-speed subsonic wind tunnel at different Reynolds numbers. The results showed that lower Reynolds number gave better torque coefficient variation with the increase of the angle of rotation for each model and Power coefficient calculated from the numerical method shows that it is always increasing with the increase of the tip speed ratio.

Wenehenubun et al., 2015, studied experimentally the effect of number of blades (2, 3 and 4 blades) on the performance of the model of the Savonius type wind turbine. The author concludes that the number of blades influences the performance of wind turbine and Savonius model with three blades has the best performance at high tip speed ratio.

Saha et al., 2008, discussed the aerodynamic performance of single-, two- and three-stage Savonius rotor systems based on experiments that are carried out to optimize the different parameters like number of stages, number of blades and geometry of the blade. And All the experiments had been conducted at different wind speed. The results showed a twisted geometry blade profile had better performance as compared to the semicircular blade geometry, the two-stage Savonius rotor had a better power coefficient as compared to the single- and three-stage rotors.

Saha and Rajkumar, 2006, tested the twisted blade in a three bladed Savonius wind rotor in a low speed wind tunnel. The experimental results showed that the potential of the twisted bladed rotor in terms of smooth running, higher efficiency and self-starting capability as compared to that of the conventional bladed rotor.

M. Jamil et al., 2013, presented Experimental Study the performance of a Combined Three Bucket H-Rotor with Savonius Wind Turbine (H-rotor WT with DUW200 airfoils). The authors concluded that Combining both Savonius and H-rotor with each other makes an efficient wind turbine which has the better self-starting ability besides higher power coefficient.

K.K. Sharma et al., 2013, presented performance measurement of three bladed combined Darrieus- Savonius rotor with Darrieus mounted on top of Savonius rotor. The authors

concluded that an optimum TSR at which the performance coefficients are the highest and an optimum overlap at which the performance coefficients are the highest.

Gupta and Biswas, 2011, studied numerically the performance of a combined three-bucket Savonius and three-bladed Darrieus turbine and measured the aerodynamic coefficients with respect to angle of attack for various tip speed ratios. The authors concluded that the power augmentation of the combined turbine occurred for low overlap in Savonius turbine due to high aerodynamic lift-to-drag coefficient of the Savonius turbine, caused by the increase of dynamic pressure from bucket-vortex interactions on the concave face of the returning bucket. And high value of overlap (20% onwards) caused vortex separations from the inner edges of the bucket destabilizing the Coanda flow for which the aerodynamic coefficients were lowered.

### **3.6 Vertical Axis Wind Turbine (VAWT)**

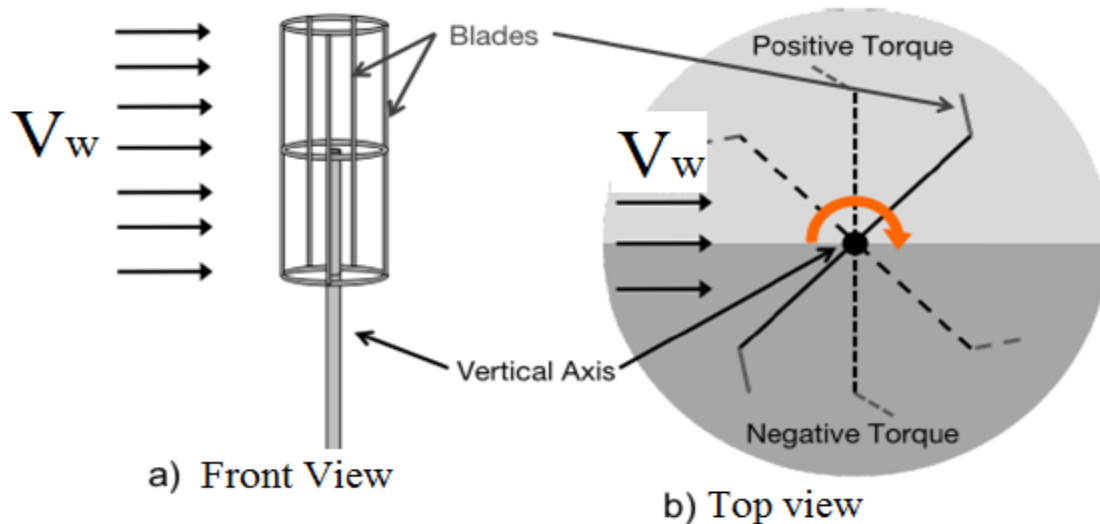
In recent years vertical axis wind turbine arrays have been shown to produce more power per unit land area than horizontal axis wind turbines, primarily due to the difference in spacing requirements between the two turbine types (Kinzel, et al., 2012; Hau, 2006). While vertical axis wind turbines (VAWTs) were the first type of wind turbine in existence. horizontal axis wind turbines (HAWTs) quickly became the prevailing wind energy converter due to their higher efficiency.

The result of this shift in focus is that horizontal axis wind turbines have gone through many more years of technical development than their counterparts. Consequently, vertical axis wind turbines have remained an immature technology (Sheldahl et al., 1977).

One significant difference between VAWTs and HAWTs is the method with which the blades interact with the wind. HAWTs orientate their rotor blades perpendicular to the wind, i.e. their power production depends on the angle between the wind direction and the rotor. With proper alignment between wind direction and the rotor, the blades continuously produce lift, which in turn keeps the rotor spinning.

In contrast, VAWTs are independent of wind direction. The blades must produce positive torque throughout half of one rotation, while minimizing any negative impact on rotor rotation as the blades are carried back upstream. This is due to the symmetry of the turbine as laid out in Figure 3.5, where a VAWT is depicted from the side (a) and from above (b).

Notably, the blade aerodynamics changes dramatically over the course of a rotation because the angle of attack changes due to the rotation.



**Figure 3.5:** Bird's eye view of a vertical axis turbine

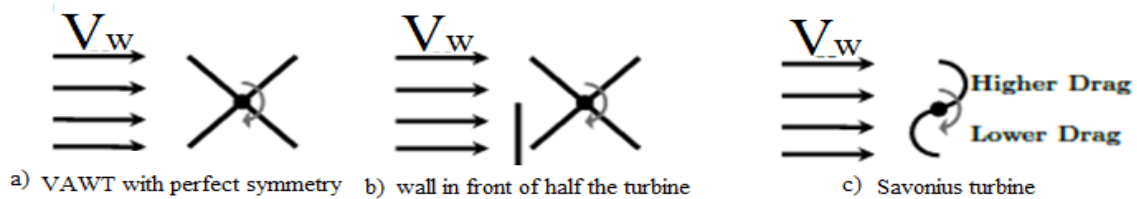
Historically, creating the necessary torque differential has been solved in two ways: the first solution was to build a wall in front of the negative torque region, preventing any forces from wind occurring on this half of the turbine (see Figure 3.6b); the second solution was to create non-symmetric blade shapes. This concept can be further divided into two categories: air foils in the case of lift-driven Darrieus rotors, or bucket-like scoops in the case of drag-driven Savonius rotors, shown in Figure 4.6c (Vogel, 1984). However, both of these solutions involve compromises.

In the case of building a wall to create flow blockage, the benefit VAWTs exhibit over HAWTs of being directionally independent of the wind direction is removed by the large wall structure forcing directional dependence. In the second case of nonsymmetrical blades, manufacturing complication, and thus additional expense, creates a suboptimal solution.

Mechanisms to prevent damage during storms are also important elements of wind turbine design. HAWTs have many mechanisms to prevent damage caused by high winds. They can either rotate the entire rotor section parallel to the wind or change the pitch of the blades to



avoid over-spinning. In contrast, VAWTs have relied on both mechanical and electrical breaks to prevent the turbine rotor from spinning too fast.



**Figure 3.6:** Geometry of vertical axis wind turbine designs as viewed from above the Turbines

From Figure 3.6;

- a. Shows a VAWT with perfect symmetry, which is therefore unable to rotate,
- b. Shows the use of a wall in front of half the turbine to impose the force differential needed for rotation,
- c. Shows a Savonius turbine, which uses geometric differences to break the symmetry of forces acting on the blades.

This body of work explores the simple solution of using at, rectangular sheets of pliable materials as the blades of a VAWT. The idea sprang from the drag enhancement as well as drag reduction qualities of shape reconfiguration. Vogel, 1984. and Crosselin, 2010, noted that pliable structures have both drag enhancing and drag reducing properties, dependent only on the angle of attack of the blade relative to its clamp and fluid flow direction. The principle was incorporated in a turbine design, which used reconfiguration to produce a torque differential across the turbine. The positive torque side would use drag enhancement, while the negative torque side would minimize forces acting on the turbine by utilizing the drag reduction.

The studied wind energy converter is a VAWT, which is a less common type of wind turbine. The VAWT is Omni-directional, i.e. it accepts wind from all directions and does not need a yawing mechanism. In addition, the vertical axis wind turbine is predictable to produce less noise than a horizontal axis wind turbine (Ribrant & Bertling, 2007).

The studied system has a turbine with straight blades, which are attached to the drive shaft via support arms. This configuration is commonly called an H-rotor as in (Eriksson et al.,

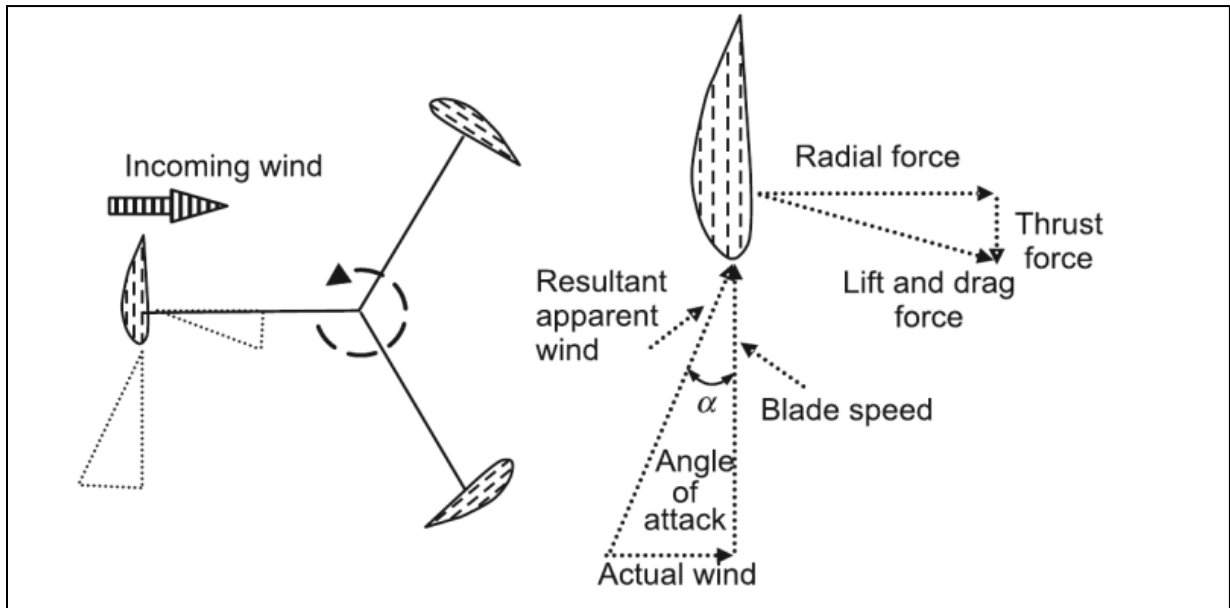
2008). The simplicity is the main advantage with this wind turbine concept. The wind turbine consists of few parts and will only have one rotating part. The omission of the gearbox, yawing system and pitch system is expected to reduce maintenance (Roynarin & Leung, 2002). The blades will be fixed, i.e. it will not be possible to turn them out of the wind. The absorbed power will be controlled by an electrical control system combined with passive stall control, i.e. the blades will be designed to stall to limit power absorption at high wind speeds. The generator of the vertical rotational axis of wind turbine is located at the bottom of the tower. This is expected to simplify installation and maintenance. The tower can be lighter for a VAWT since the nacelle is excluded, which reduces structural loads and problems with erecting the tower (Angelin et al., 1981). The generator design is focused on efficiency, cost and minimizing maintenance, as the size of the generator is not the main concern. In advantage, the control system can also be located at ground level facilitating access (Earnest, 2014). There is an apparent difference in the drive train between a HAWT and a VAWT with a ground based generator (apart from turbine configuration): the length of the drive shaft. The long drive shaft of this type of VAWT is interesting to field of study. Although, the long drive shaft is not unique for this system; it has been used in hydropower. In Järnvägsforsen, Sweden, a hydropower station with two turbine-generator systems of the long shaft type was installed, each having a rated power of 60 MVA, a drive shaft length of 45 meters and a shaft outer diameter of 1.4 meters (Abzug & Larrabee, 2002).

### **3.6.1 Working Principle of VAWT**

In the VAWT design which may be two-bladed, three-bladed or four-bladed, the blades are symmetrically arranged around a vertical axis and the angles of the blades are set optimally in such a manner so that it works on the lift principle.

For a rotating VAWT, the blades encounter two forces its own rotating speed and the incoming wind speed (see Figure 3.5). There is a tangential force pulling the blade around and radial force acting against the bearing of vertical axis. Both speeds get added vectorially yielding a total apparent wind speed at an incoming angle of attack. The incoming air stream which is parallel to the blade yields high and low pressure regions on the blade, yielding overall lift and drag forces. The resulting oblique lift force creates a torque on the shaft to which the blades are attached making them rotate in the direction of the blades in which they

are already travelling. The VAWT yield an overall positive torque that can be extracted as electrical power through the generator.

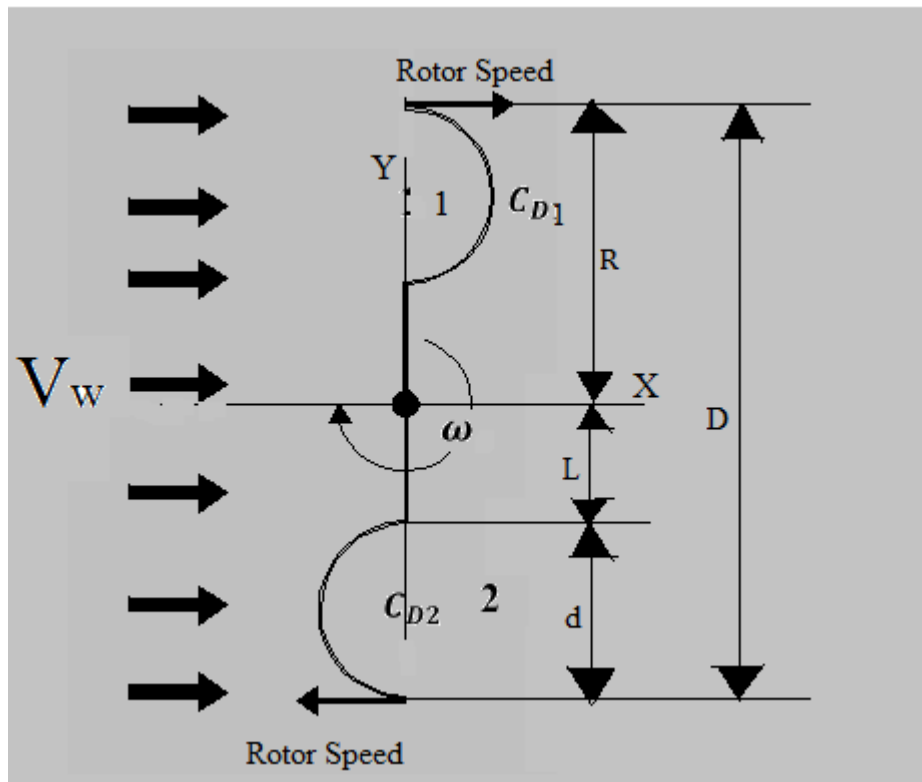


**Figure 3.7:** Lift principle of three-bladed VAWT Rotor: The aerofoil of the blades are adjusted

A major limitation of the VAWT is that it is not self-starting due to symmetry of the blades. Hence, to generate a torque on its own, starting is achieved by operating the electrical generator as a motor and then speeding up the VAWT sufficiently for the wind to pass over the blade aerofoil to create the lift force and then run in the generating mode. Torque is caused by change in the apparent wind direction relative to the moving blades (Burton, 2001).

### 3.7 Estimate the Torque and Mechanical Power Output

As discussed earlier, the Savonius type rotor is a drag-based wind turbine because it's the drag component of the aerodynamic force that powers the Savonius turbine to rotate. We can estimate the torque, and mechanical power output of a Savonius rotor using a simplified model, Figure 3.8. This simplified model, however, neglects the effect of rotor on the wind flow characteristics.



**Figure 3.8:** Simplified model of C-section Wind turbine

Let's assume that the rotor has mean radius  $R$  and it is rotating with an angular speed  $\omega$ . The circumferential velocity of the rotor,  $v_r$ , at the mean radius is equal to:

$$v_r = \omega R \quad (3.12)$$

during the rotation, the wind velocity is broken into two components:  $X$ , and  $Y$  as shown in Figure 3.9. Vertical flows were not considered in this research, and could be a topic for future exploration. Assuming that the axis of the C-section vertical axis wind turbine rotor is

the upward-pointing Y-axis, the flow experienced in the X-direction is the sum of the free-stream flow in the X-direction, and the X-aspect of rotational velocity (see Figure 3.10).

Let assume that the rotor is not rotating (see Figure 3.8), then the average relative velocities of the wind  $v_{rel,1}$  and  $v_{rel,2}$  at the first and second rotating drums are given by following expressions, respectively (see Figure 3.9).

$$v_{rel,1} = v_w - v_r \quad (3.13)$$

$$v_{rel,2} = v_w + v_r \quad (3.14)$$

The resulting drag forces  $F_{D,1}$  and  $F_{D,2}$  on the rotating drums are given as:

$$F_{D,1} = \frac{1}{2} \rho C_{D,1} v_{rel,1}^2 A = \frac{1}{2} \rho C_{D,1} A (v_w - v_r)^2 = \frac{1}{2} \rho C_{D,1} A v_w^2 \left(1 - \frac{v_r}{v_w}\right)^2 \quad (3.15)$$

$$F_{D,2} = \frac{1}{2} \rho C_{D,2} v_{rel,2}^2 A = \frac{1}{2} \rho C_{D,2} A (v_w + v_r)^2 = \frac{1}{2} \rho C_{D,2} A v_w^2 \left(1 + \frac{v_r}{v_w}\right)^2 \quad (3.16)$$

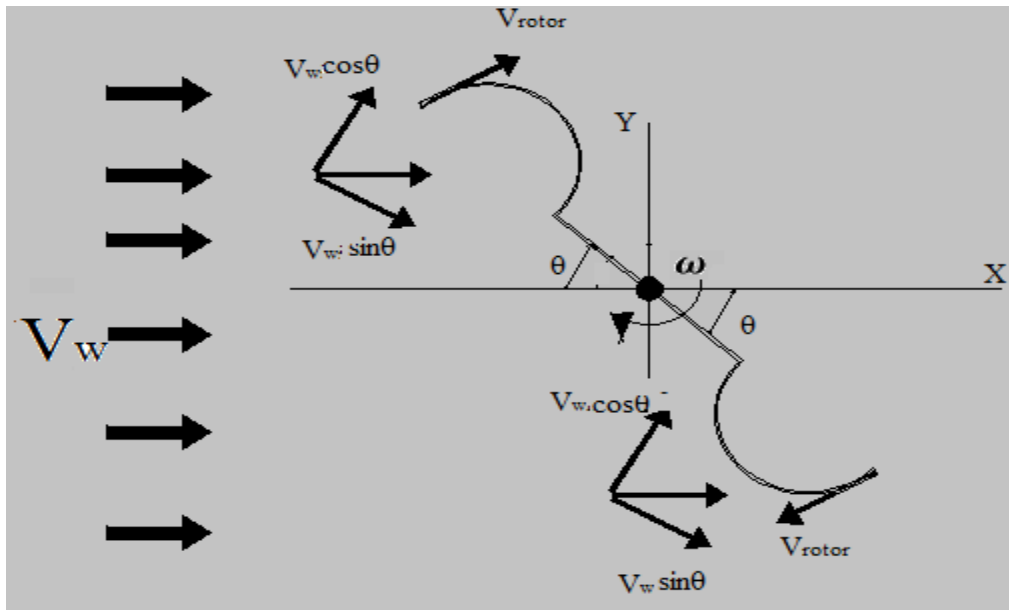
where, A denotes projected area of the drums. The aerodynamic torque along the central axis is calculated as:

$$\begin{aligned} T &= (F_{D,1} - F_{D,2}) \left(L + \frac{d}{2}\right) \\ &= \frac{1}{2} \rho C_{D,1} A v_w^2 \left[ C_{D,1} \left(1 - \frac{v_r}{v_w}\right)^2 - C_{D,2} \left(1 + \frac{v_r}{v_w}\right)^2 \right] \left(L + \frac{d}{2}\right) \end{aligned} \quad (3.17)$$

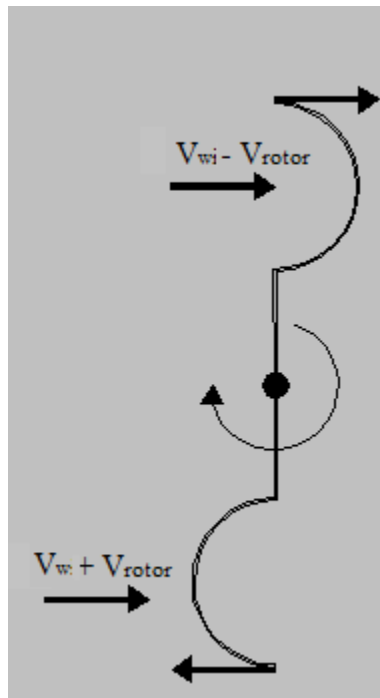
The mechanical power by the turbine can be then determined using the following equation

$$\begin{aligned} P &= T\omega = \frac{1}{2} \rho C_{D,1} A v_w^2 \left[ C_{D,1} \left(1 - \frac{v_r}{v_w}\right)^2 - C_{D,2} \left(1 + \frac{v_r}{v_w}\right)^2 \right] \omega \left(L + \frac{d}{2}\right) \\ &= \frac{1}{2} \rho C_p v_w^3 A \end{aligned} \quad (3.18)$$

The expression  $\left[ C_{D,1} \left(1 - \frac{v_r}{v_w}\right)^2 - C_{D,2} \left(1 + \frac{v_r}{v_w}\right)^2 \right]$  is defined as power coefficient,  $C_p$ . It can be noted from equation (3.15) that the mechanical power produced by a C-section turbine is directly proportion to the total projected area by the rotor and the cube of upstream wind speed  $v_w$  (Priya et al., 2013).



**Figure 3.9:** Vector components of the wind speed of C-section rotor



**Figure 3.10:** Scheme of a C-section rotor showing the velocity of the rotor and wind speed

### **3.8 Rotational Speed**

The aim of the wind turbine designer is the production of energy at minimum cost, subject to constraints imposed by environmental impact considerations. However, blade designs optimized for a number of different rotational speeds but the same rated power produce substantially the same energy yield, so the choice of rotational speed is based on machine cost rather than energy yield. One of the key cost drivers is the rotor torque at rated power, as this is the main determinant of the drive train cost. For a given tip radius and machine rating, the rotor torque is inversely proportional to rotational speed, which argues for the adoption of a high rotational speed. However increasing the rotational speed has adverse effects on the rotor design, which are explored in the following sections (Burton, 2001).

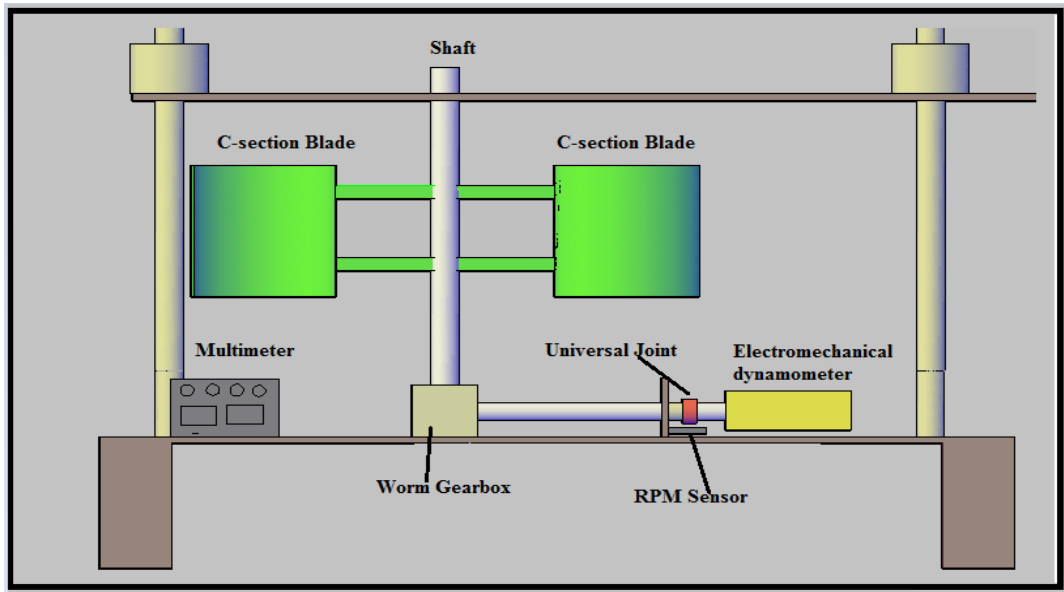
## CHAPTER 4

### METHODOLOGY

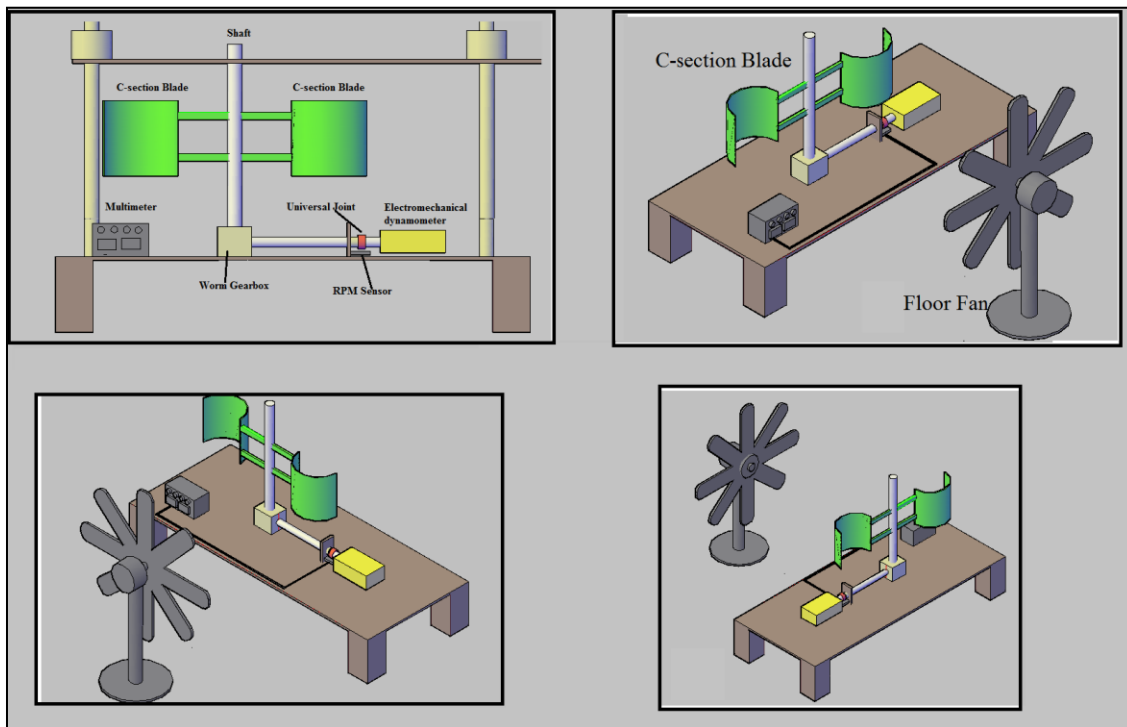
#### 4.1 Vertical Axis C-Section Wind Turbine

The experiment used a model of C-section vertical axis wind turbine with two, three and four blades. Figure 4.1 and 4.2 show the experimental setup with two blades C-section vertical axis wind turbine as an example. The shaft and blades of the C-section rotor is made of stainless steel and PVC material, respectively. Different number of blades and smooth surface design is intended to increase the capability of wind energy capture. The C-section vertical axis wind turbine is connected to the electromechanical dynamometer through a worm gearbox to produce mechanical power, and then convert it into electricity for domestic powered generation. The turbine captures wind and moves due to the presence of drag forces, which cause it to rotate around its fixed axis as shown in Figure 4.1 and 4.2. The dimensions of C-section vertical axis wind turbine model are the diameter of the blade,  $D$ , ( $D = 7, 10$  and  $15\text{cm}$ ), blade height,  $H$ , ( $H = 30$  and  $40$  cm), rotor radius,  $R$ , ( $R = 28, 12.5$  and  $5.5$  cm) is shown in Table 4.1 and Figure 4.3. Additionally, a floor fan is used as the wind source for doing experiments with C-section wind turbine as shown in Figure 4.2. The wind velocity,  $V_w$ , was set at 4, 8 and 10 m/s by adjusting the distance between the floor fan and C-section wind turbine and the wind speed switch settings on the fan to see the performance of the turbine under this controlled environment.





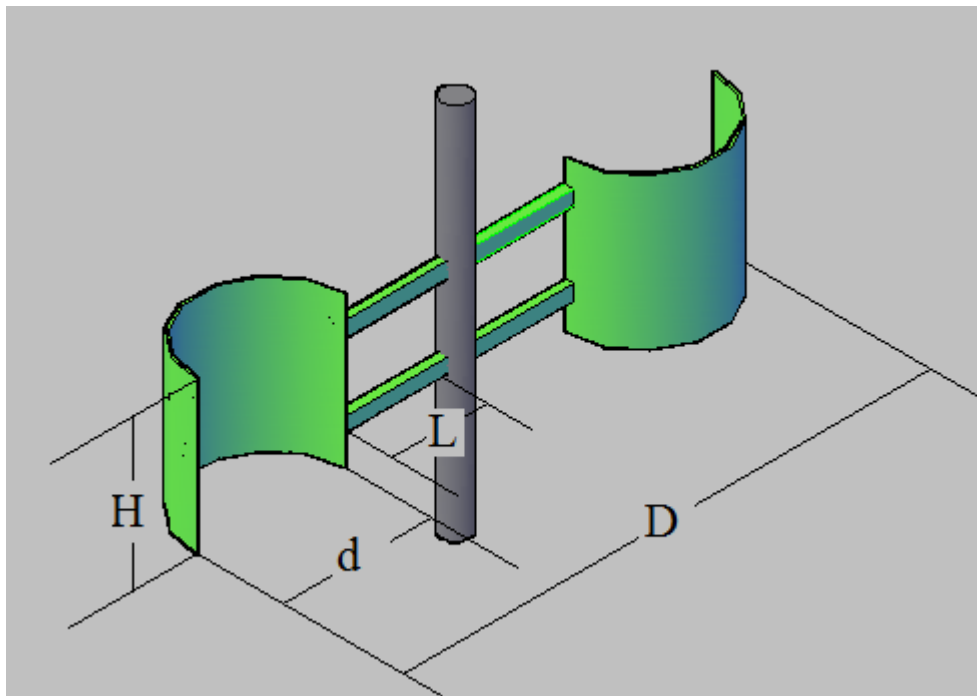
**Figure 4.1:** Schematic of representation of the experimental setup used to measure torque and rotational speed of the shaft



**Figure 4.2:** Three dimensional views of experimental setup used to measure torque and rotational speed of the C-section rotor wind turbine.

**Table 4.1.** Different fixed and variable parameters considered in the design analyses.

<i>Category</i>	<i>Design parameter</i>	<i>Value</i>
<b>Physical features</b>	1. Blade	C-section
	2. Number of blades (N)	N = 2, 3 and 4 blades
<b>Dimensional</b>	3. Blade diameter (D)	D = 7, 10 and 15 cm
	4. Blade height (H)	H = 30 and 40 cm
	5. Beam Length (L)	L = 28, 12.5 and 5.5 cm
<b>Operational</b>	6. Rated wind speed ( $V_w$ )	$V_w = 4, 6$ and $10$ m/s



**Figure 4.3:** Design parameter of C-section wind turbine

## 4.2 Measuring Wind Speed Experimentally

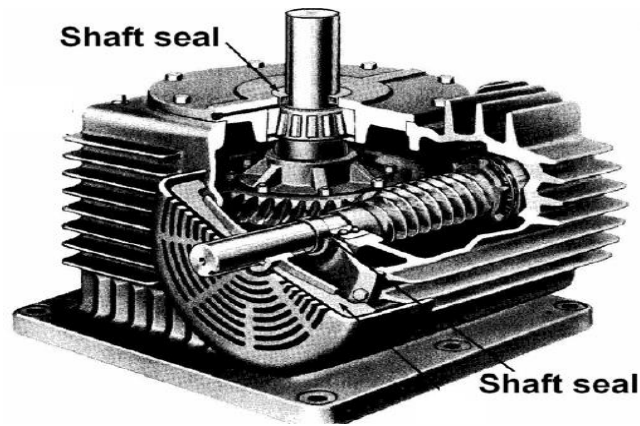
Wind speed is an important parameter for evaluating the mechanical power performance of wind turbine. Hence, when testing a wind turbine, wind speed must always be measured. Anemometry is used to measure the wind speed in the project as shown in Figure 4.4.



**Figure 4.4:** Anemometry device

## 4.3 Worm Gear

Gears can be used to change the direction or speed of movement. In this project, Worm gear is used for transmitting power between two non-parallel, non-intersecting shaft (see Figure 4.1 and 4.2). Worm gears involve one wheel gear (a pinion) and one shaft with a screw thread wrapped around it as shown in Figure 4.5. Worm gears change the direction of motion as well as the speed. Worm gear efficiency varies significantly when lead angle, friction factor and gear ratio changes and worm gear efficiencies range from 50% to 90%.



**Figure 4.5:**The cut section of a worm gearbox

#### **4.4. Measuring the Torque of Vertical Axis Wind Turbine Experimentally**

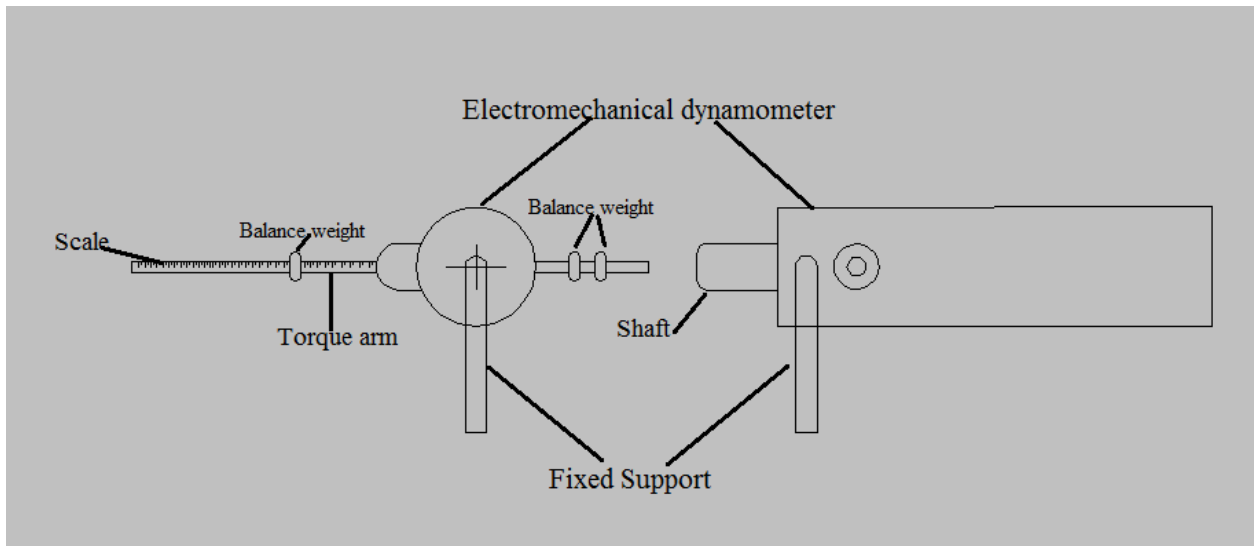
The procedure for measuring the torque and mechanical power of the C-section wind turbine, the first step is to build the turbines with the different sizes. This was done using PVC material for the blade (C-section shape) of 0.5 mm thick with different height and diameter as shown in Table 4.1. The shaft of the C - section rotor is made from stainless steel with 2 cm diameter and 1 m long. The finished turbine was then attached to a worm gearbox (Worm gear is used for transmitting power between two non-intersecting shaft), which was attached to electromechanical dynamometer and was placed in front of a floor fan. Electromechanical dynamometer is used to measure force and torque from a rotating shaft of C-section vertical axis wind turbine as shown in Figure 4.1 and 4.2. The electromechanical dynamometer system is consisted water level, arms, weight and balance weight for measuring the output torque of wind as shown in Figure 4.6. Also, it consists of a direct current (DC) machine with the stator cradle-mounted on anti-friction bearings. The rotor is connected to the shaft of the machine under test. The stator is constrained from rotating by a radial arm of known length to which is attached a scale for measuring the force required to prevent rotation. Torque is described as force acting along a distance. Torque is something that creates twisting and tries to make something rotate. The turbine is arranged with the stator mounted free to revolve but restrained from revolving by a brake arm attached to it and fastened to weighing scales. The force,  $F$ , shown on the scales becomes a torque,  $T$ , when multiplied by the lever distance,  $d$ , from the centre of rotation. Power,  $P$ , is measured as the torque operating at the rotational speed of the generator shaft. The RPM sensor is used to measure the rotational speed of the

shaft which was placed under the special universal joint as shown in Figure 4.1 and 4.2. This RPM sensor is connected to multimeter device reader. However, the multimeter device reader is device used to read the RPM of the shaft as shown in Figure 4.2. The floor fan was turned into low power and adjusting the distance between the floor fan and C-section wind turbine, where it would be emitting a wind speed of 4 m/s. The RPM reading on the multimeter and wind speed result on the anemometry were recorded, as well as the distance and weight for calculating the torque of the C-section turbine. Then, floor fan is turned to medium and high power, and recorded the same data. The same method is used to make and test the other turbines, and recorded the same data.

The formula for torque and power are:

$$T = F \times d \quad [N.m] \quad (4.1)$$

$$P = T \times \omega \quad [Watt] \quad (4.2)$$



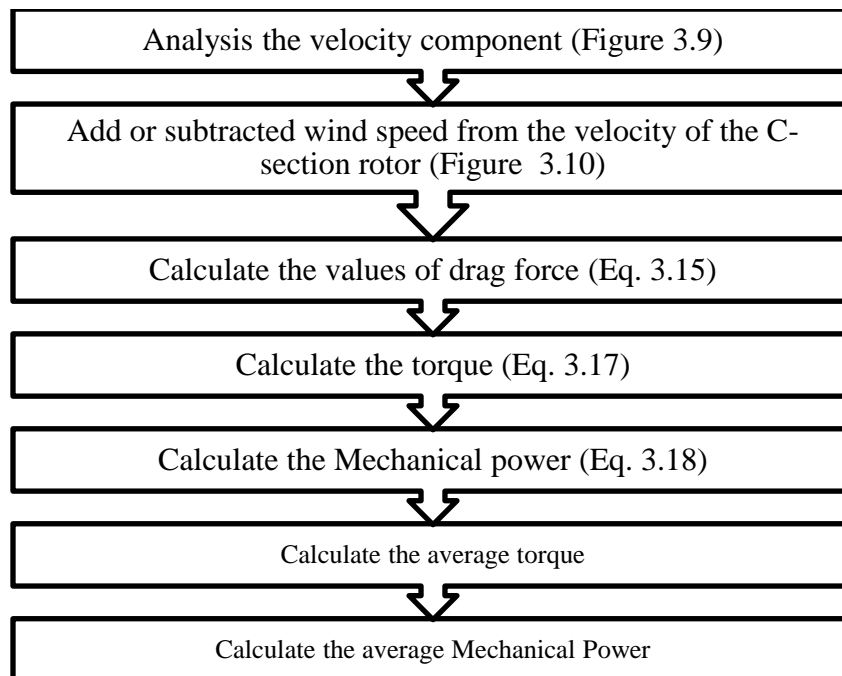
**Figure 4.6:** Scheme of electromechanical dynamometer (Front and right views) showing the components of electromechanical dynamometer

#### 4.4 Theoretical Procedures for Calculating the Mechanical Power

As mentioned in the previous chapter, the procedures of power calculation of C-section vertical axis wind turbine can be described as the following steps and shown in Figure 4.7:

1. Analysis the velocity component into X-axis and Y-axis which depends on the position of the blade as shown in Figure 3.9.

2. Add or subtract wind speed from the velocity of the C-section rotor which depends on the direction of the velocity X-component (see Figure 3.10).
3. Find out the values of the drag coefficient,  $C_D$ , which depends on the position of the blade.
4. Calculate the values of drag force,  $F_D$ , (pressure force) for two, third and fourth blade (the blades are different by  $180^\circ$ ,  $120^\circ$  and  $90^\circ$  from each other respectively).
5. Calculate the torque,  $T$ , for each blade (Eq. 3.17)
6. Calculate the total values of torque of this rotor for the preparation of Mechanical power calculation (Eq. 3.18)
7. Calculate the average torque for the preparation of average Mechanical power calculation.



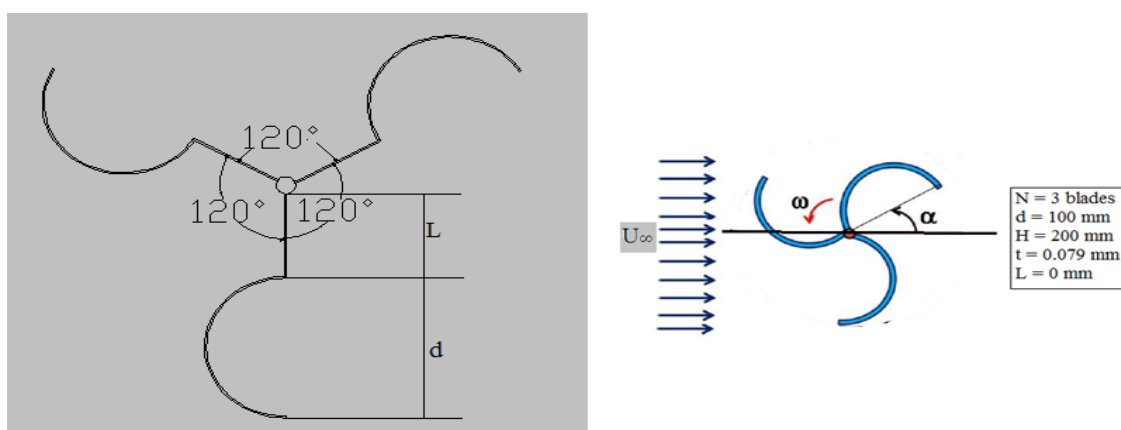
**Figure 4.7:** The procedure for calculating mechanical power of the C - section rotor

## CHAPTER 5

### RESULTS AND DISCUSSIONS

#### 5.1 Comparison of Theoretical study and Experimental<sup>1</sup> Torque of Three blade C-section Savonius Wind Turbine Rotor

Before applying the theoretical study in C-section wind turbine, a comparative study has been done between the theoretical studies with Mohammed, 2013, by using the same dimension of C-section Savonius wind turbine, wind speed and angular rotation. The blade of a Savonius wind turbine was made of semi-cylindrical scoops of diameter ( $d = 100$  mm), height of ( $H = 200$  mm) and thickness of ( $0.079$  mm). The three blades of Savonius wind turbine are different by  $120^\circ$  from each other as shown in Figure 5.1. The theoretical was compared with the experimental data which obtained from an article Mohammed, 2013, at wind speed  $4$  m/s and  $410$  RPM. Figure 5.2, Figure 5.3 and Table 5.1 show the comparison between experimental and theoretical predictions data torque and torque coefficient of the Savonius (C-section Blade) wind turbine rotor. Also, the percentage of error between them is shown in Table 2. As can be seen, the percentage of error between the theoretical predictions and experimental data at  $60^\circ$ ,  $90^\circ$ ,  $180^\circ$ ,  $210^\circ$ ,  $300^\circ$ , and  $330^\circ$  is about 5percent and at  $30^\circ$  and  $270^\circ$  is about 6 percent. Whereas, at  $0^\circ$ ,  $120^\circ$ ,  $240^\circ$ , and  $360^\circ$  the percentage error between the experimental and theoretical data is in the range between 38 and 65 percent.



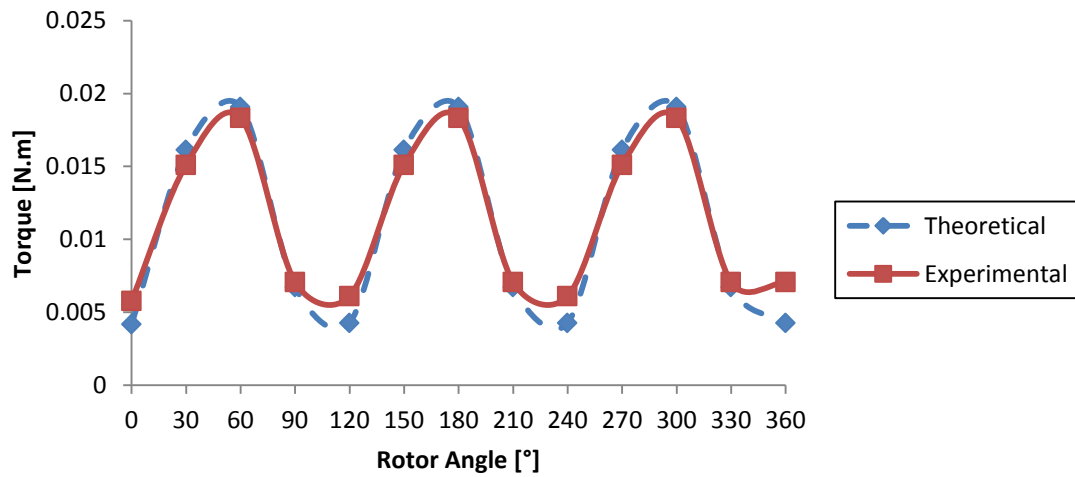
**Figure 5.1:** Scheme of a Savonius rotor with  $L=0$  mm

<sup>1</sup>Experimental data of Savonius wind turbine rotor which was done by experiments are taken from reference Mohammed, 2013.

**Table 5.1:** Theoretical and experimental values of torque and torque coefficient of Savonius (C-section blade) wind turbine.

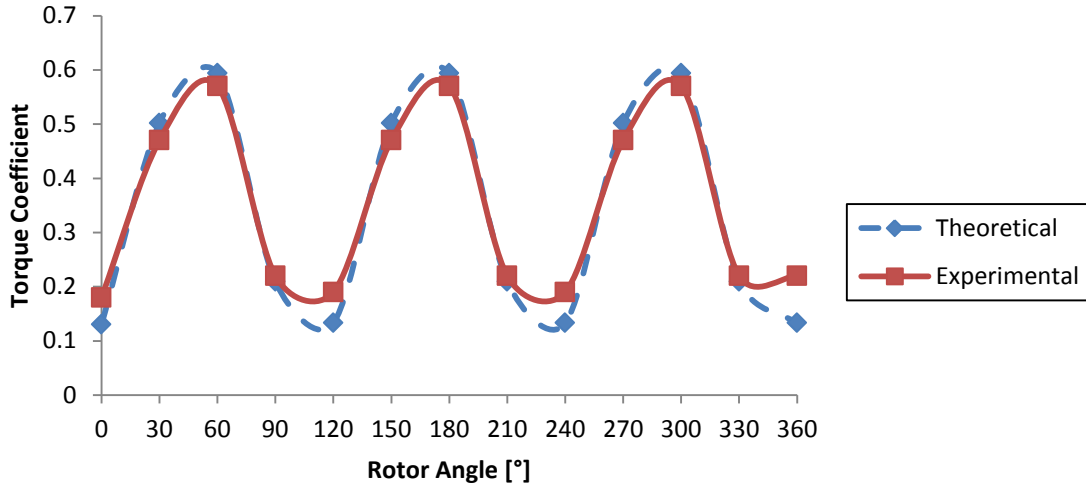
Rotor Angle [°]	Torque [N.m]			Rotor Angle [°]	Torque Coefficient		
	Th.	Exp.	Absolute Error [%]		Th.	Exp.	Absolute Error [%]
0	0.004184	0.0058	38.36	0	0.13	0.18	38.36
30	0.016132	0.0151	6.31	30	0.5	0.47	6.31
60	0.019084	0.0183	3.96	60	0.59	0.57	3.96
90	0.006734	0.0071	5.05	90	0.21	0.22	5.05
120	0.004276	0.0061	42.90	120	0.13	0.19	42.90
150	0.016132	0.0151	6.31	150	0.5	0.47	6.31
180	0.019084	0.0183	3.96	180	0.59	0.57	3.96
210	0.006734	0.0071	5.05	210	0.21	0.22	5.05
240	0.004276	0.0061	42.90	240	0.13	0.19	42.90
270	0.016132	0.0151	6.31	270	0.5	0.47	6.31
300	0.019084	0.0183	3.96	300	0.59	0.57	3.96
330	0.006734	0.0071	5.05	330	0.21	0.22	5.05
360	0.004276	0.0071	65.46	360	0.13	0.22	65.46

Th.: Theoretical                      Exp.: Experimental



**Figure 5.2:** Theoretical predictions and experimental torque of Savonius wind turbine rotor





**Figure 5.3:** Theoretical predictions and experimental torque coefficient of Savonius wind turbine rotor

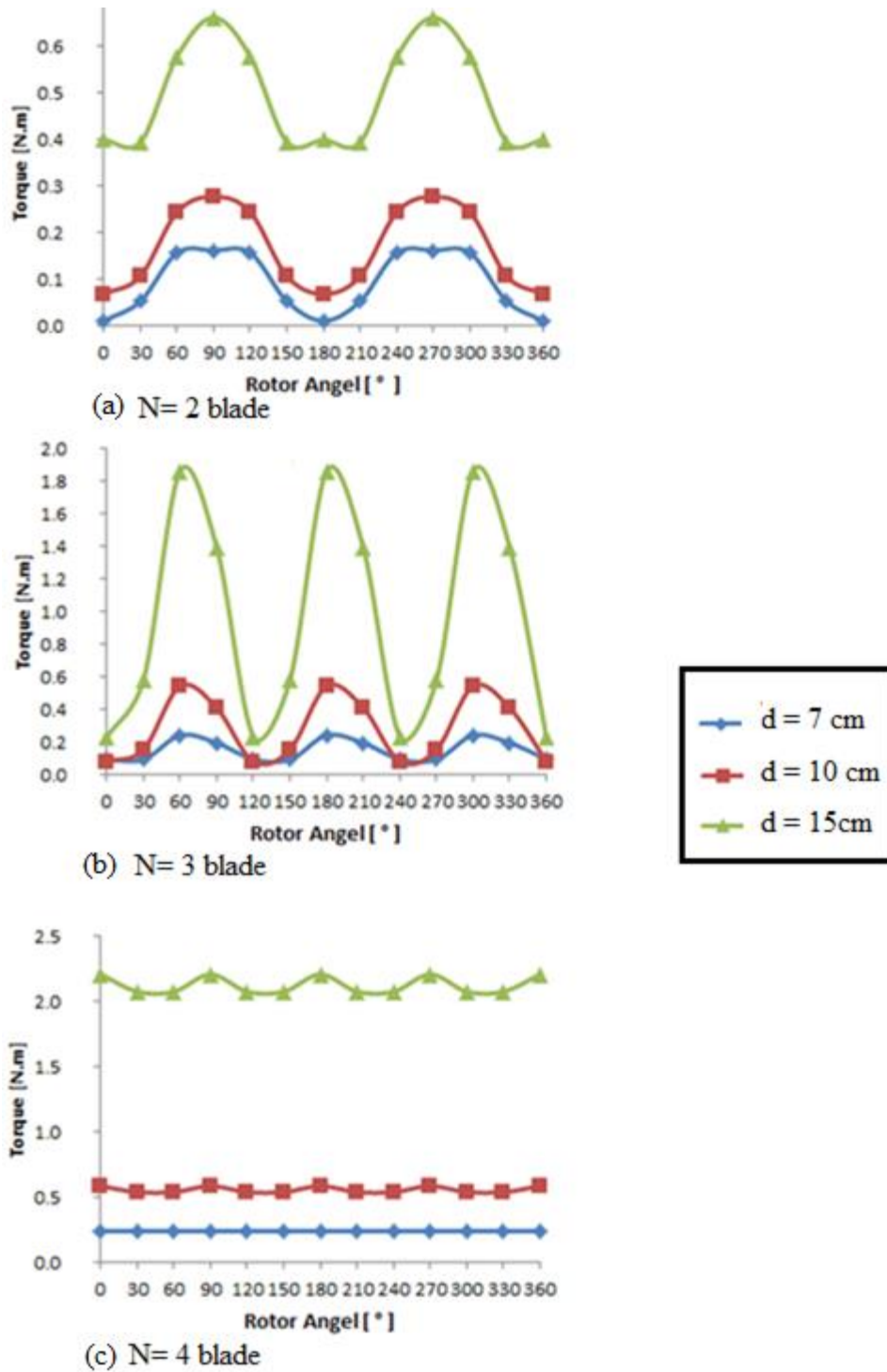
## 5.2. Theoretical Results of Torque of C-section Rotor

As mentioned previously, Torque and mechanical power of the C-section rotor were calculated for varying numbers and sizes of C-section blades and varying rotor diameter.

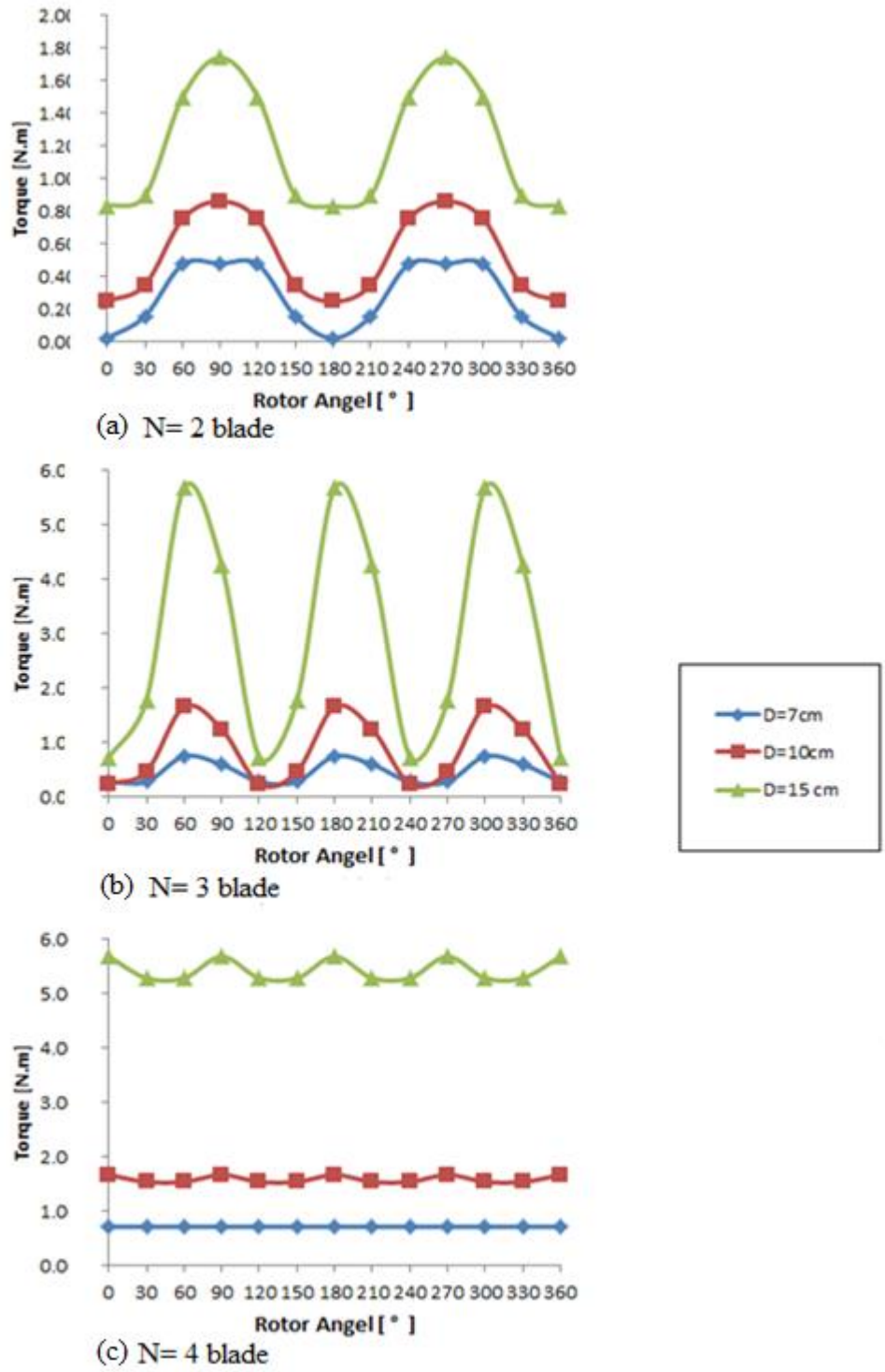
Figures 5.4, 5.5 and 5.6 show the torque varies with the change in rotor angle for different number of blades (2, 3, 4) and blade diameter (7, 10 and 15cm) with fixed blade height (40 cm) and wind speed (4m/s) which were chosen randomly. For two, three, and fourth C-section blades of vertical axis wind turbine, the blades are different by 180°, 120°, and 90° from each other respectively. As shown in Figure 5.4, 5.5 and 5.6, the torque increases when the number and size of blade increased. Furthermore, the periodic motion of the graph of two, three, and four blades of C-section is very obvious and the motion repeats itself in a regular fashion. As can see, as the number blades increase than 3 blades, the torque values of C-section rotor are slightly increased.

Figure 5.6 shows how the torque varies with the change in the rotor angle with a different blade numbers and wind speed with fixed blade rotor radius and blade diameter where was chosen randomly. As shown in Figure 5.7, the torque increases when the number of blade and wind speed are increased. Furthermore, the periodic motion of the graph of two, three and four blades of C-section is very obvious and the motion repeats itself in a regular pattern. The increasing in rotor radius leads to increase the torque of C-section blade with fixed blade

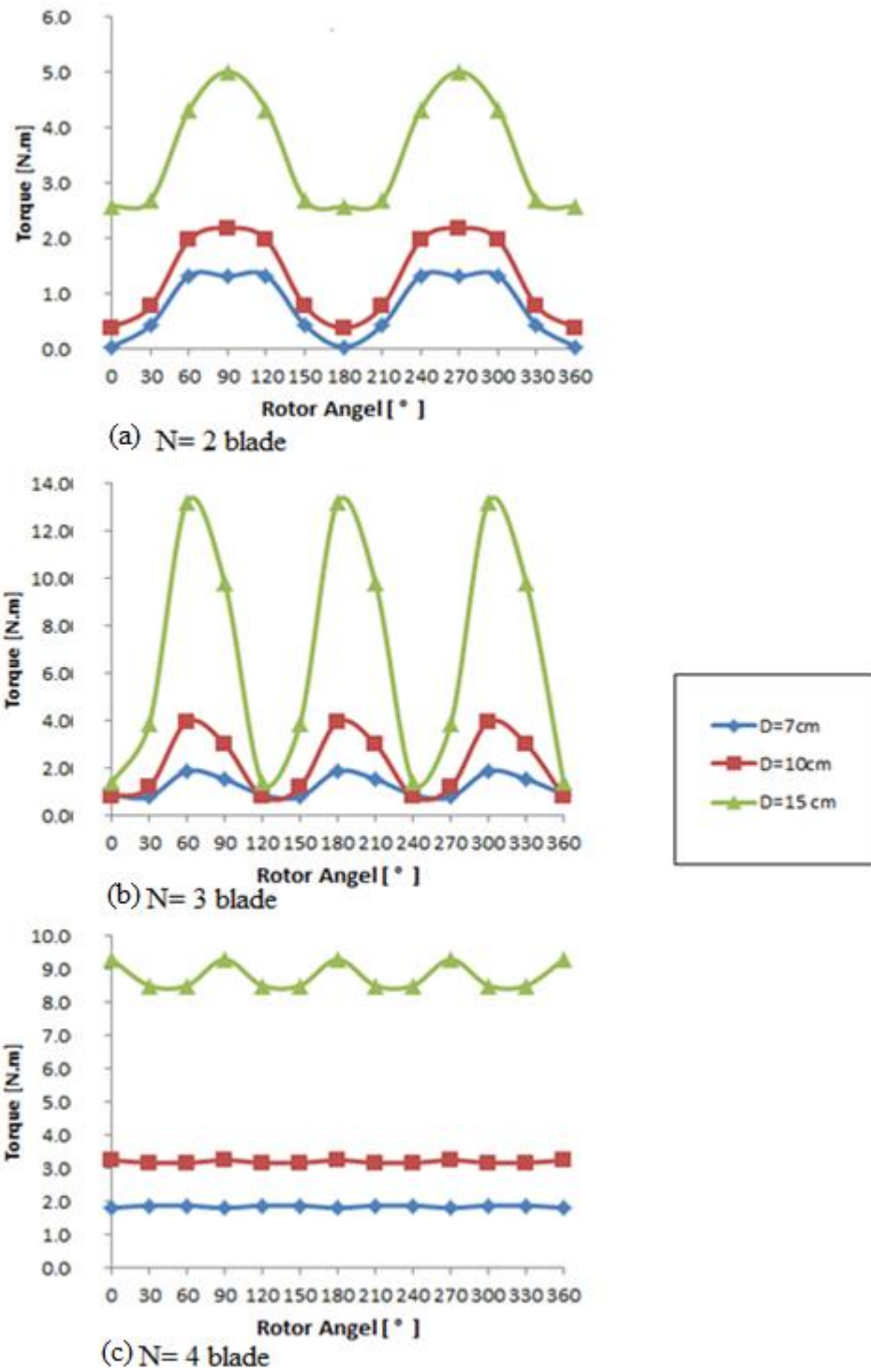
size and wind speed as shown in Figure 5.8.



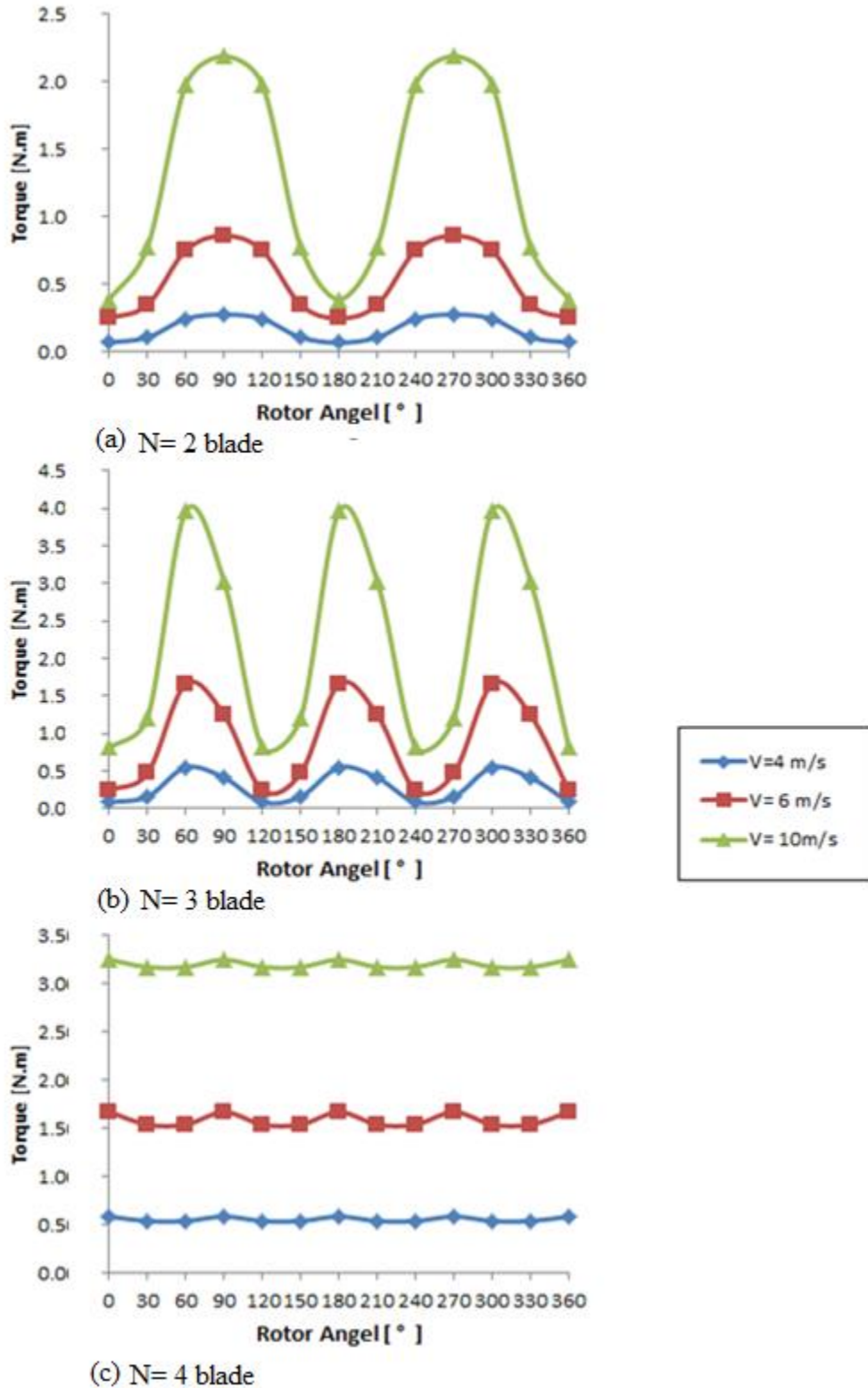
**Figure 5.4:** Torque versus Angle of rotation for different diameter with fixed  $V = 4\text{m/s}$  ,  $H = 40$  cm and  $R = 28\text{cm}$



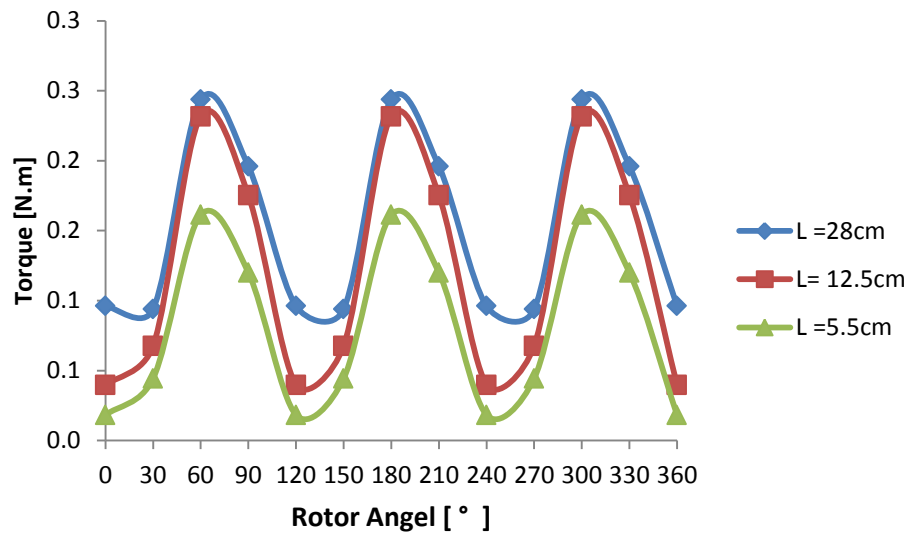
**Figure 5.5:** Torque versus Angle of rotation for different diameter with fixed  $V = 6\text{m/s}$  ,  $H = 40\text{ cm}$  and  $R = 28\text{cm}$



**Figure 5.6:** Torque versus Angle of rotation for different diameter with fixed  $V = 10\text{m/s}$  ,  $H = 40\text{ cm}$  and  $R = 28\text{cm}$



**Figure 5.7:** Torque versus Angle of rotation for different wind speed with fixed  $d = 10\text{cm}$ ,  $H = 40\text{ cm}$  and  $R = 28\text{cm}$

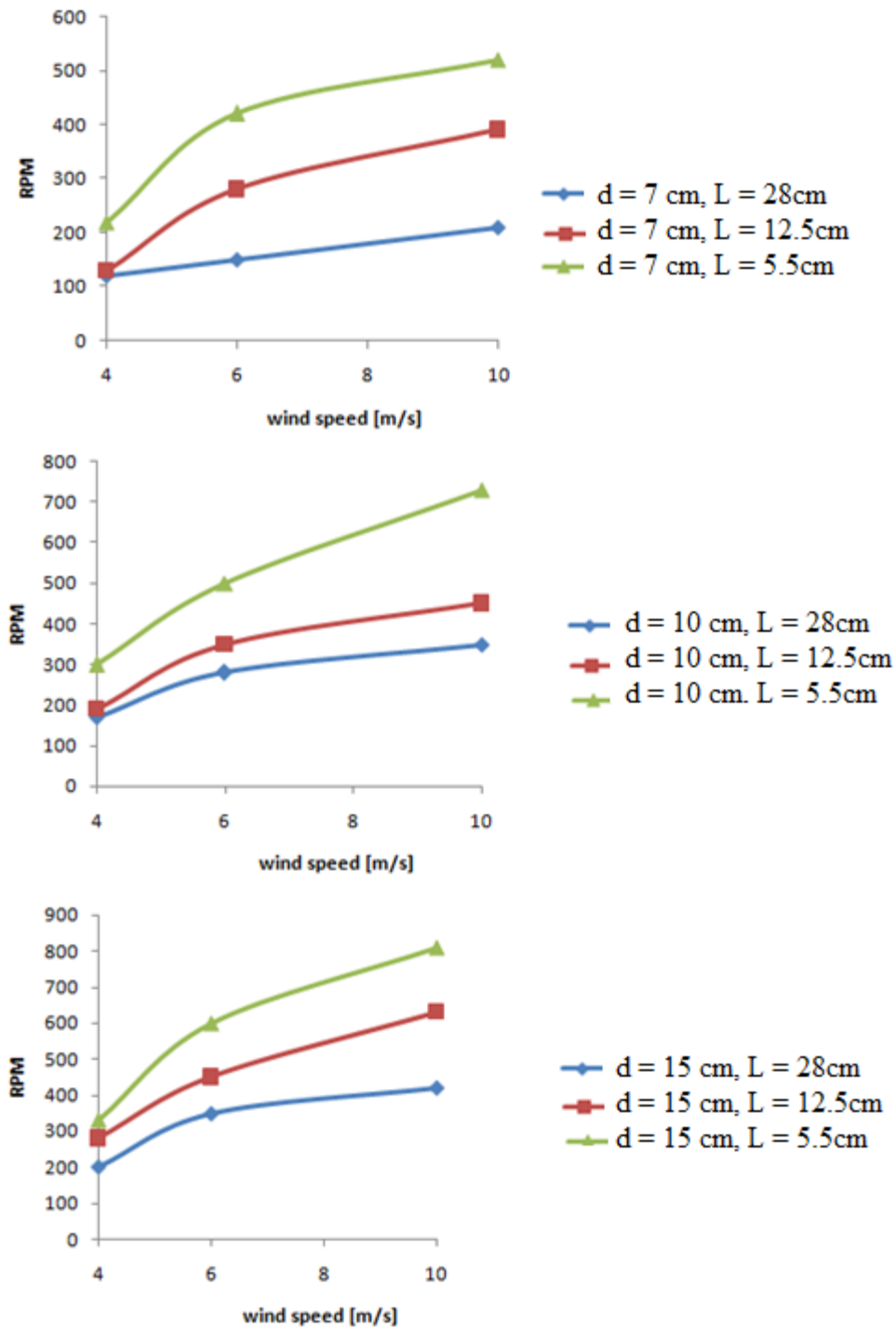


**Figure 5.8:** Torque versus Angle of rotation for different rotor radius with a fixed  $d = 7\text{cm}$ ,  $H = 40\text{cm}$  and  $V = 4\text{m/s}$

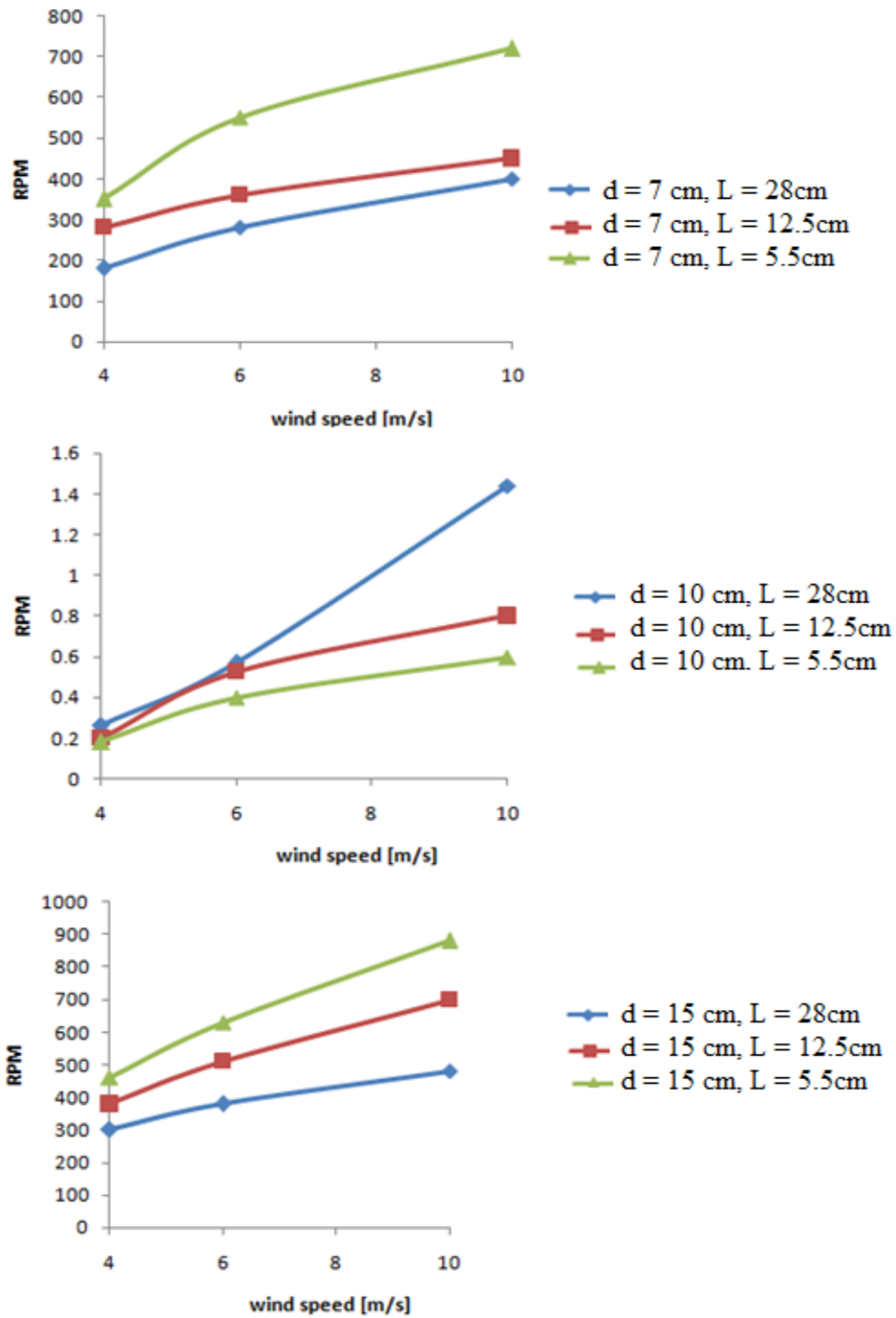
### 5.3. Relationship Between Rotor Speed and Wind Speed with Variable Blade Size and Rotor Diameter

It is instructive to investigate the relationship between rotor speed, angular rotational speed, and wind speed, and these quantities are plotted against each other in Figure 5.9 to 5.14 with different some parameters which are blade diameter, blade height, blade number and rotor radius.

For a given blade diameter, blade number and rotor radius, the rotor speed is proportional to wind speed, However, increasing the wind speed, number blades and blade size lead to increase the rotor speed of C-section blade. Additionally, the rotor speed is inversely proportional to rotor radius. Therefore, decreasing the rotor radius has adverse effects on the rotor speed.

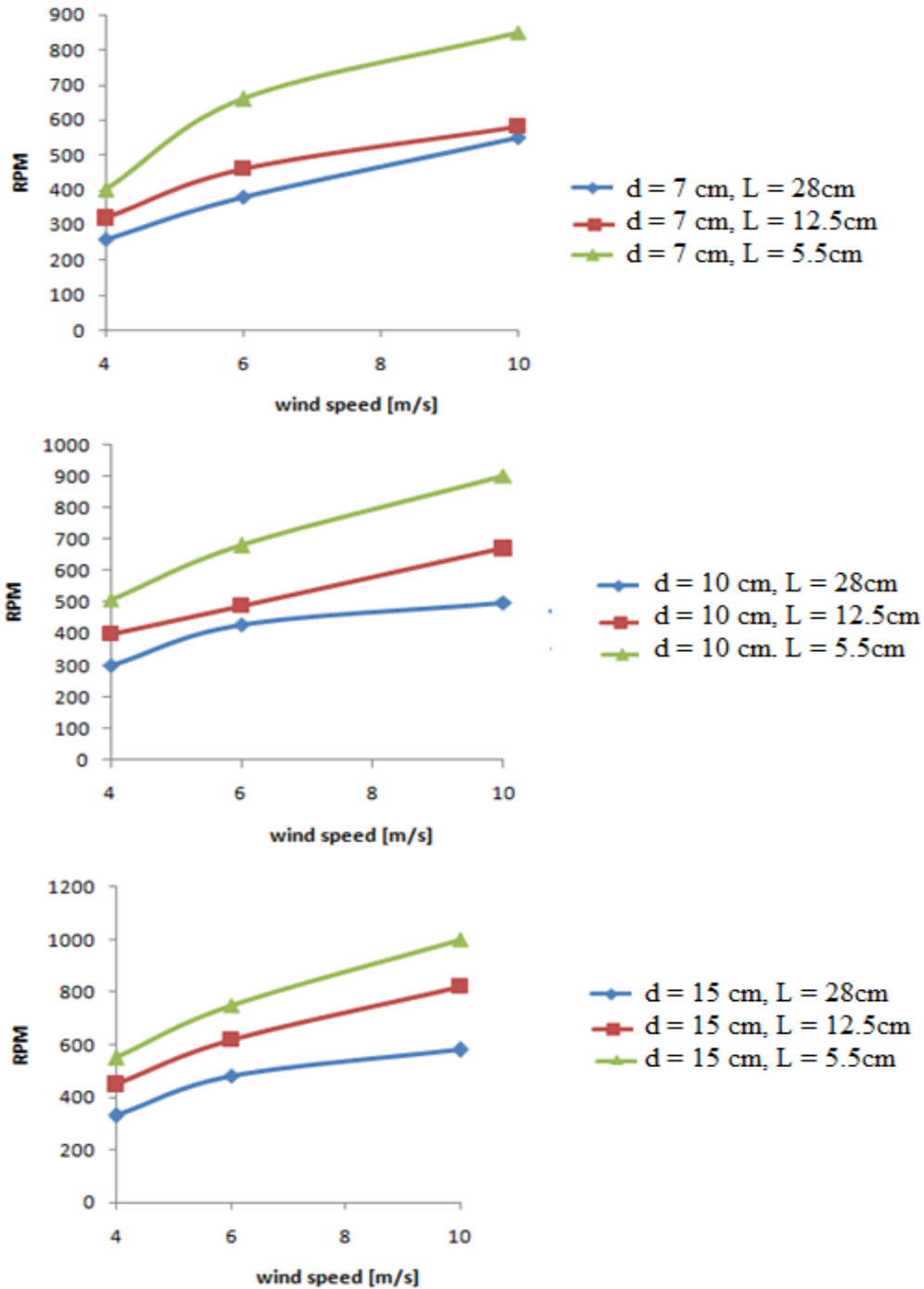


**Figure 5.9:** RPM versus wind speed for different rotor radius and blade diameter with a fixed  $H = 30$ cm and  $N = 2$  blades

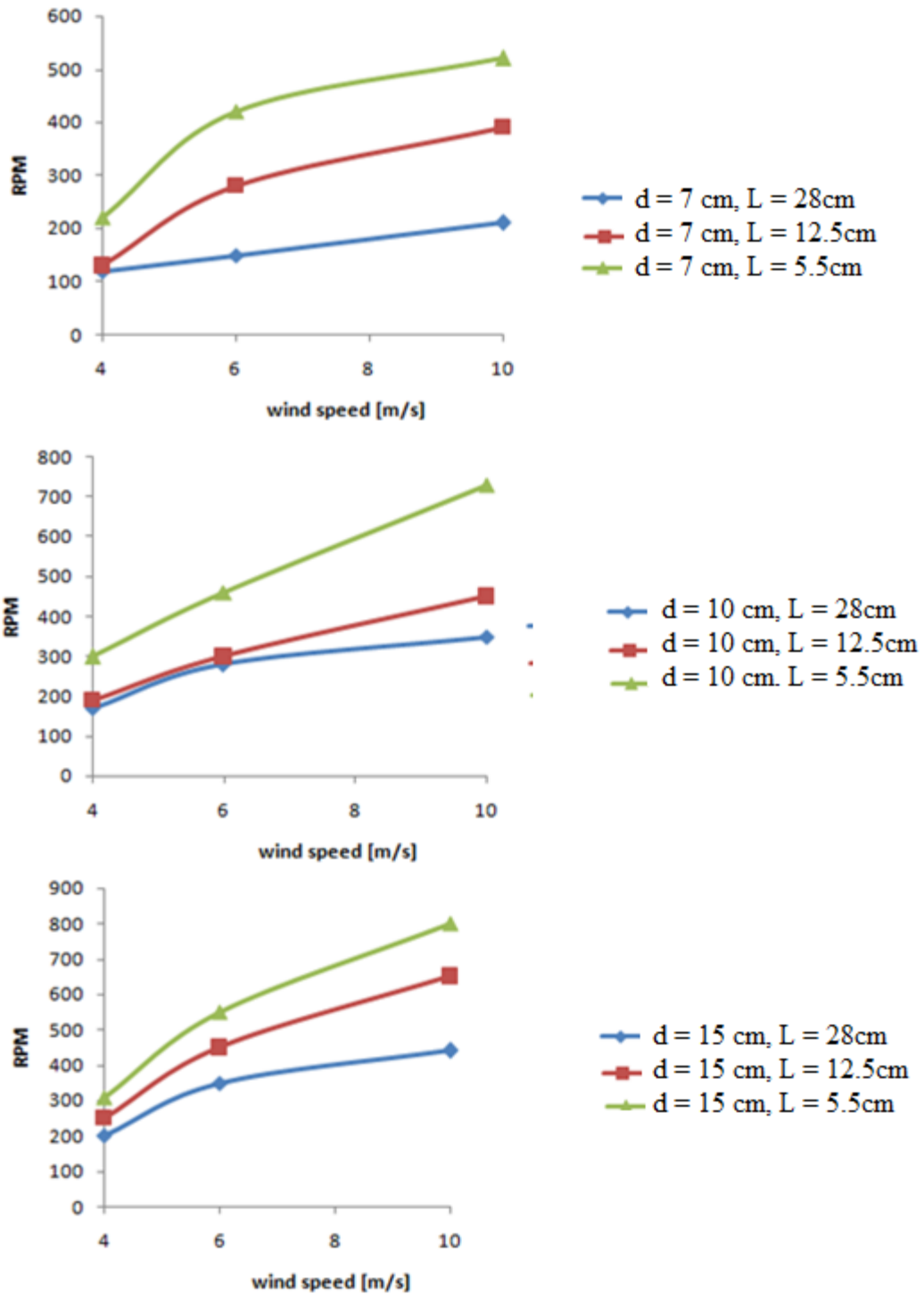


**Figure 5.10:** RPM versus wind speed for different rotor radius and blade diameter with a fixed  $H = 30\text{cm}$  and  $N = 3$  blades

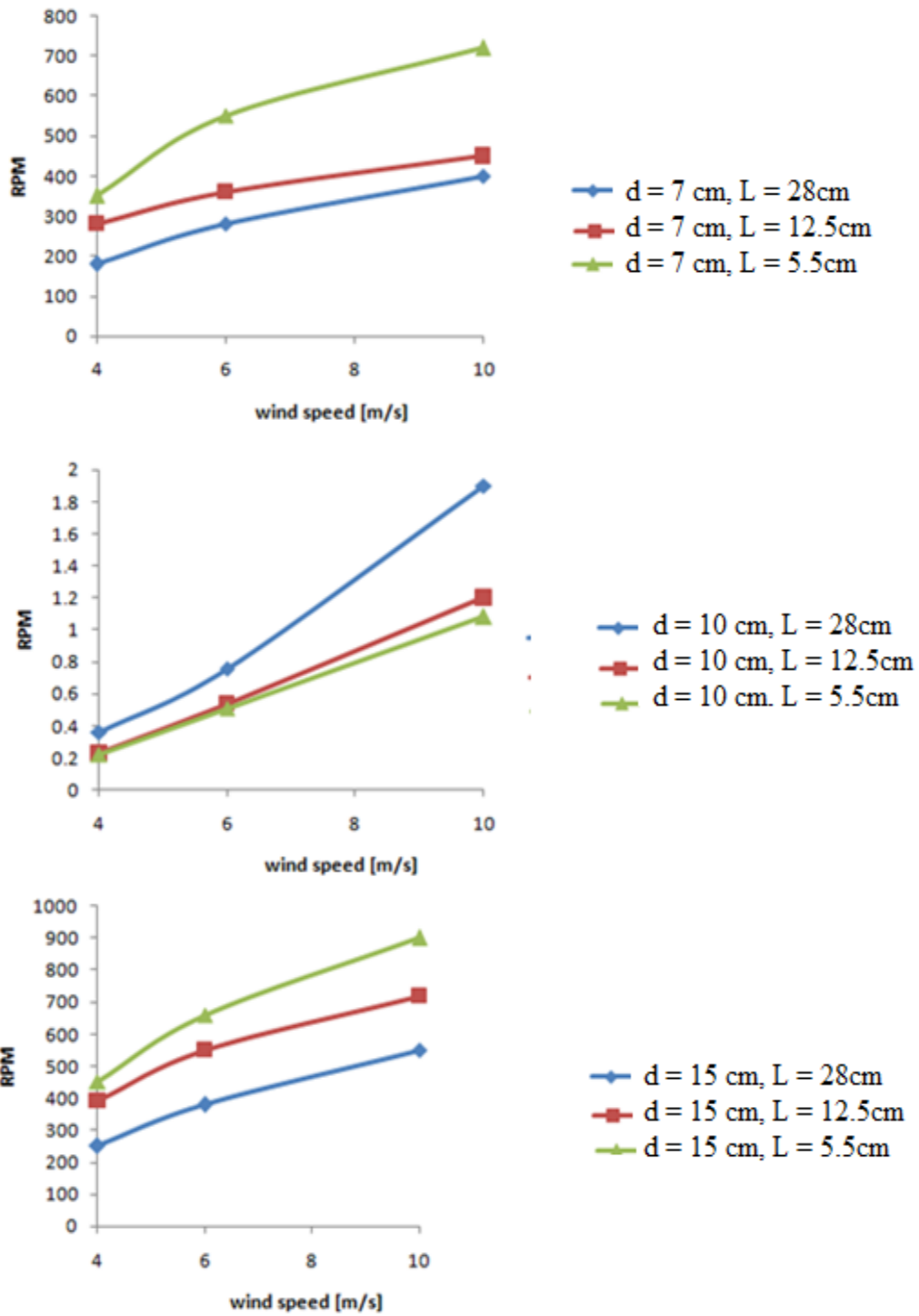




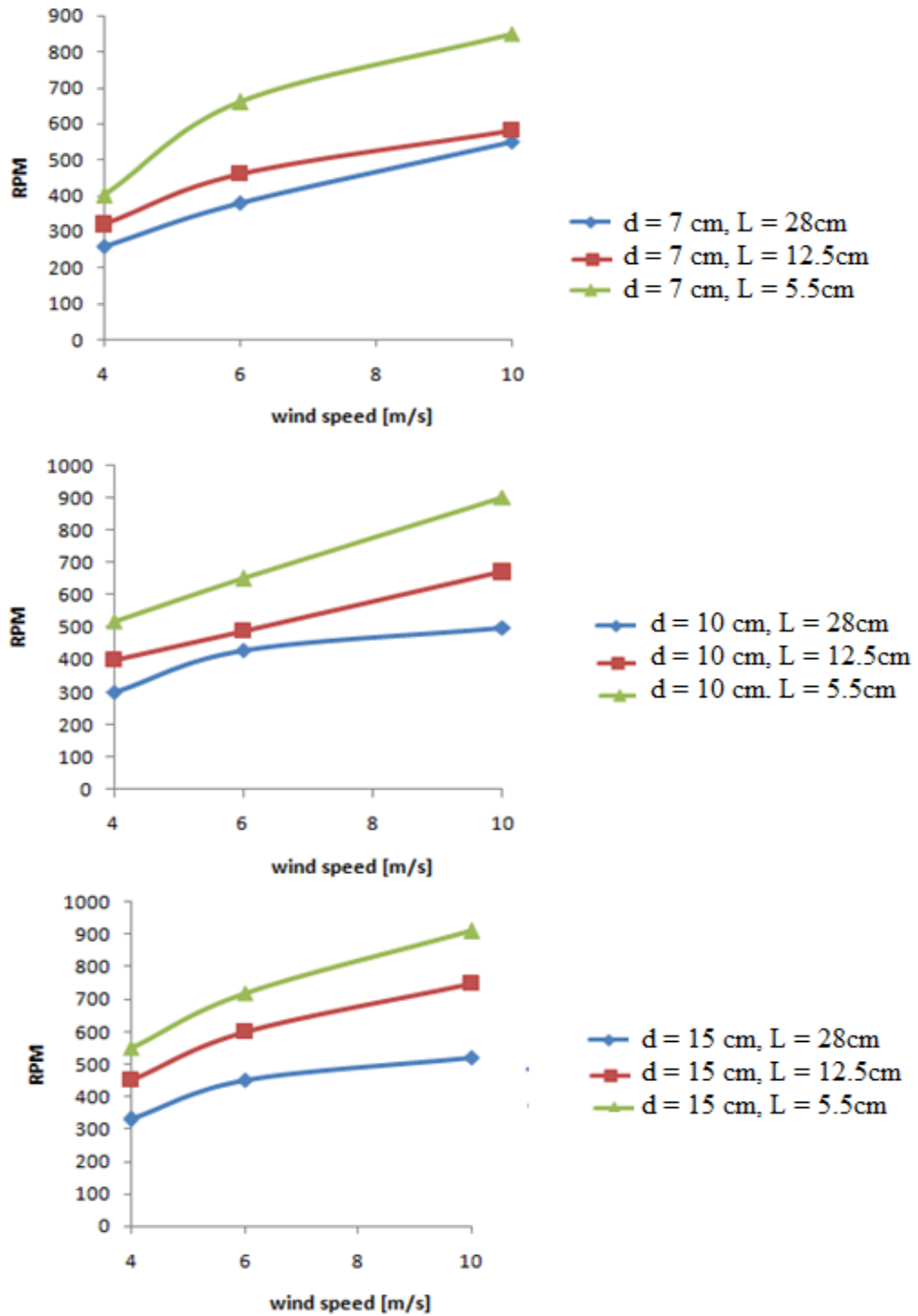
**Figure 5.11:** RPM versus wind speed for different rotor radius and blade diameter with a fixed  $H = 30\text{cm}$  and  $N = 4$  blades



**Figure 5.12:** RPM versus wind speed for different rotor radius and blade diameter with a fixed  $H = 40\text{cm}$  and  $N = 2$  blades



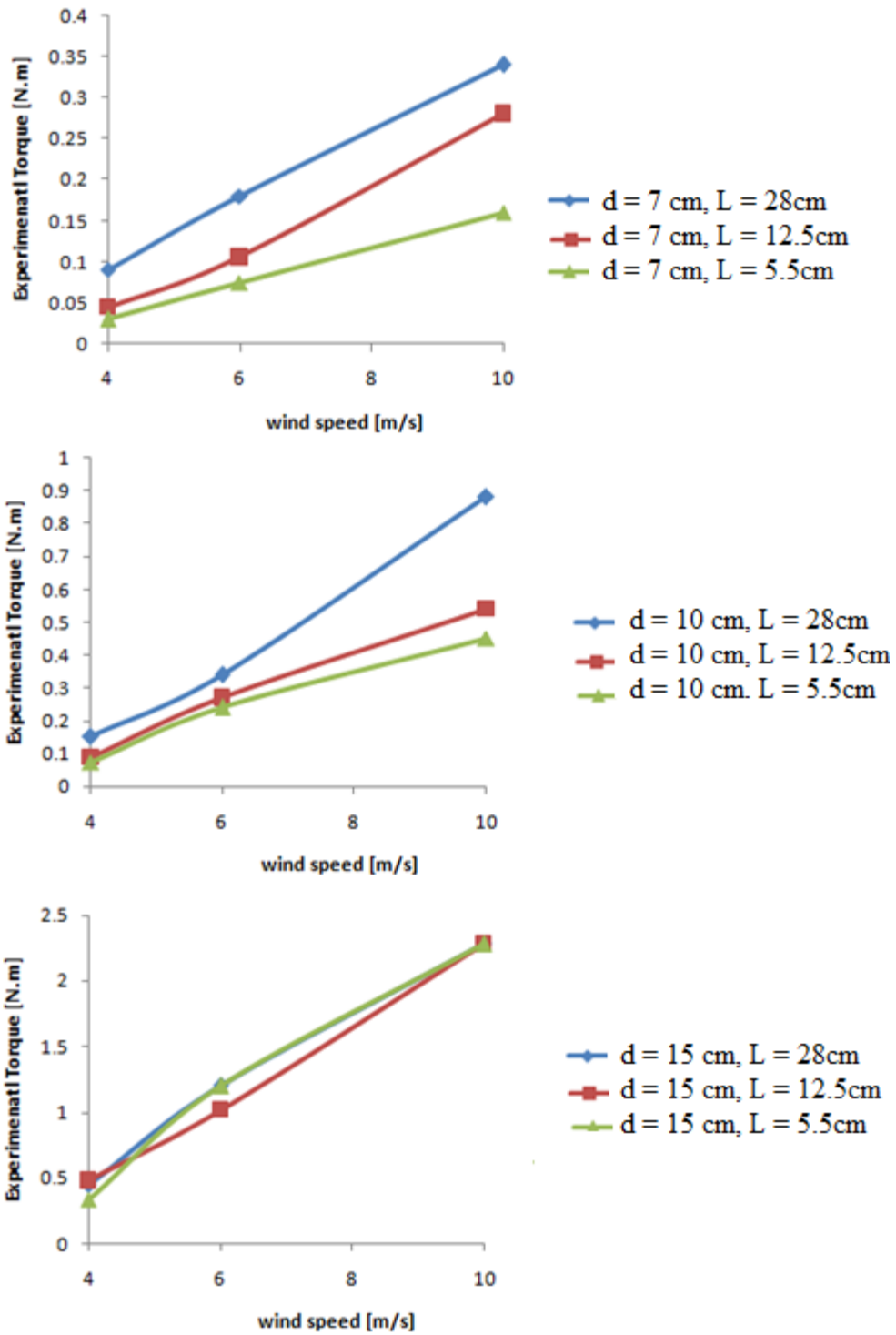
**Figure 5.13:** RPM versus wind speed for different rotor radius and blade diameter with a fixed  $H = 40\text{cm}$  and  $N = 3$  blades



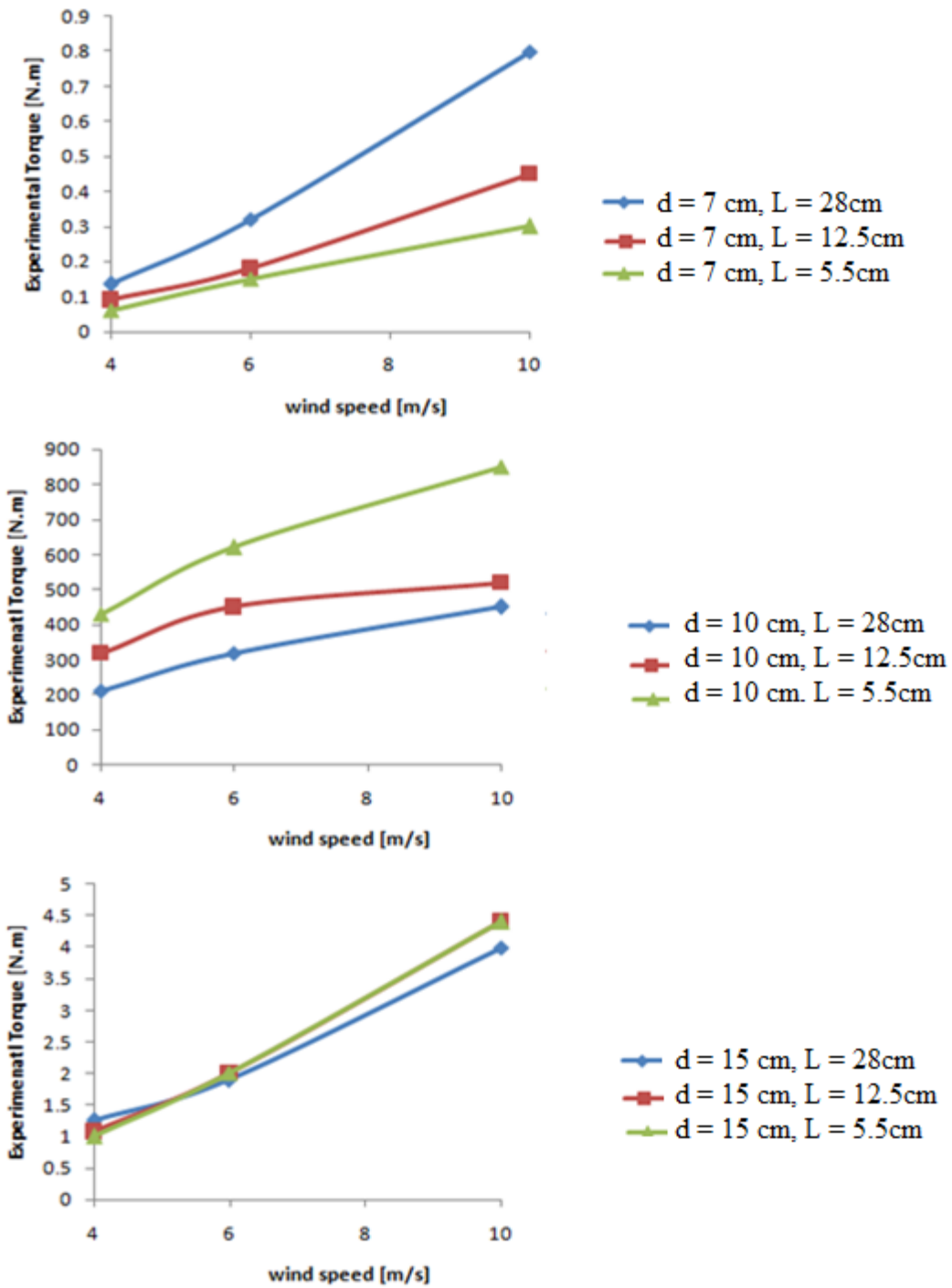
**Figure 5.14:** RPM versus wind speed for different rotor radius and blade diameter with a fixed  $H = 40\text{cm}$  and  $N = 4$  blades

#### **5.4. Relationship Between Torque and Wind Speed with Variable Blade Size and Rotor Diameter**

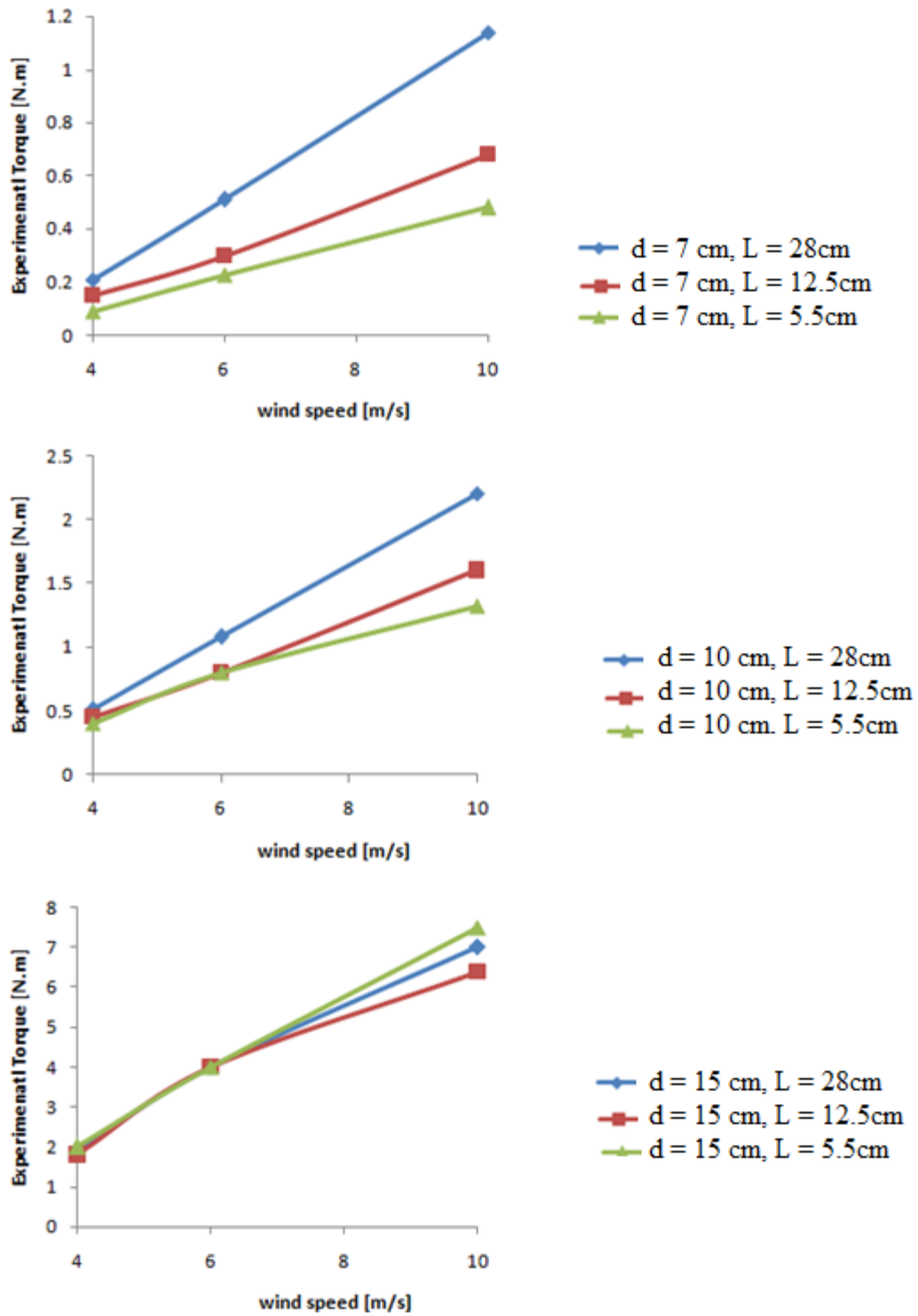
As observed in Figure 5.15 to 5.20, torque increases with increasing wind speed, blade diameter, blade height and rotor radius. It can notice that the torque increases when the blades number of C-section rotor. The author noticed that the torque is increased proportional to wind speed, blade number, blade size and rotor diameter as shown in Figure 5.15 to 5.20.



**Figure 5.15:** Torque versus wind speed for different rotor radius and blade diameter with a fixed  $H = 30\text{cm}$  and  $N = 2$  blades

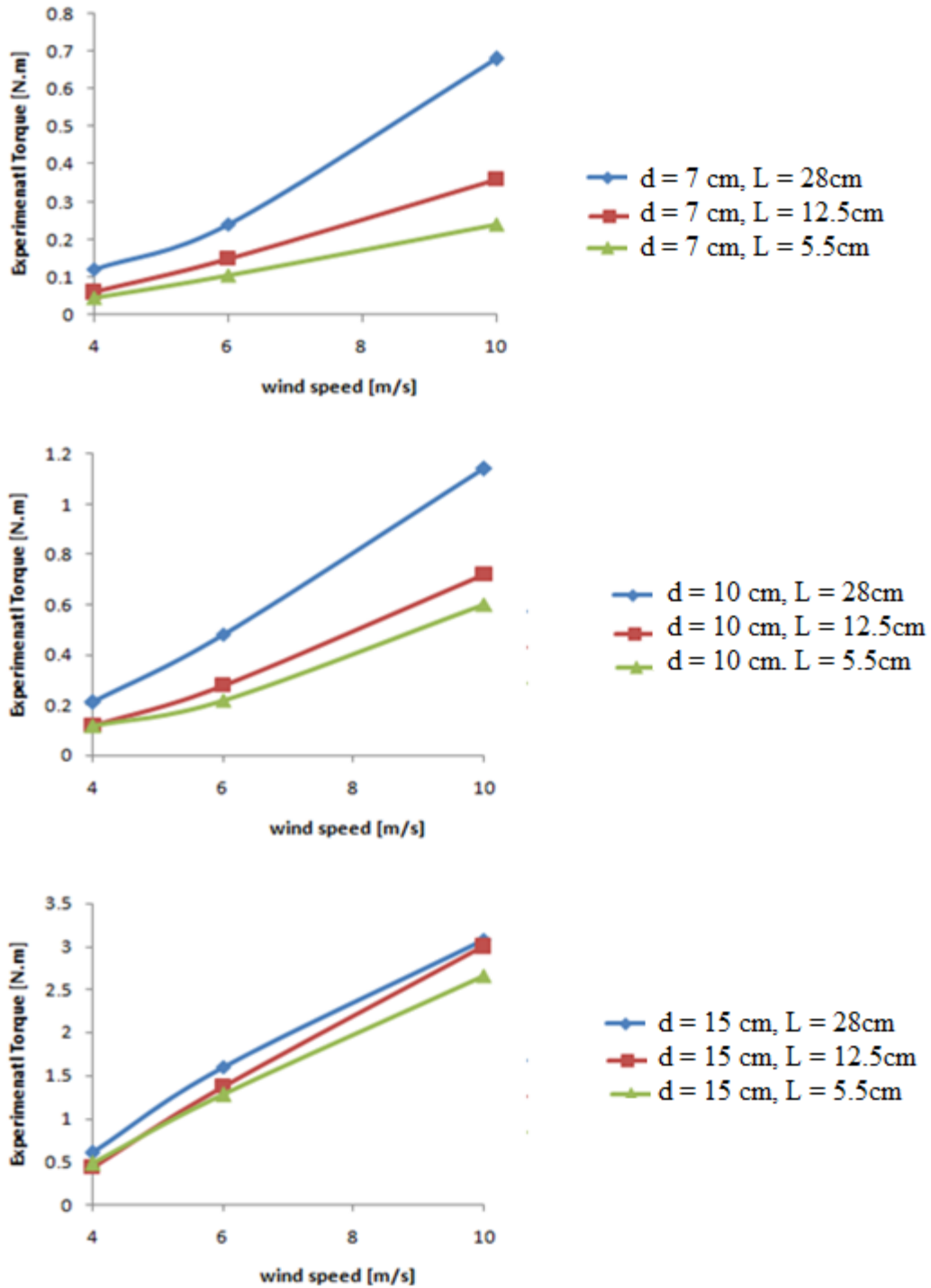


**Figure 5.16:** Torque versus wind speed for different rotor radius and blade diameter with a fixed  $H = 30\text{cm}$  and  $N = 3$  blades

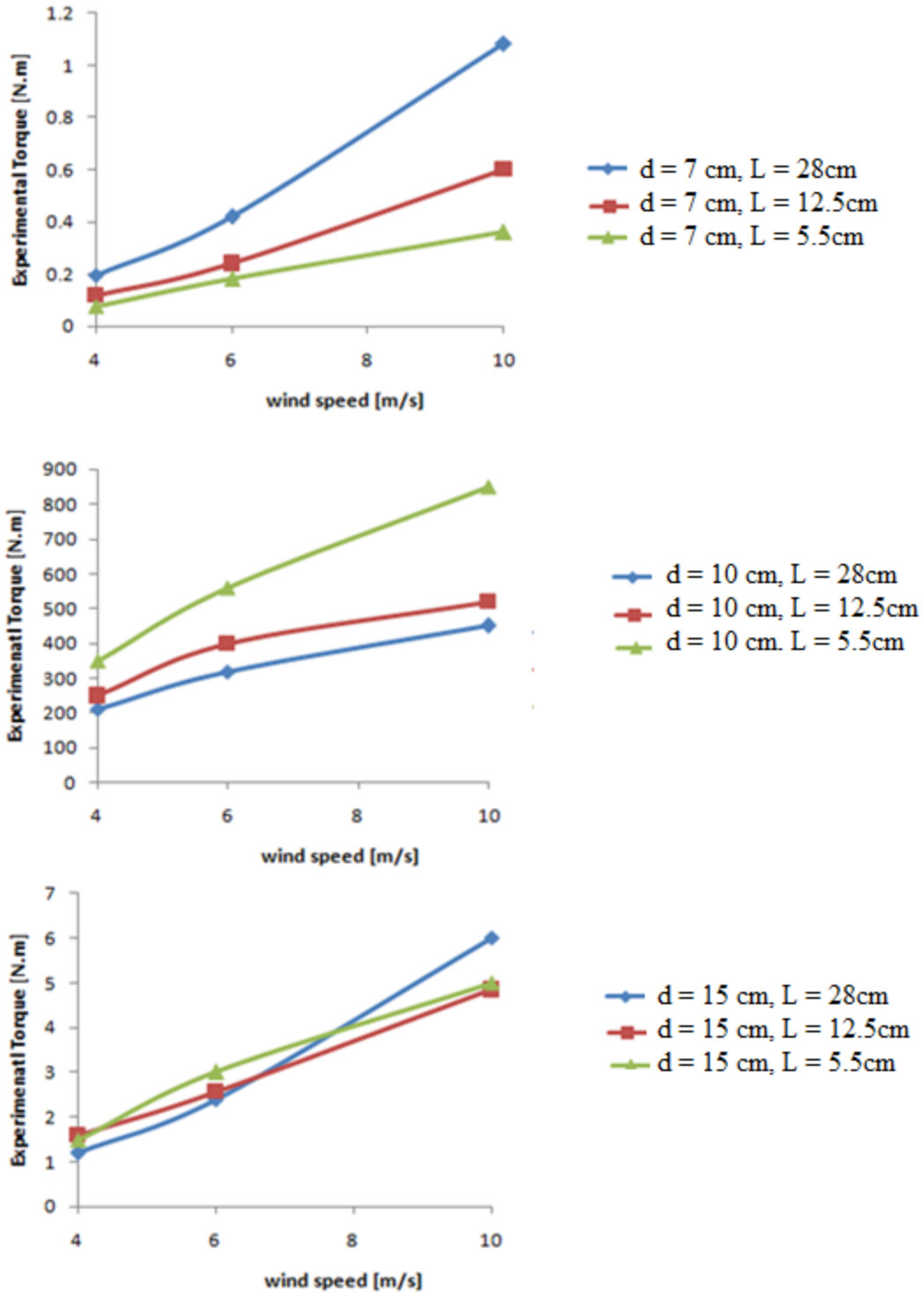


**Figure 5.17:** Torque versus wind speed for different rotor radius and blade diameter with a fixed  $H = 30\text{cm}$  and  $N = 4$  blades

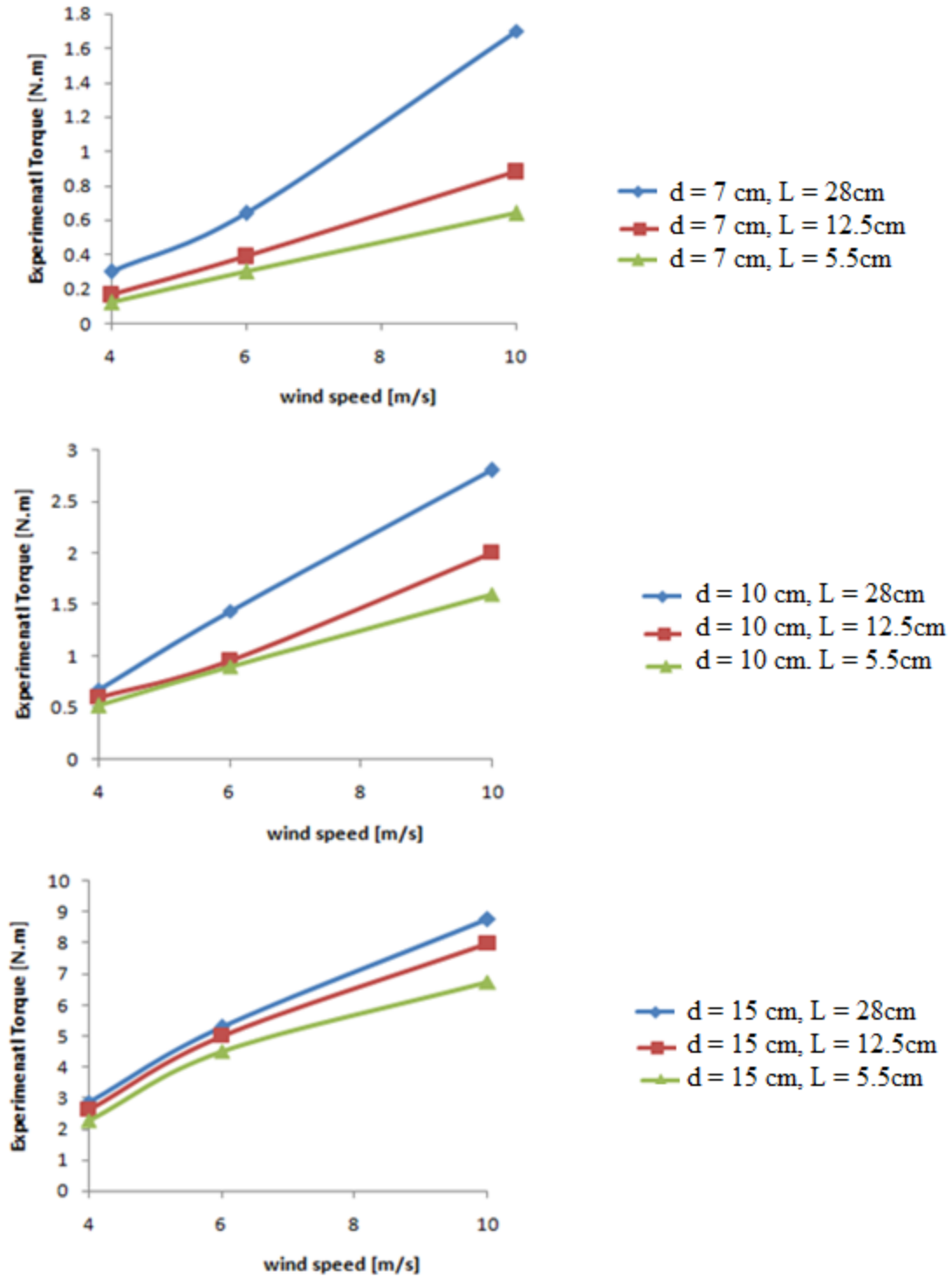




**Figure 5.18:** Torque versus wind speed for different rotor radius and blade diameter with a fixed  $H = 40\text{cm}$  and  $N = 2$  blades



**Figure 5.19:** Torque versus wind speed for different rotor radius and blade diameter with a fixed  $H = 40\text{cm}$  and  $N = 3$  blades



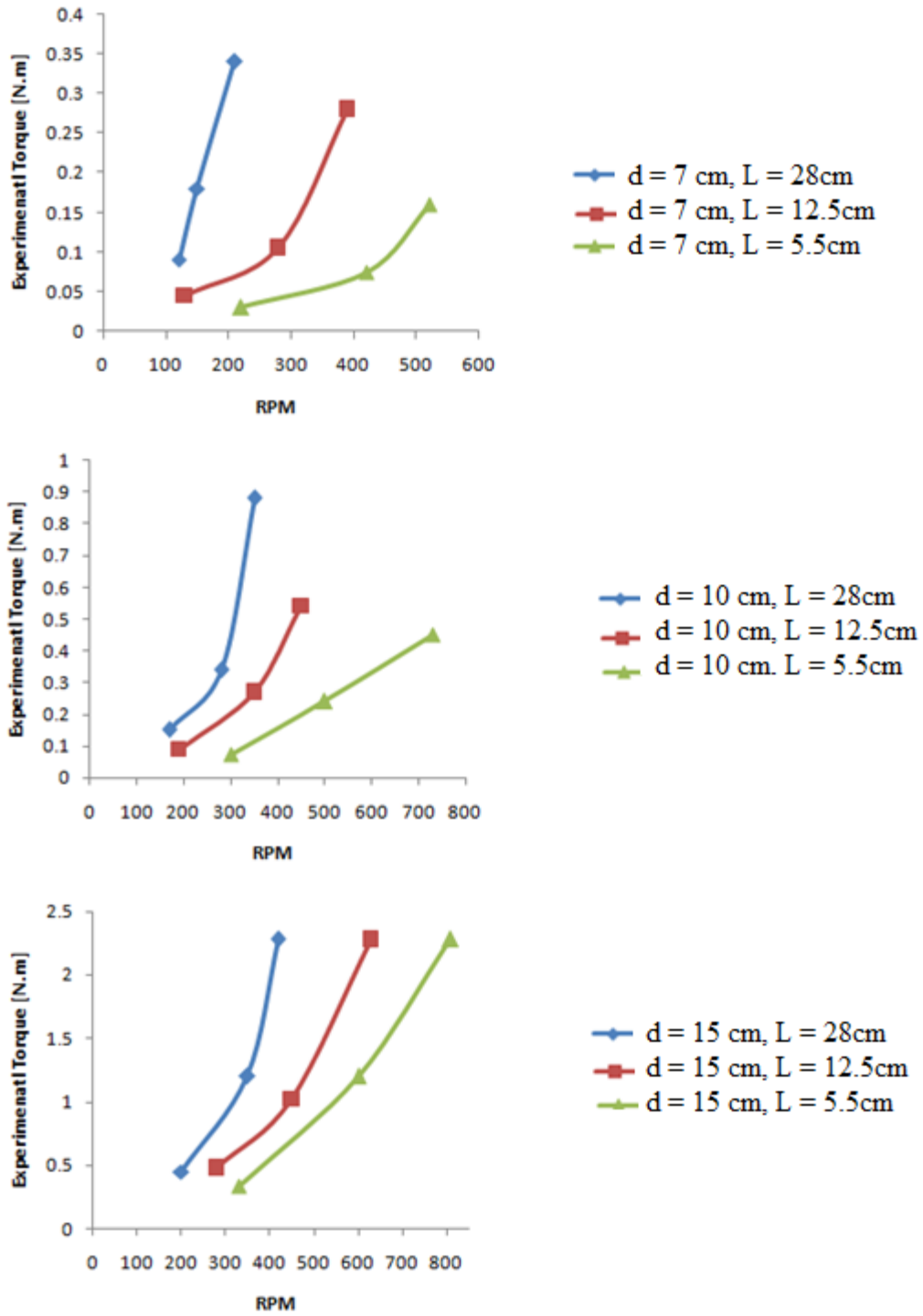
**Figure 5.20:** Torque versus wind speed for different rotor radius and blade diameter with a fixed  $H = 40\text{cm}$  and  $N = 4$  blades

## **5.5. Relationship between Torque and Rotor Speed with Variable Blade Size and Rotor Diameter**

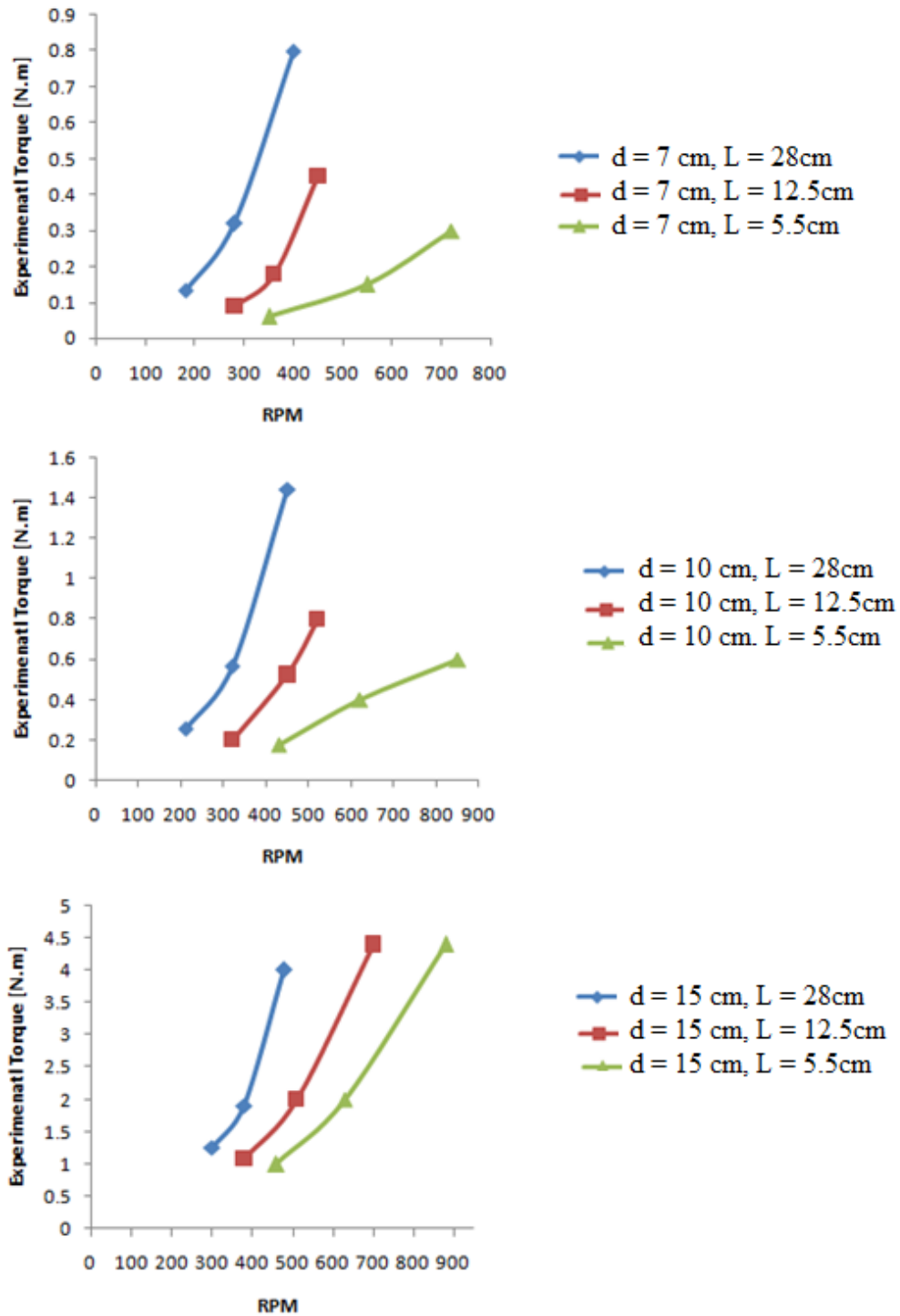
Figures 5.21 to 5.26 show the relationship between torque and rotor speed, RPM, at different blade size and rotor radius. The torque decreases as the rotor speed, RPM, with the C-section rotor increase. Additionally, they show that the increasing blade number, blade size leads to increase RPM and Torque. Whereas, RPM increased when the rotor radius of the C-section rotor decreases. However, the torque is inversely proportional to rotor speed,  $\text{RPM}^2$ . However, at constant blade size and blade number, when the torque of C-section rotor increases, the rotational speed, RPM, decreases as shown in Figures 5.21 to 5.26.

---

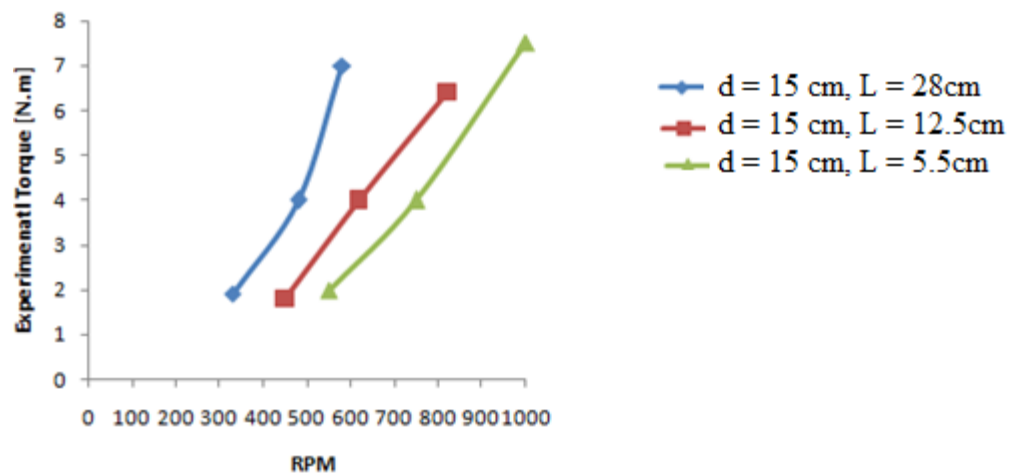
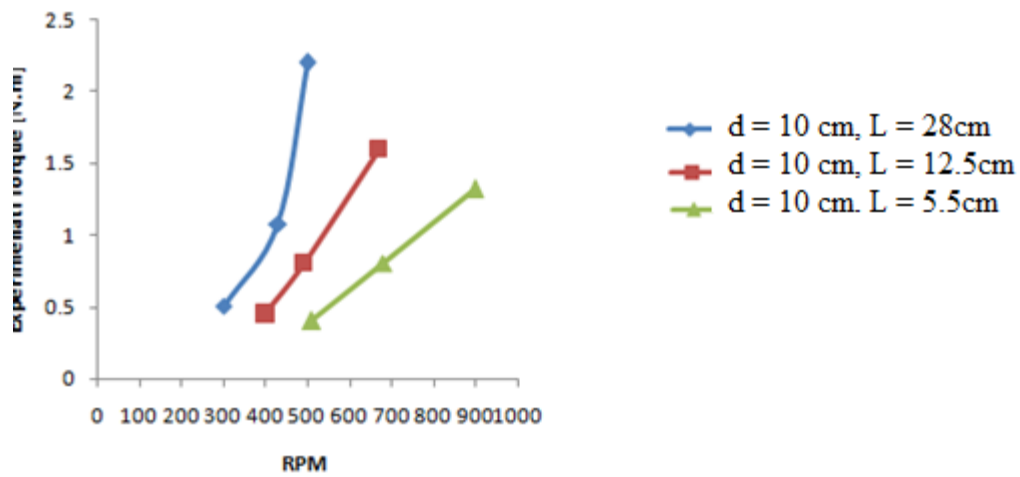
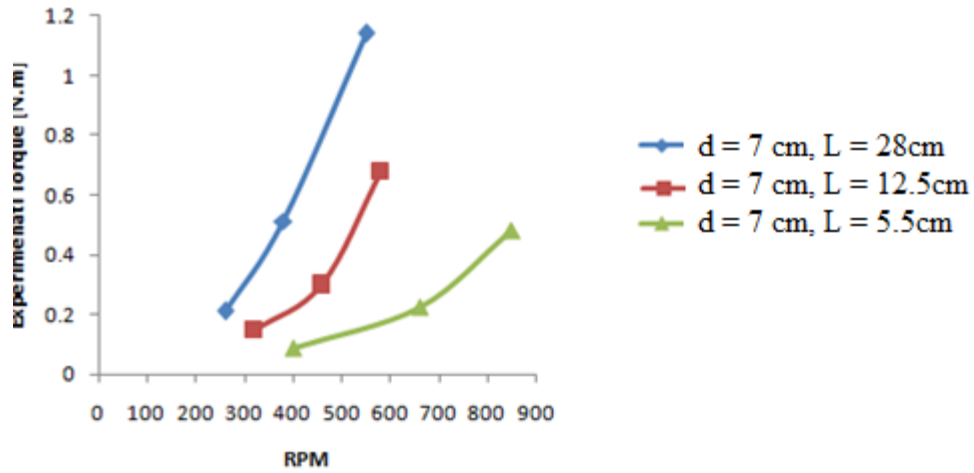
<sup>2</sup> The relationship between rotational speed and torque as in references [46]



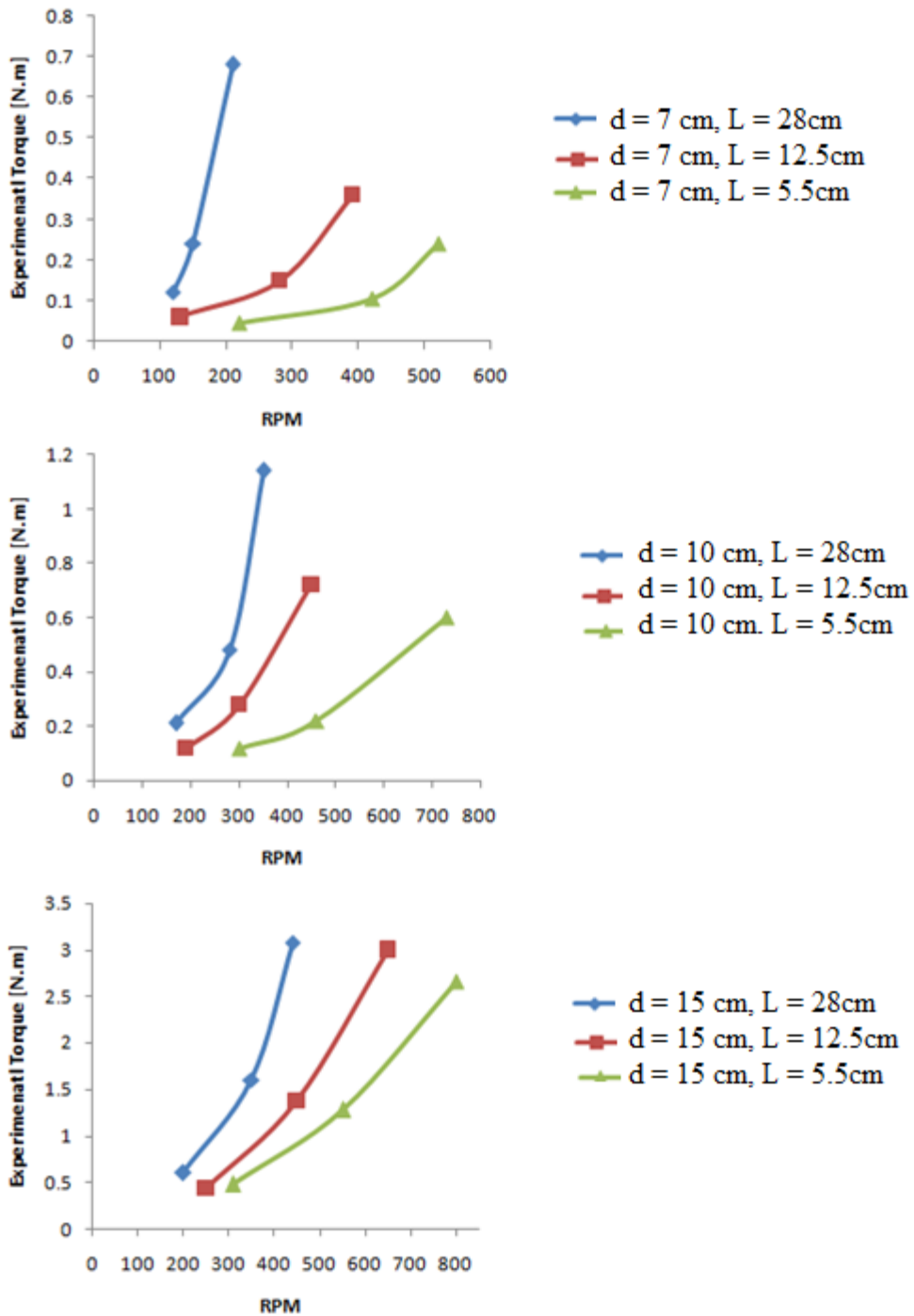
**Figure 5.21:** Torque versus Rotor speed, RPM, for different rotor radius and blade diameter with  $H = 30\text{cm}$  and  $N = 2$  blades



**Figure 5.22:** Torque versus Rotor speed, RPM, for different rotor radius and blade diameter with  $H = 30\text{cm}$  and  $N = 3$  blades

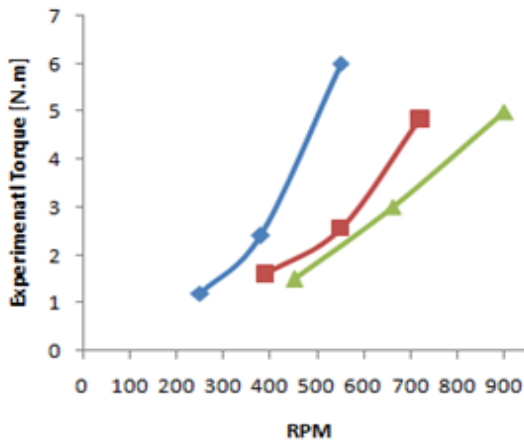
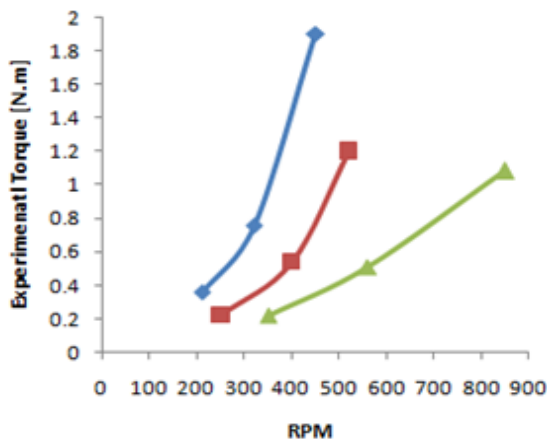
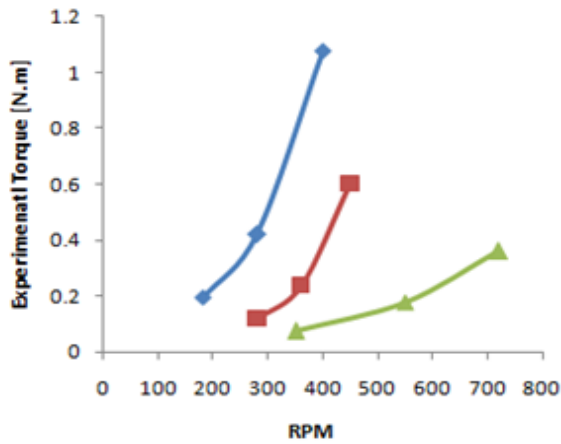


**Figure 5.23:** Torque versus Rotor speed, RPM, for different rotor radius and blade diameter with  $H = 30\text{cm}$  and  $N = 4$  blades

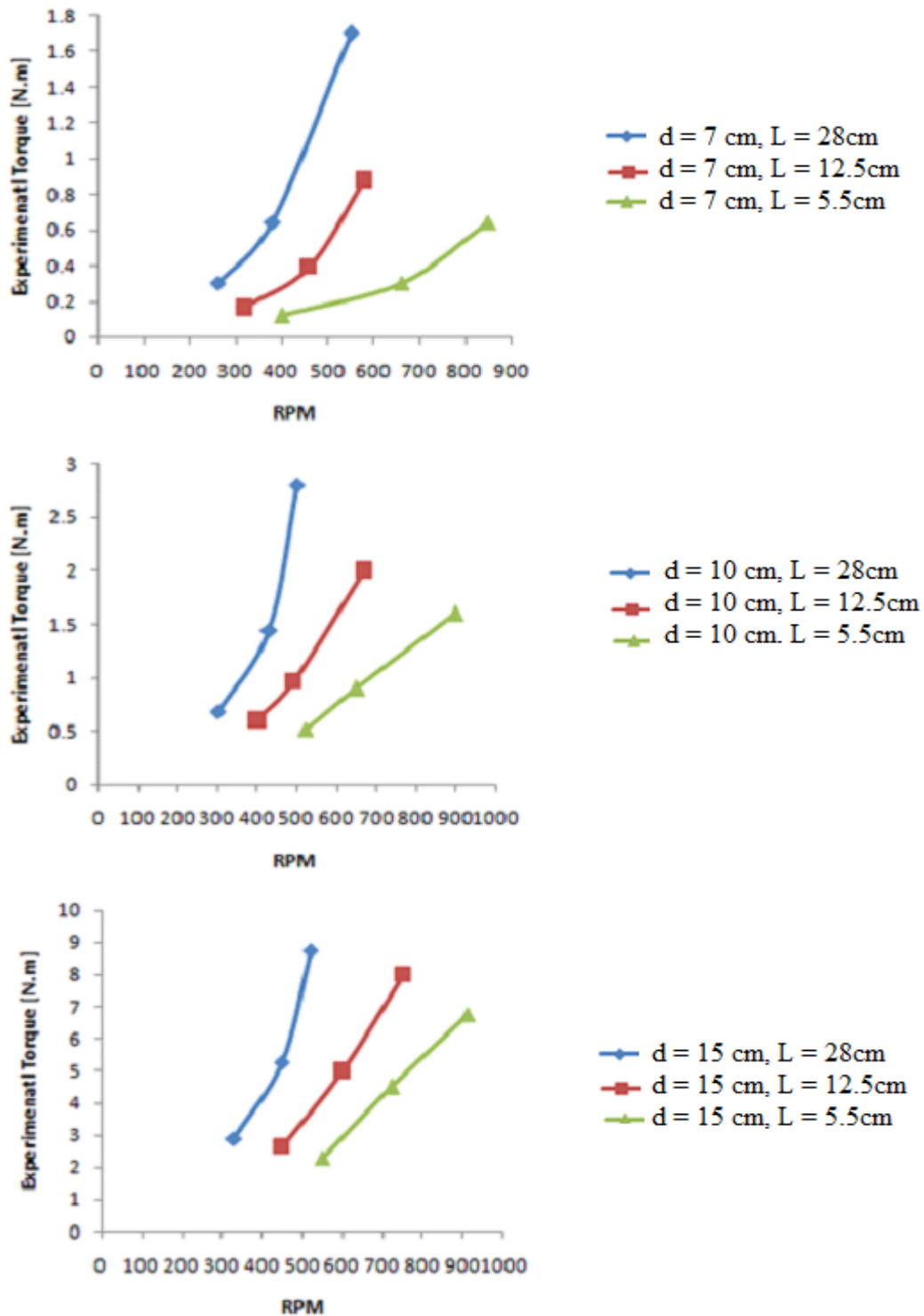


**Figure 5.24:** Torque versus Rotor speed, RPM, for different rotor radius and blade diameter with  $H = 40\text{cm}$  and  $N = 2$  blades





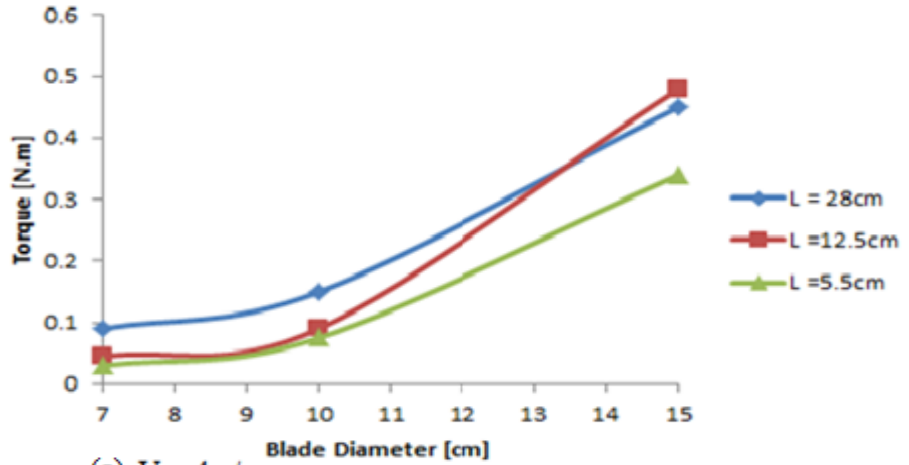
**Figure 5.25:** Torque versus Rotor speed, RPM, for different rotor radius and blade diameter with  $H = 40\text{cm}$  and  $N = 3$  blades



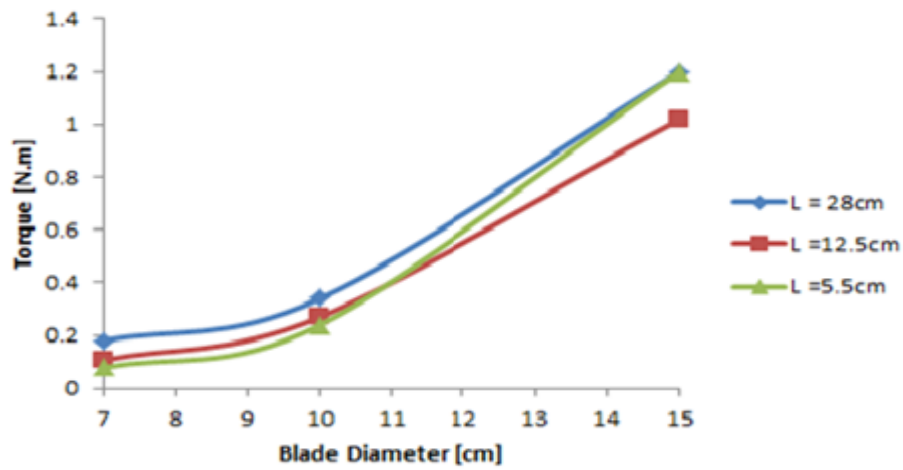
**Figure 5.26:** Torque versus Rotor speed, RPM, for different rotor radius and blade diameter with  $H = 40\text{cm}$  and  $N = 4$  blades

### 5.6 Relationship between Torque and Blade Diameter with Variable Blade Height, Wind Speed and Rotor Diameter

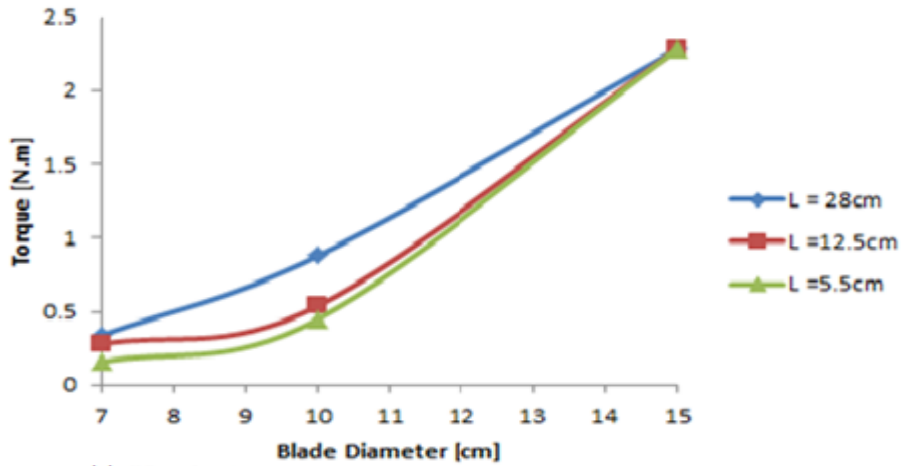
Figures 5.27 to 5.31 show the relationship between torque and blade diameter at different blade height and rotor radius. The torque increases as the blade diameters of C-section rotor increase. Additionally, they show that the increasing blade number, blade height and wind speed lead to increase the torque of C-section vertical axis wind turbine. However, the torque is proportional to blade size, wind speed and number of blade. Also, at constant blade height, wind speed and blade number, when the blade diameter increases, the torque of C-section rotor will increase as shown in Figures 5.27 to 5.31.



(a)  $V = 4\text{m/s}$

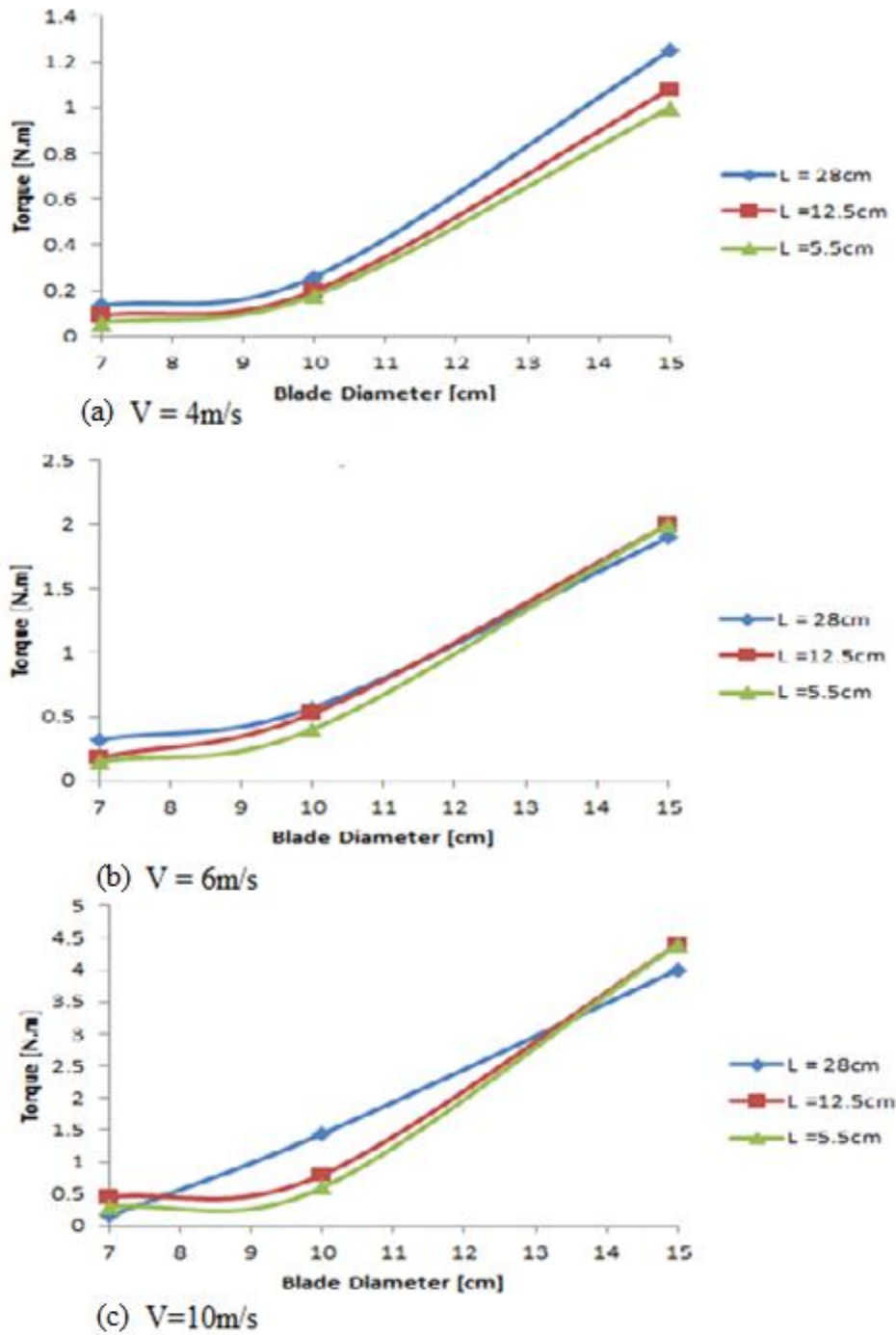


(b)  $V = 6\text{m/s}$

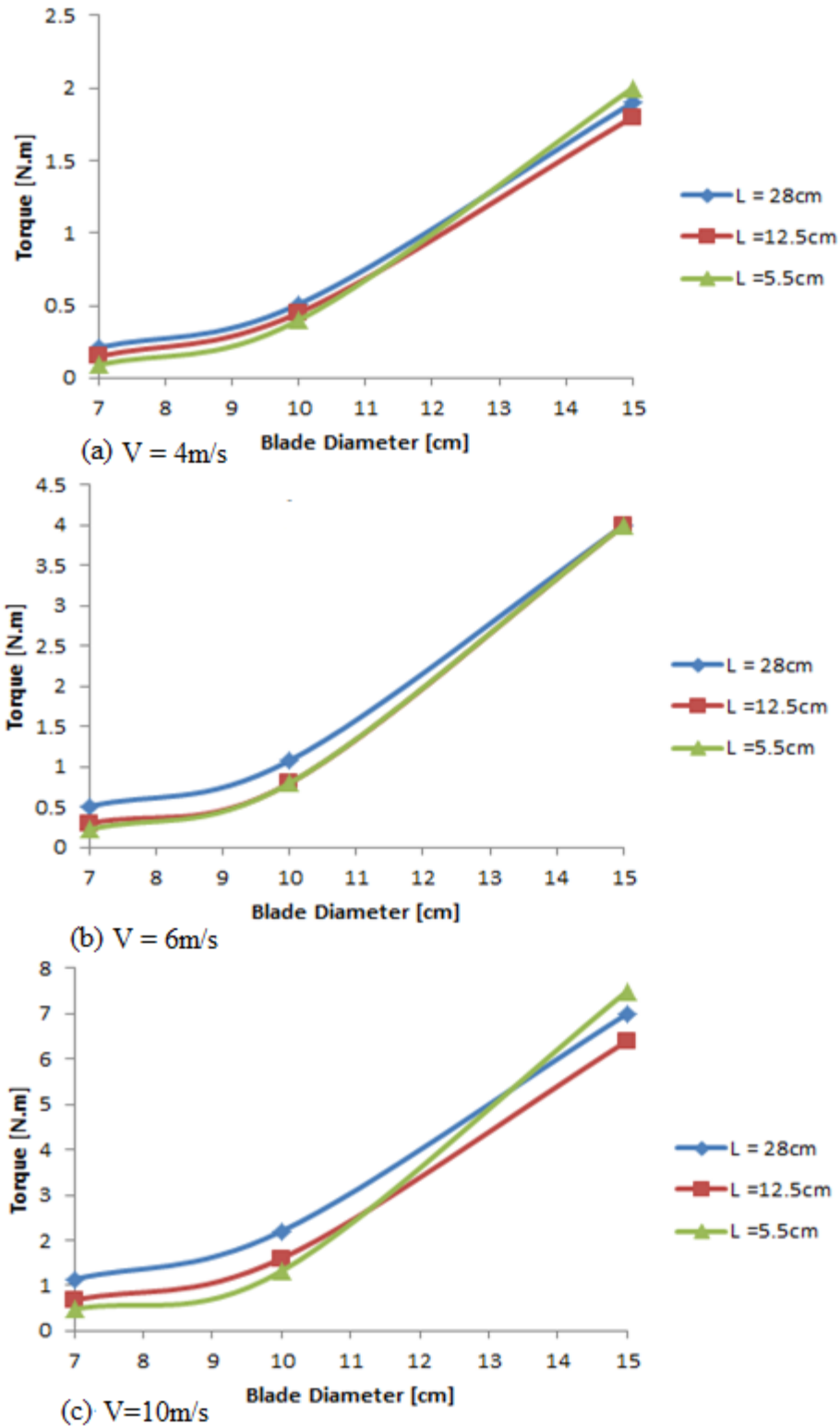


(c)  $V = 10\text{m/s}$

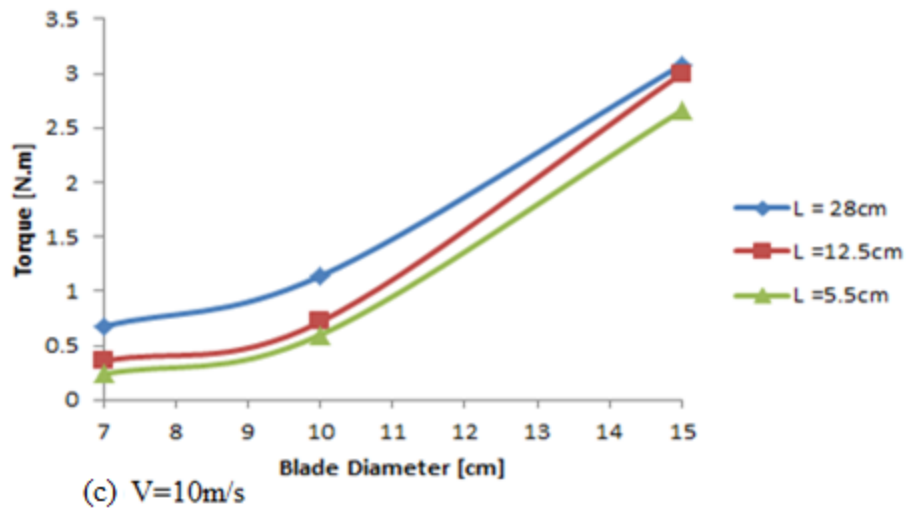
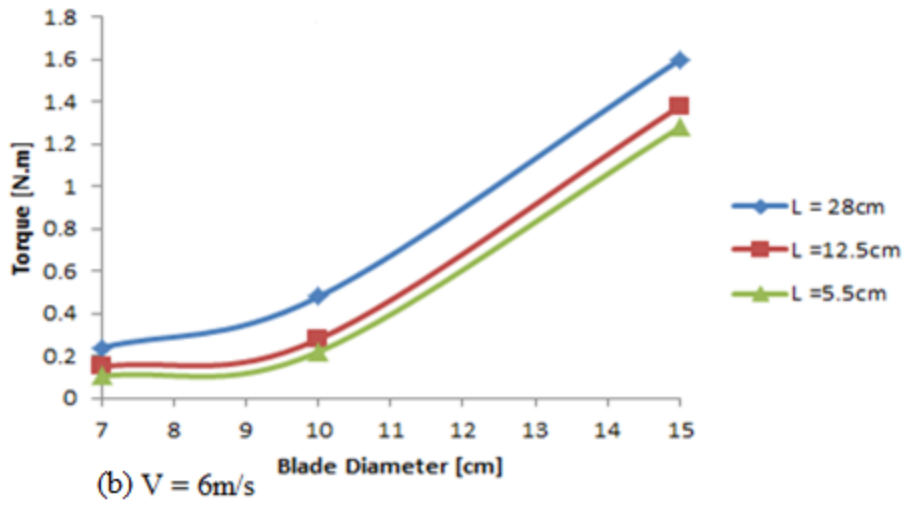
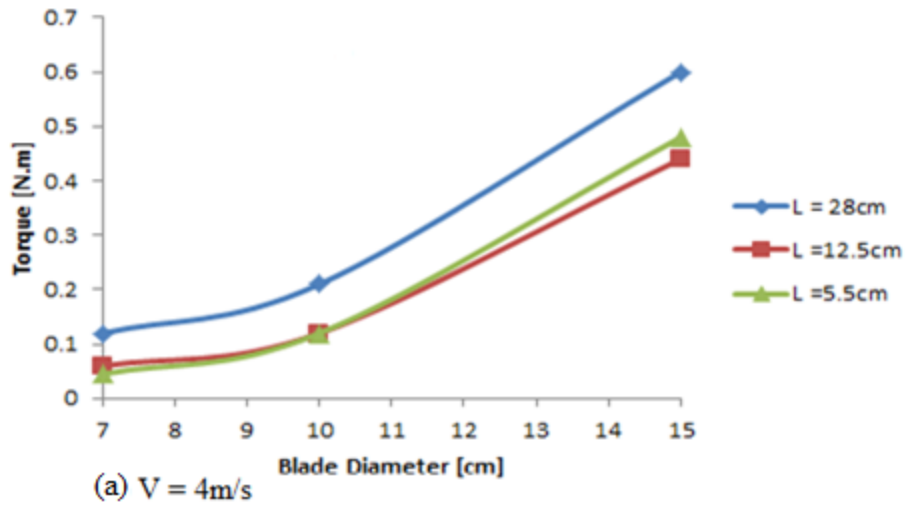
**Figure 5.27:** Torque versus blade diameter for different rotor radius with fixed  $H = 30\text{ cm}$  and  $N = 2$  blades



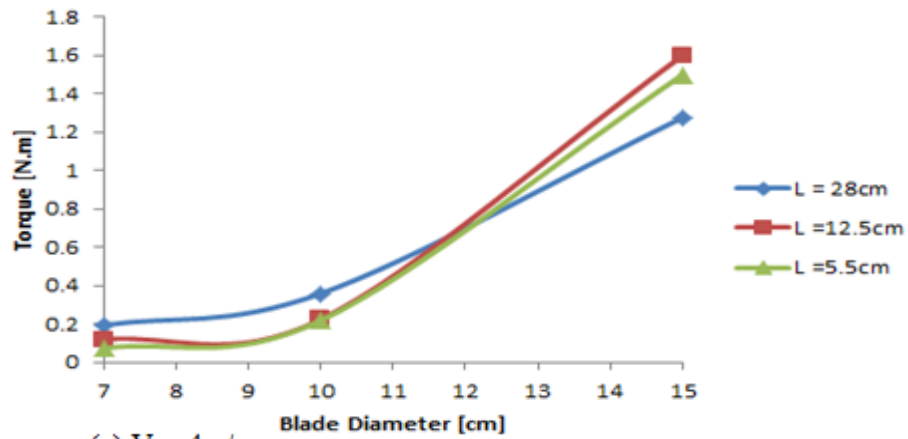
**Figure 5.28:** Torque versus blade diameter for different rotor radius with fixed  $H = 30$  cm and  $N = 3$  blades



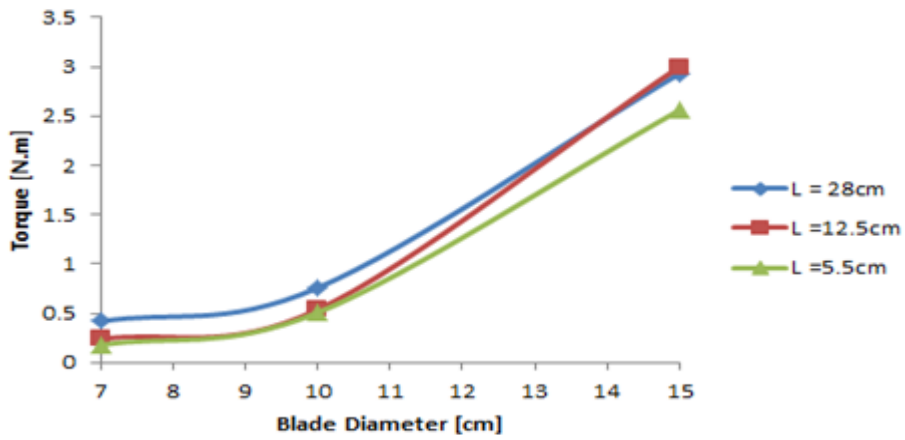
**Figure 5.29:** Torque versus blade diameter for different rotor radius with fixed  $H = 30\text{ cm}$  and  $N = 4$  blades



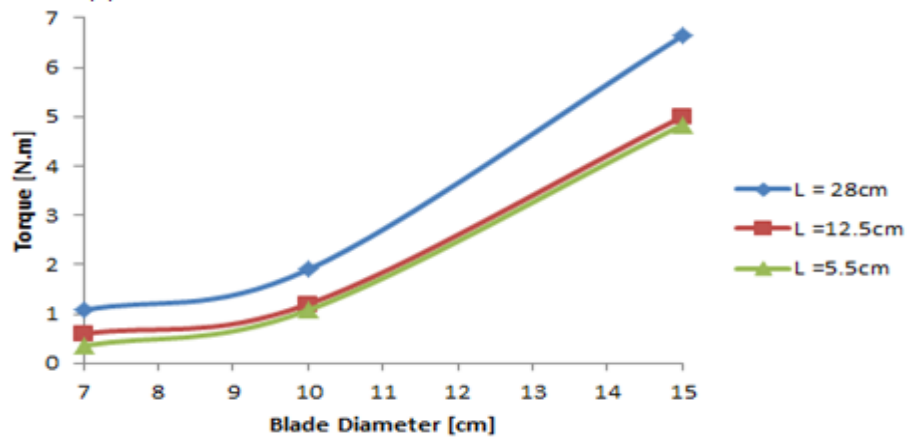
**Figure 5.30:** Torque versus blade diameter for different rotor radius with fixed  $H = 40\text{ cm}$  and  $N = 2$  blades



(a)  $V = 4\text{m/s}$



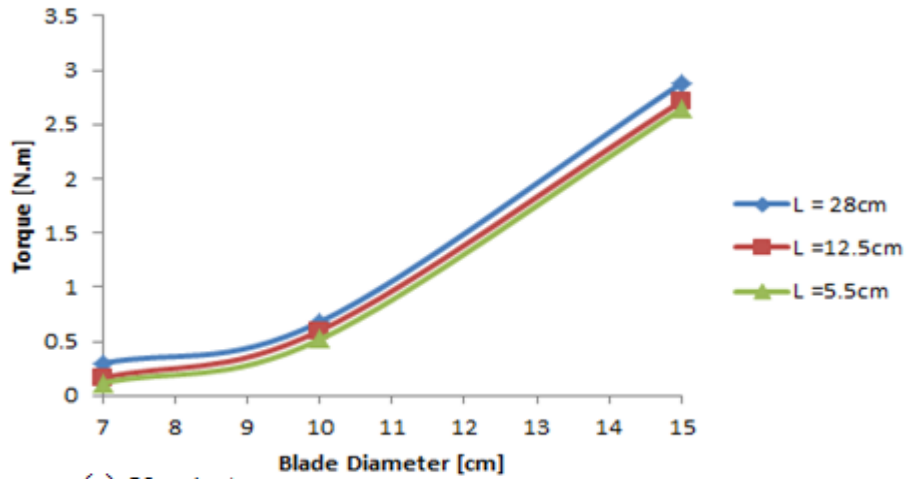
(b)  $V = 6\text{m/s}$



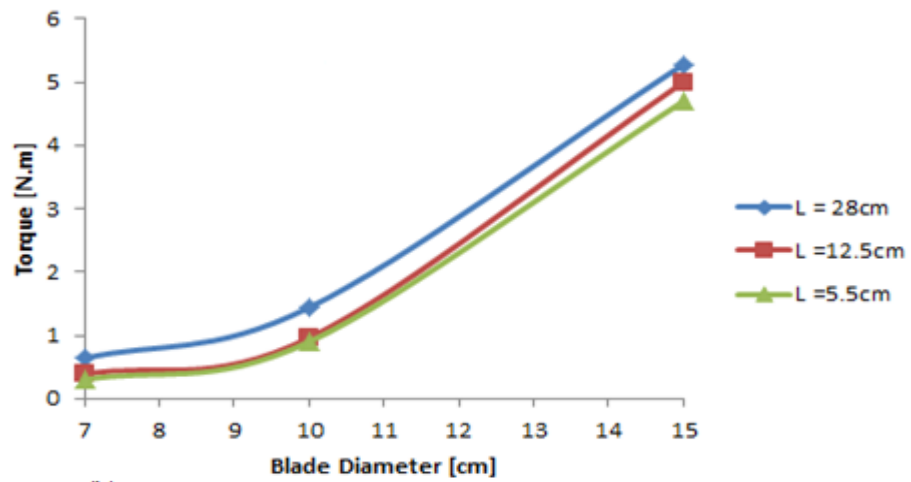
(c)  $V = 10\text{m/s}$

**Figure 5.31:** Torque versus blade diameter for different rotor radius with fixed  $H = 40\text{ cm}$  and  $N = 3$  blades

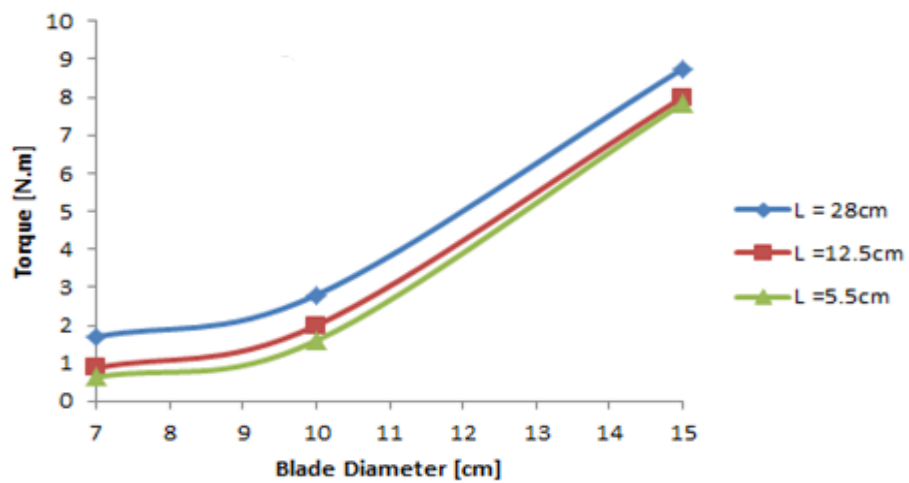




(a)  $V = 4\text{m/s}$



(b)  $V = 6\text{m/s}$



(c)  $V = 10\text{m/s}$

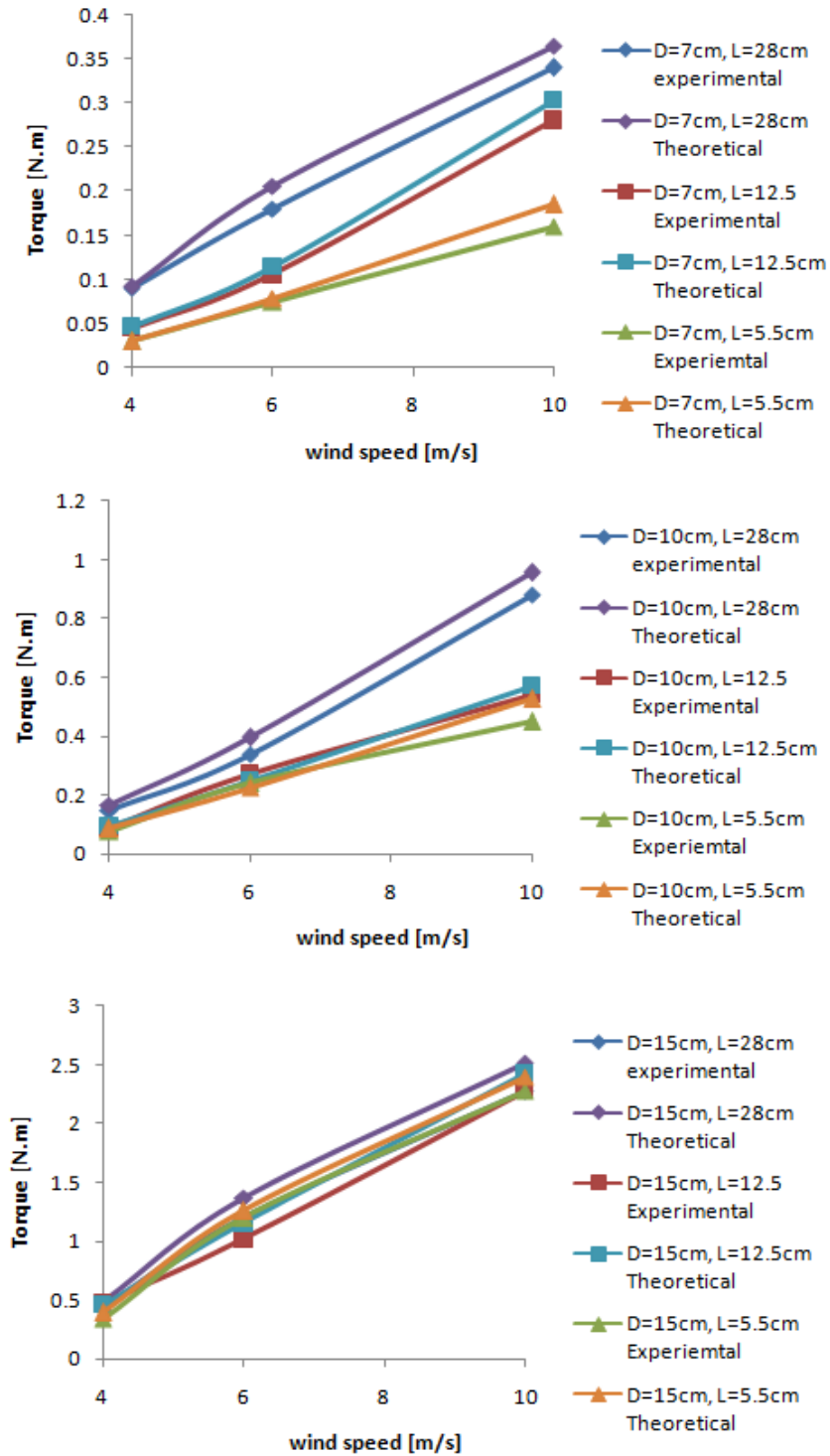
**Figure 5.32:** Torque versus blade diameter for different rotor radius with fixed  $H = 40\text{ cm}$  and  $N = 4$  blades;

## 5.7 Comparison of Theoretical Study and Experimental Torque of C-section Wind Turbine Rotor

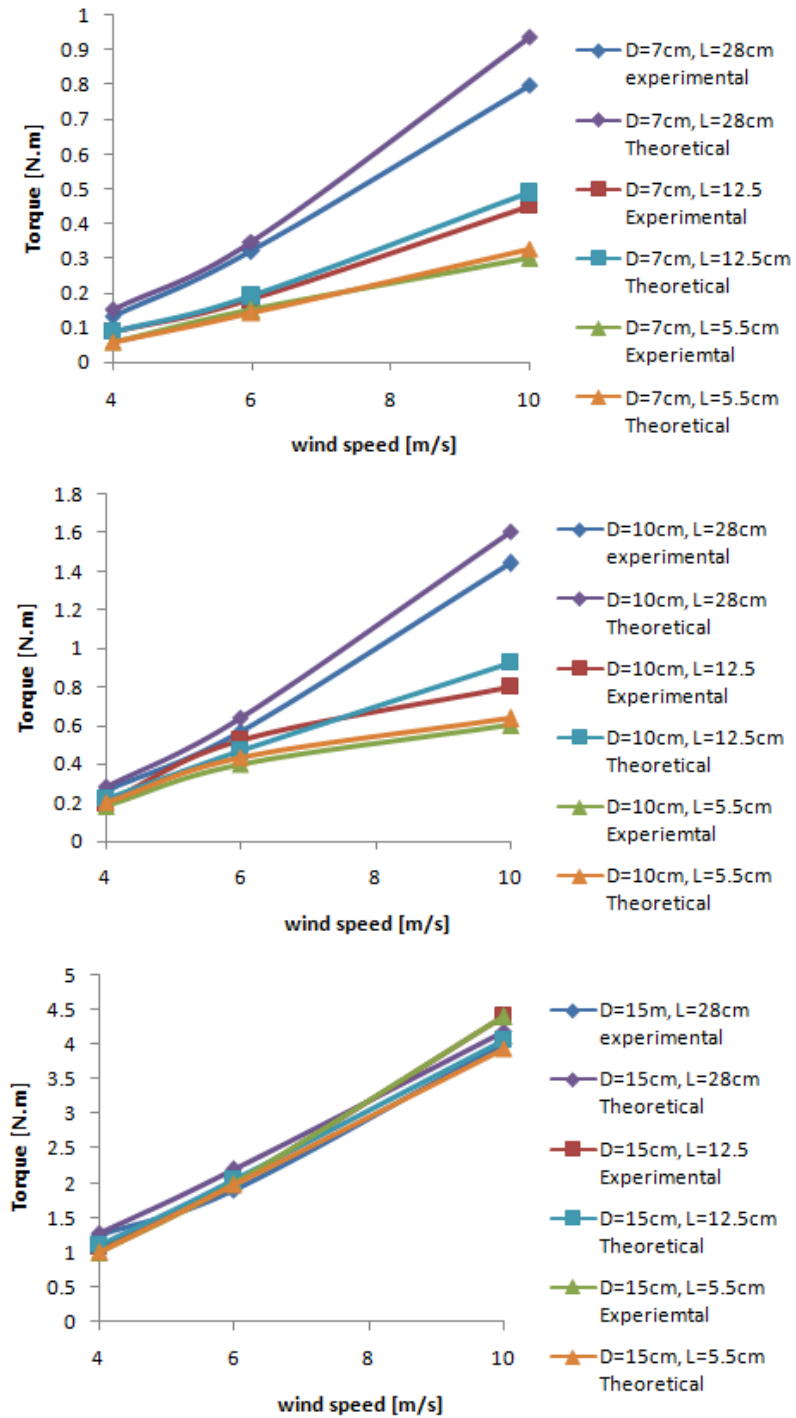
Theoretical average torque, traditionally, average torque is calculated by dividing the sum of all values of theoretical torque at a different rotor angle by a number of the values. It is given by the formula

$$T_{\text{average}} = \frac{\sum_{i=1}^n T_i}{n} \quad (5.1)$$

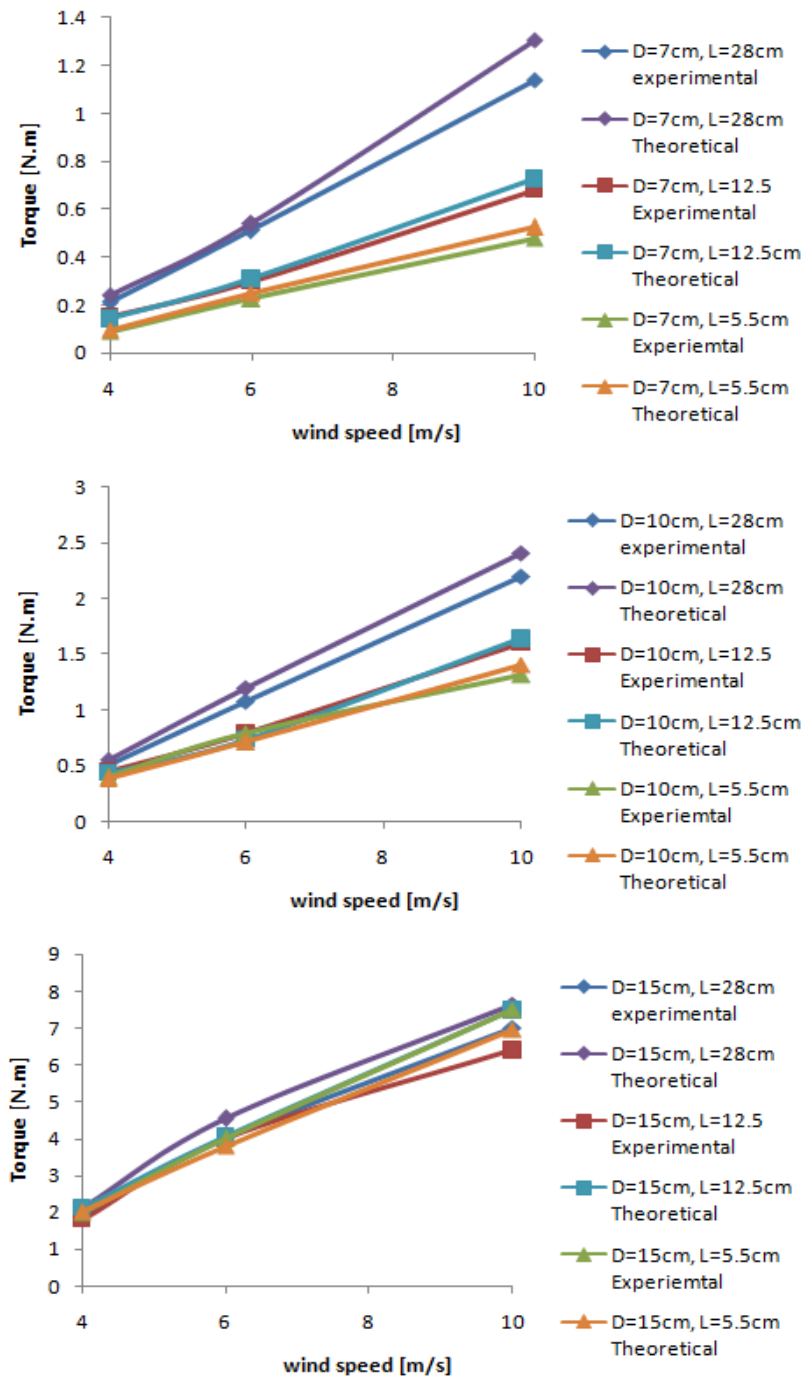
Figures 5.33 to 5.38 illustrate the amount of theoretical average torque produced from the different number of C-section blades with different size at the different wind speed. Additionally, the comparison between the theoretical predictions and experimental torque are shown in Figures 5.33 to 5.38. It can notice that the torque, Theoretical and experimental, is rapidly increasing with the increase in the number of blades, the size of the blades and wind speed. The absolute error between them is between rang 0 and 15% as shown in Figures. However, from these Figures, it is clear that as the number of blades, blade size, and wind speed increase, the torque of C-section rotor wind turbine will increase.



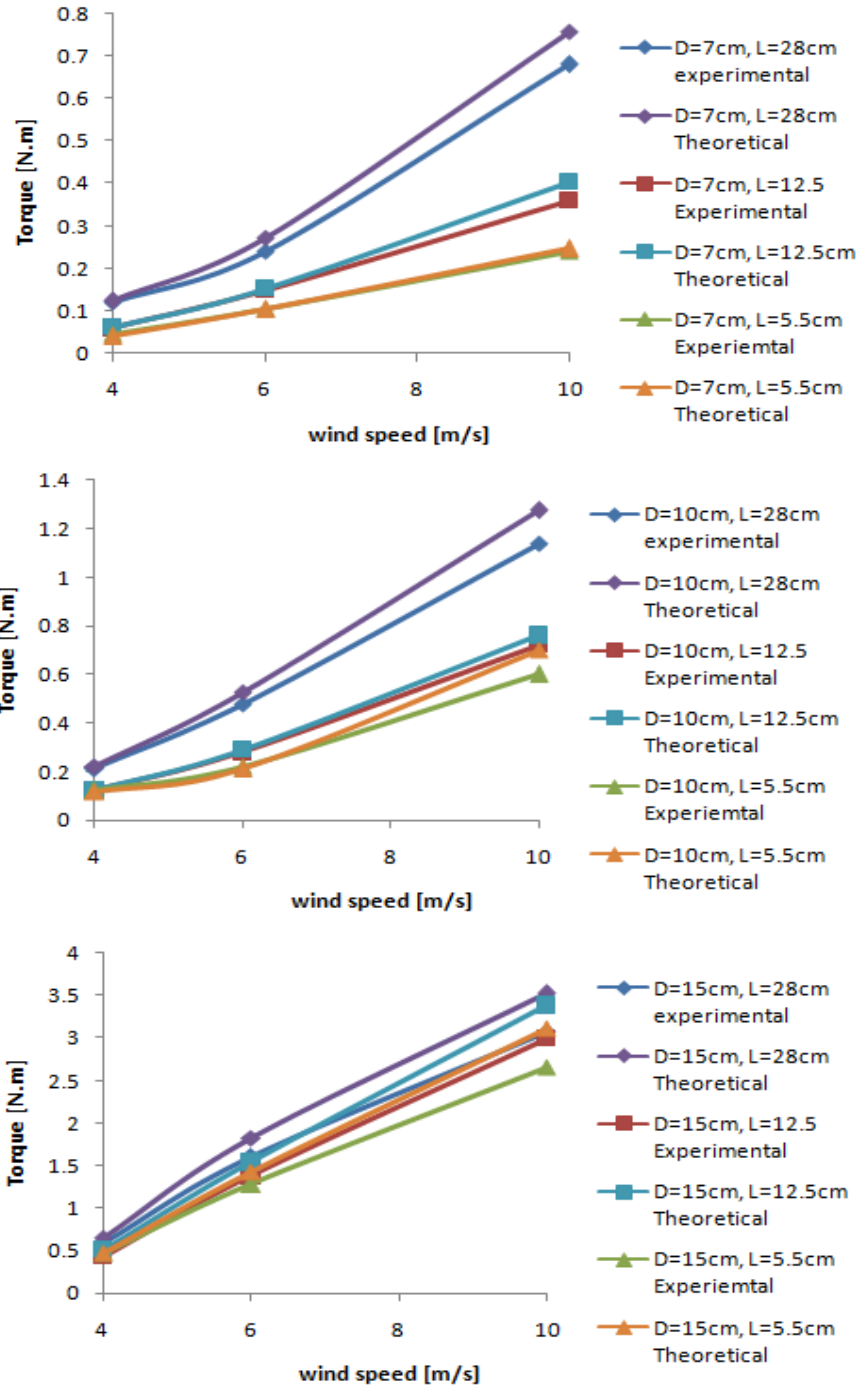
**Figure 5.33:** The theoretical result and experimental torque of C-section wind turbine rotor versus wind speed for different rotor radius and blade diameter with a fixed  $H=30\text{cm}$  and  $N=2$  blades



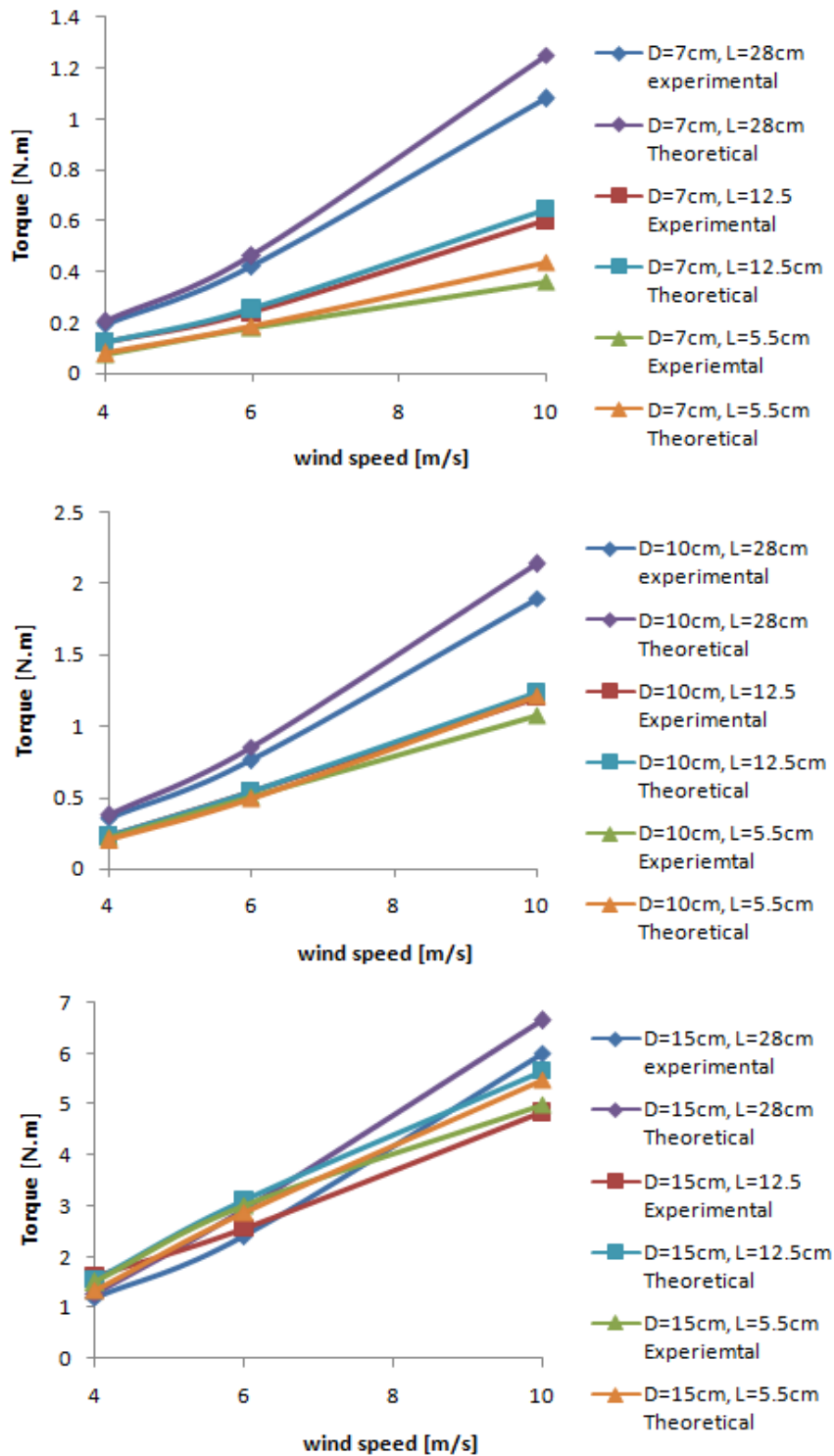
**Figure 5.34:** The theoretical result and experimental torque of C-section wind turbine rotor versus wind speed for different rotor radius and blade diameter with a fixed  $H=30\text{cm}$  and  $N=3$  blades



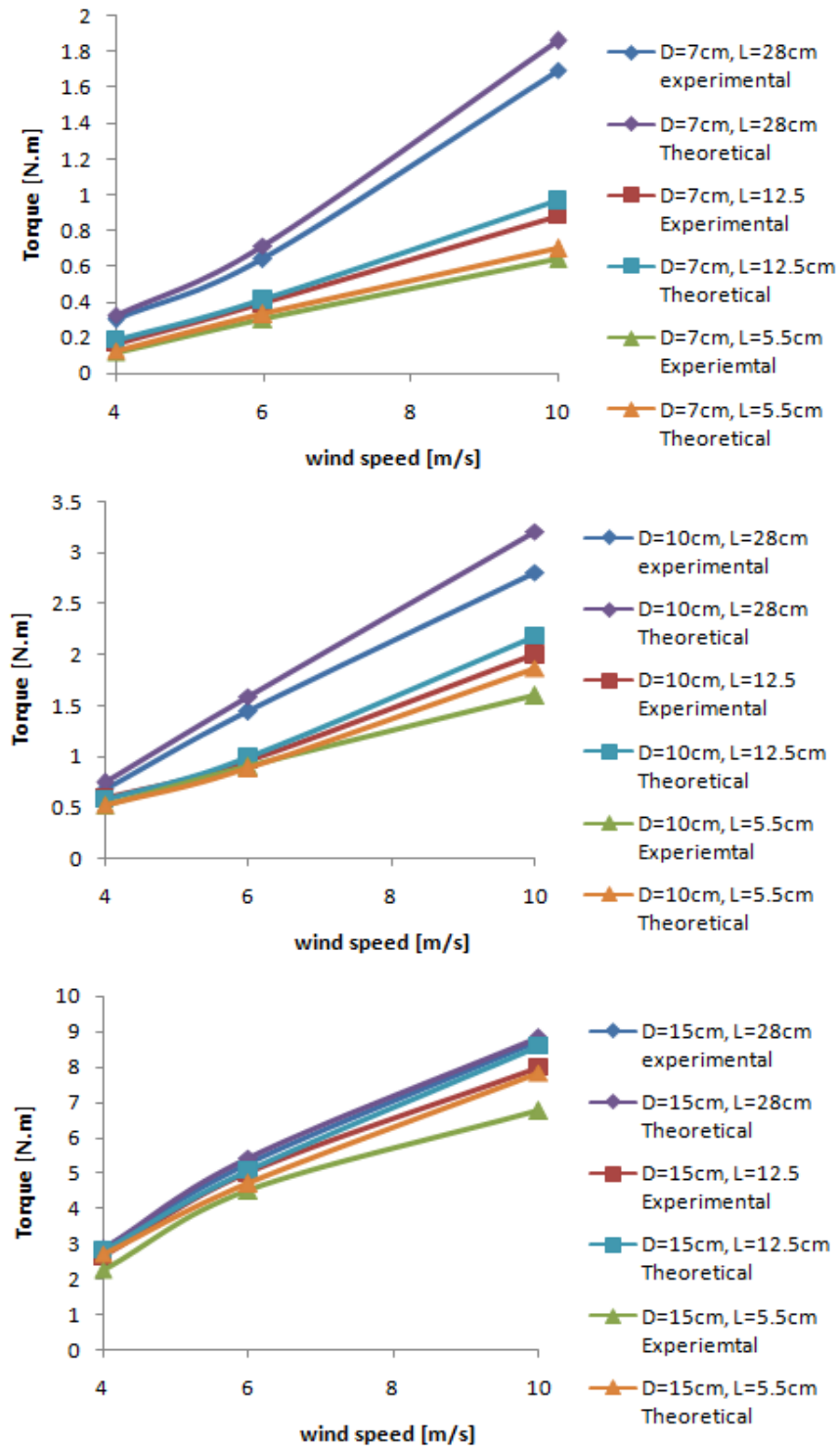
**Figure 5.35:** The theoretical result and experimental torque of C-section wind turbine rotor versus wind speed for different rotor radius and blade diameter with a fixed H=30cm and N=4 blades



**Figure 5.36:** The theoretical result and experimental torque of C-section wind turbine rotor versus wind speed for different rotor radius and blade diameter with a fixed H=40cm and N=2 blades



**Figure 5.37:** The theoretical result and experimental torque of C-section wind turbine rotor versus wind speed for different rotor radius and blade diameter with a fixed H= 40cm and N=3 blades



**Figure 5.38:** The theoretical result and experimental torque of C-section wind turbine rotor versus wind speed for different rotor radius and blade diameter with a fixed H=40cm and N=4 blades

### 5.8. Comparison of Theoretical Study and Experimental Power of C-section Wind Turbine Rotor

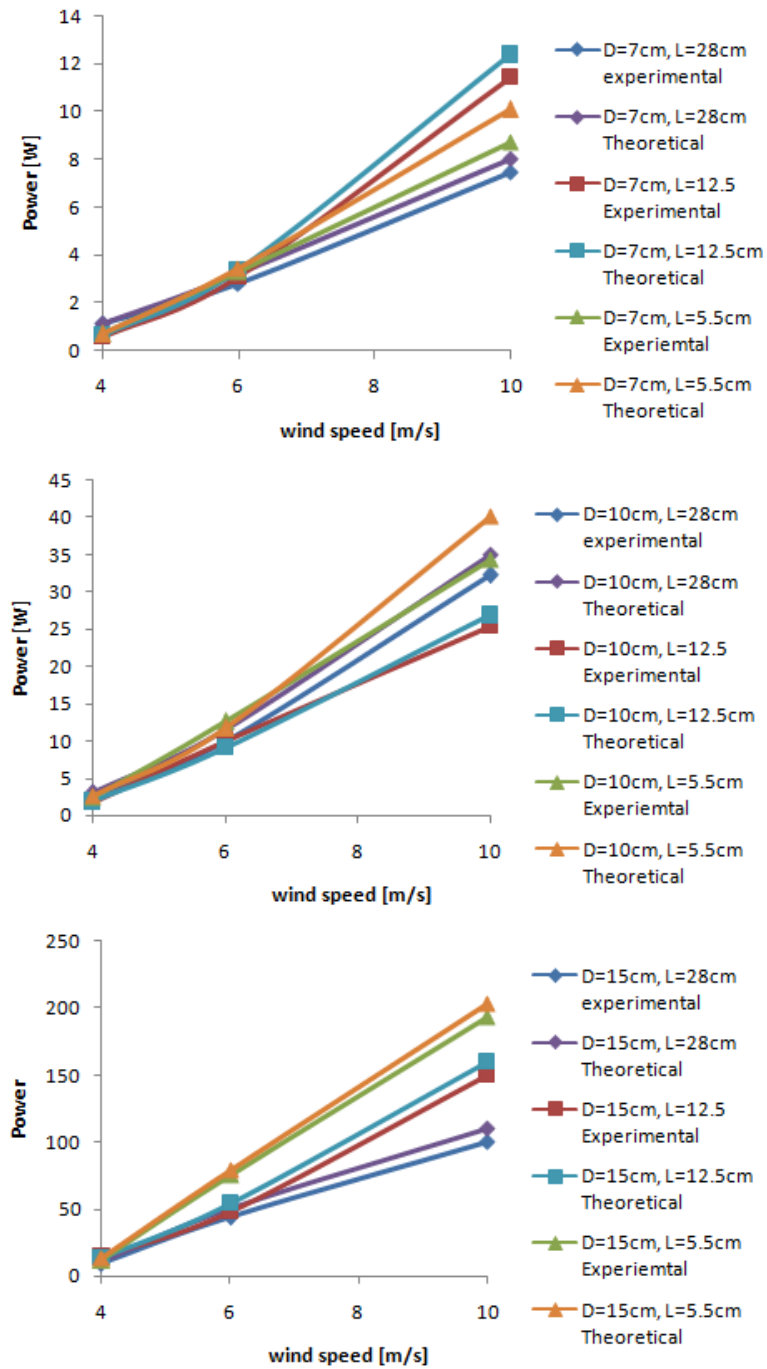


Theoretical average Mechanical power, traditionally average mechanical power is calculated by multiplying the average torque by angular speed, rotor speed,. It is given by the formula

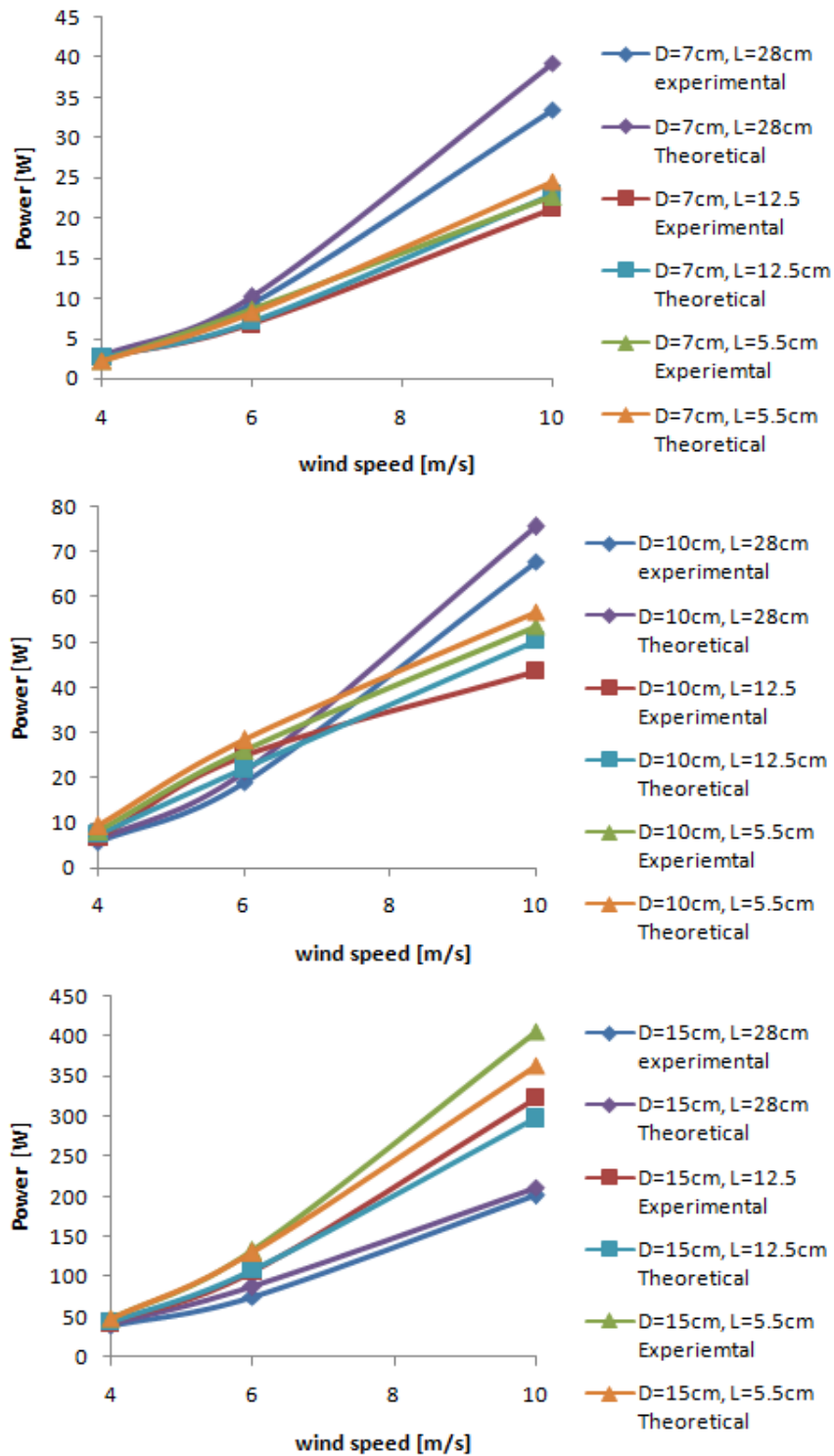
$$P_{\text{average}} = T_{\text{average}} \times \omega \quad (5.2)$$

Figures 5.39 to 5.44 illustrated the relationship between the average of theoretical mechanical power and experimental mechanical power and size and number of blades with variable wind speed. Additionally, it is observed that the absolute error between them is between rang 0 and 15% as shown from these Figures. However, from these figures, it is clear that as the number of blades, blade size, and wind speed increase, the C-section rotor wind turbine will produce more mechanical power.

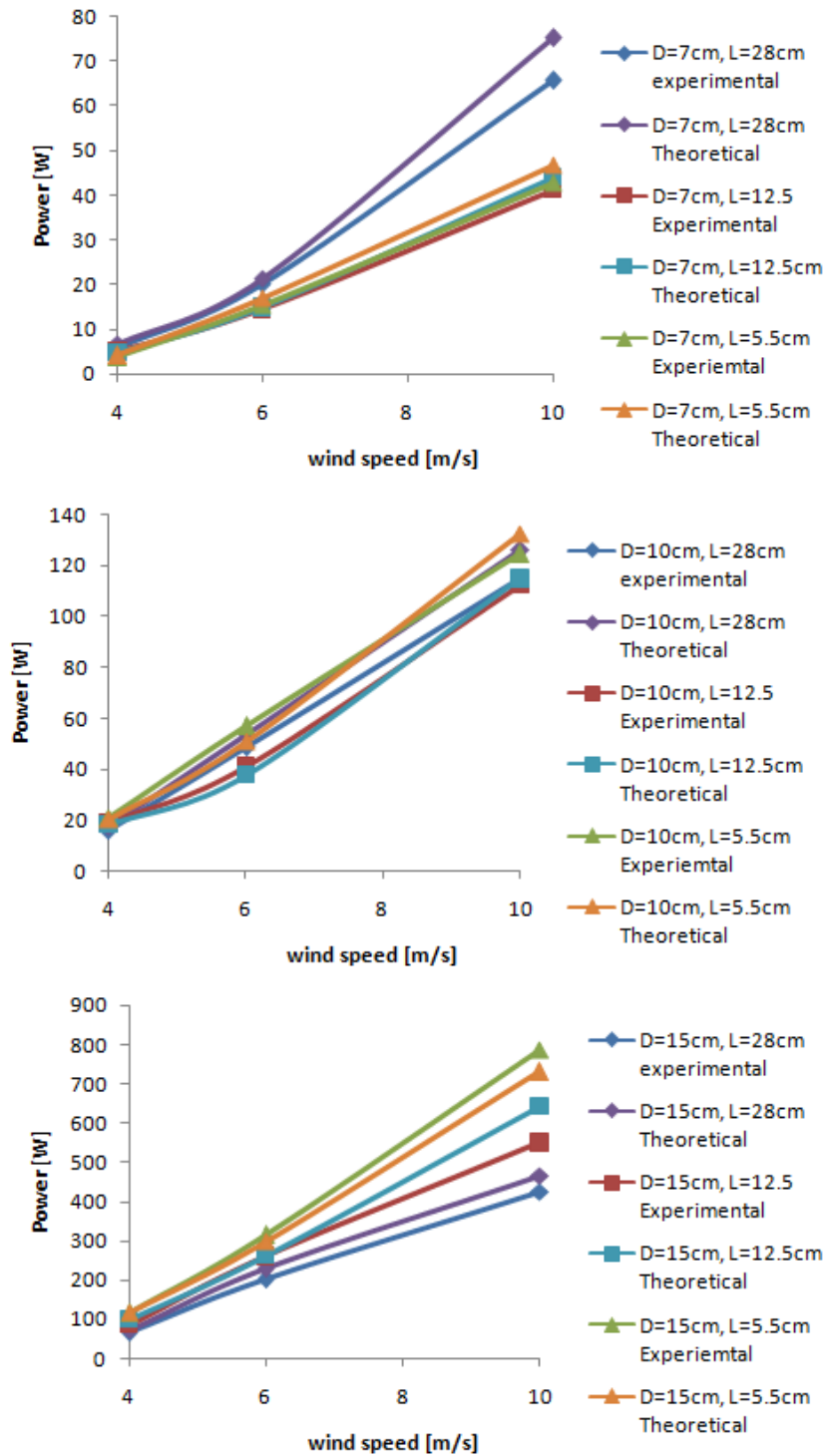
It can notice from the figures that a greater number of blades increase the weight to be turned by the turbine. On the other hand, more blades provide a greater available surface area for the wind to push, so it would produce more turning power. Having fewer blades could be beneficial because it will not be as heavy, and will be easier to turn than a greater number of blades, but it will also be somewhat inefficient because it produces less turning power.



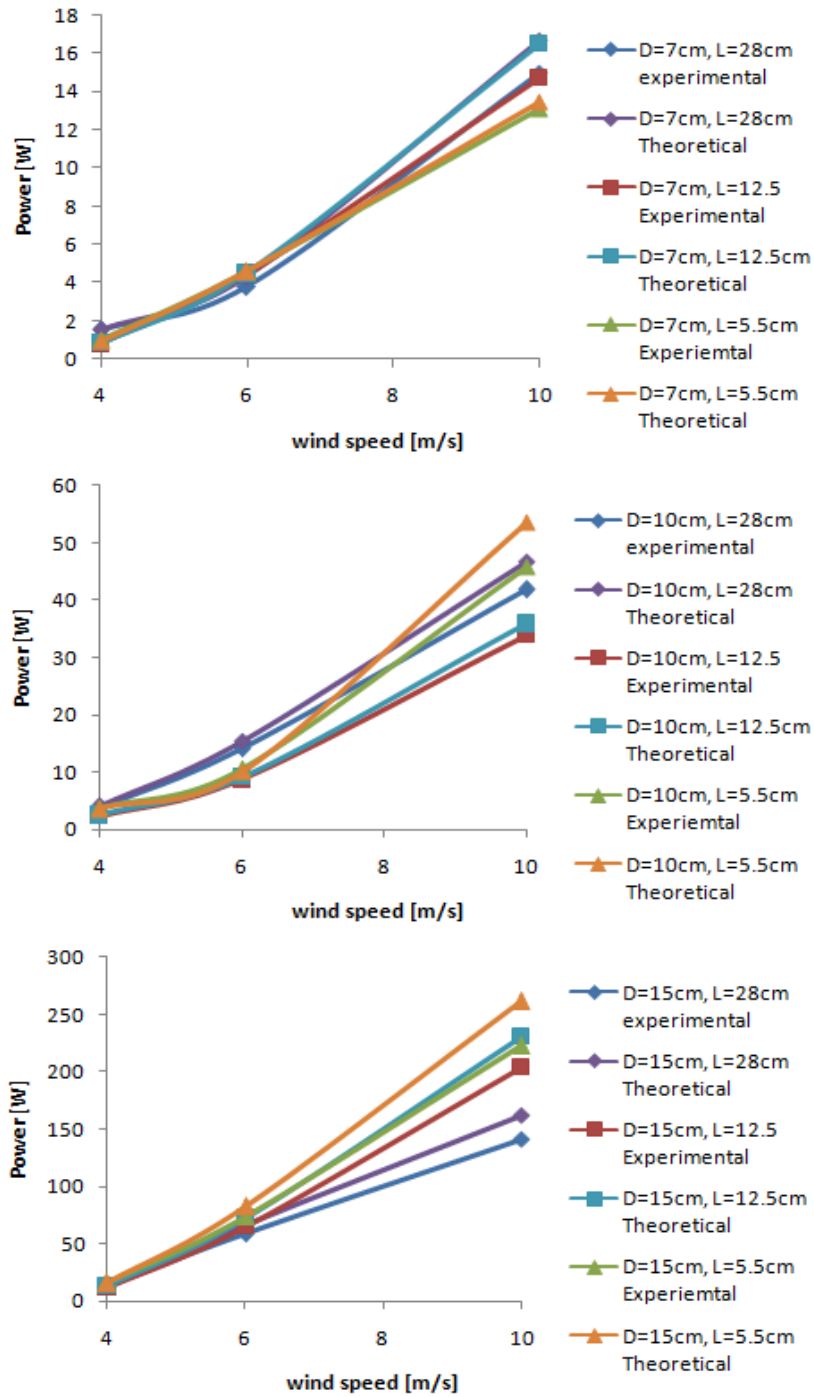
**Figure 5.39:** The theoretical result and experimental torque of C-section wind turbine rotor versus wind speed for different rotor radius and blade diameter with a fixed H= 30cm and N= 2 blades



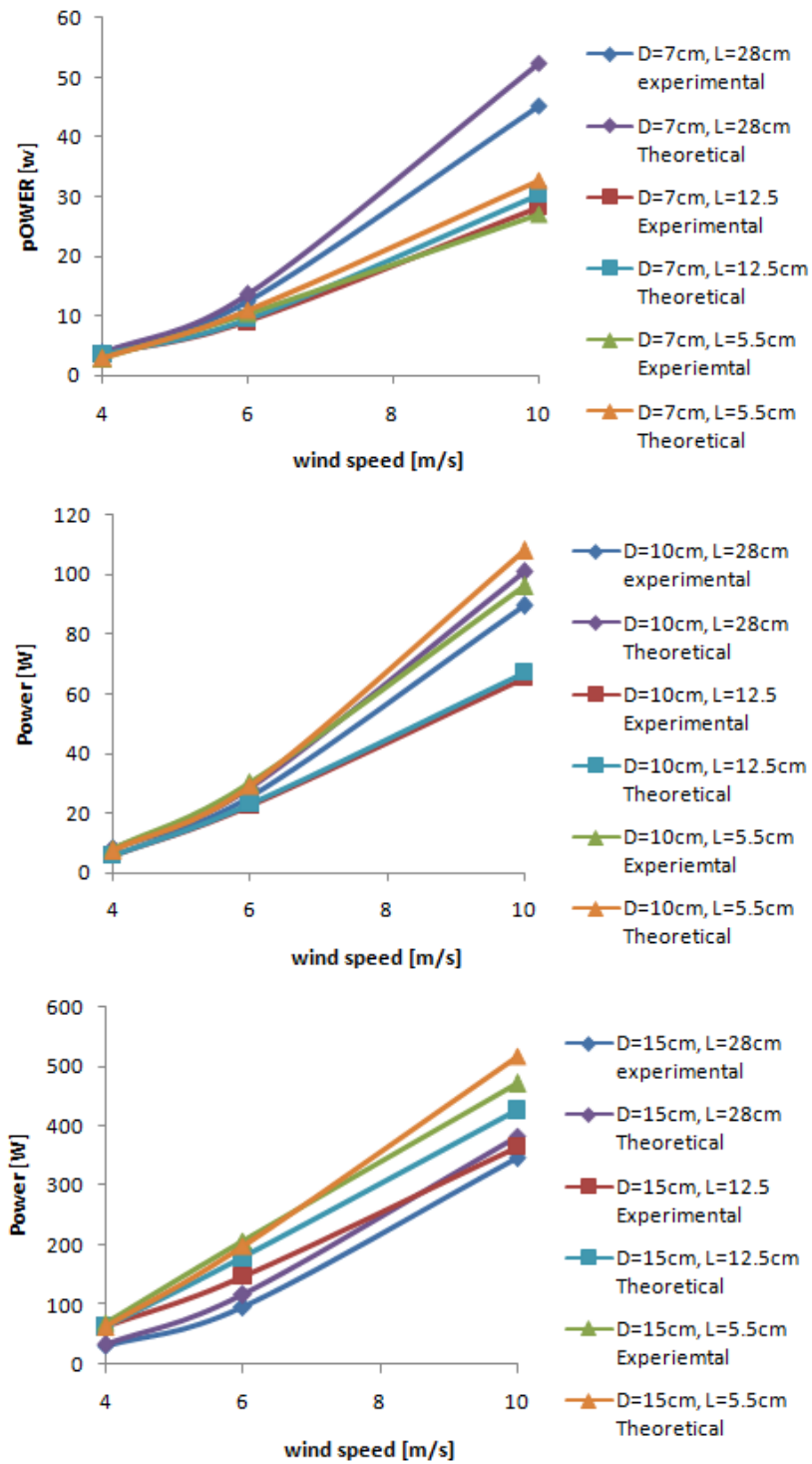
**Figure 5.40:** The theoretical result and experimental torque of C-section wind turbine rotor versus wind speed for different rotor radius and blade diameter with a fixed  $H=30\text{cm}$  and  $N=3$  blades



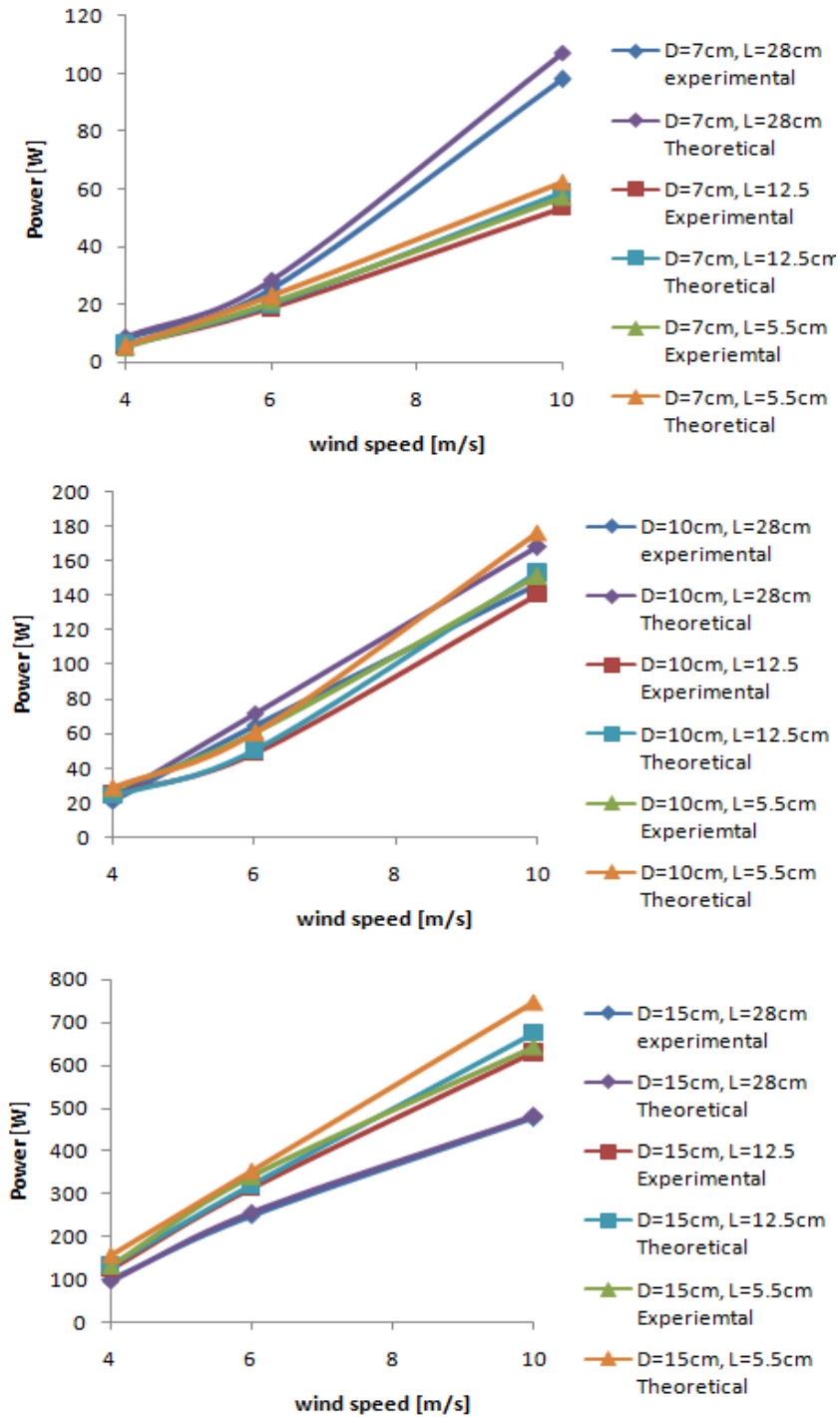
**Figure 5.41:** The theoretical result and experimental torque of C-section wind turbine rotor versus wind speed for different rotor radius and blade diameter with a fixed H= 30cm and N=4 blades



**Figure 5.42:** The theoretical result and experimental torque of C-section wind turbine rotor versus wind speed for different rotor radius and blade diameter with a fixed  $H=40\text{cm}$  and  $N=2$  blades



**Figure 5.43:** The theoretical result and experimental torque of C-section wind turbine rotor versus wind speed for different rotor radius and blade diameter with a fixed H 40cm and N=3 blades



**Figure 5.44:** The theoretical result and experimental torque of C-section wind turbine rotor versus wind speed for different rotor radius and blade diameter with a fixed H= 40cm and N=4 blades

## CONCLUSIONS AND FUTURE WORKS

Based on the research work, the aims and objections of the research project have been achieved. The significant findings are summarized below.

### 6.1 Conclusions

The primary objective of this thesis is to analyze the effect of aerodynamic on the performance of a prototype C-section vertical axis wind turbine and study the effect of turbine geometry on the mechanical power produced at low wind speed.

The independent variables were wind speed, blade size, rotor diameter and blade number. The different wind speeds were 4, 6 and 10 m/s. The blade lengths and diameters were 30 and 40 cm and 7, 10 and 15cm, respectively. The blades were made from PVC material. For each blade length and blade diameter, there were six turbines, each with a different number of blades, 2, 3, or 4. All tests were conducted indoors to reduce interfering wind and other elements. The models of the C-section vertical axis wind turbine were tested under the same environment. The main conclusions of this thesis are:

- The performance of the turbine can be best evaluated by the theoretical study as experimental evaluation consumes time and money. Another advantage of theoretical study is that the experimental results can be verified if there is a geometrical similarity between experimental and theoretical.
- The increasing wind speed leads to increase the mechanical power of C-section vertical axis wind turbine.
- The mechanical power and torque of C-section rotor increases when blade number and blade size increase.
- From comparisons between the theoretical study and experimental test, it was found that the absolute error is in range 0 and 15 percent.
- From comparisons between 2, 3 and 4 blades, it was found that maximum power is higher for 4 bladed of C-section rotor compared to 2 and 3 blades. The maximum power is obtained blade height 40 cm, blade diameter 15cm, rotor radius 28cm and wind speed 10 m/s.



- For three blades of 10 cm diameter, was found to be more efficient than other diameter and 2 and 4 blades.
- From the results, it can be concluded that a four-bladed turbine should have about double or more weight to turn compared to a two and three blade turbine of the same size; but a four-bladed turbine has nearly quadrupled and double the pushing power compared to two blade and three blade turbine of the same size, respectively.
- It was also found that the largest bladed turbine shook violently during testing. This shows that at high wind speeds, turbines with larger blades are unstable. This may reduce the performance of the turbine, and it may break down.
- It can be concluded that the C-section vertical axis wind turbine is capable of producing electricity power even with low wind velocity for domestic used.

## **6.2 Future Works**

Future work should include computer modeling of the rotor to study its flow profile and predict its performance in terms of torque and power coefficient. The results of these analyses could provide a better understanding of the fluid dynamic characteristics of our wind turbine design. Ideally, CFD (Computational fluid dynamics) could be performed to compare with the results from the testing performed with naturally occurring wind.

Another viable method would be to fabricate a scale model of the turbine to test in a wind tunnel with controlled wind speeds and real-time flow profiles from smoke-dyed wind. These studies will significantly advance the possibility for the widespread implementation of vertical-axis wind turbines in the future.

## REFERENCES

- Abzug, M., & Larrabee, E. (2002). *Airplane stability and control*. Cambridge, UK: Cambridge University Press.
- Ali, M. (2013). Experimental Comparison Study for Savonius Wind Turbine of Two & Three Blades At Low Wind Speed. *International Journal of Modern Engineering Research*, 3(5), 2978-2986.
- Ali, M.H. (2012). *Wind energy systems*. Boca Raton, FL: Taylor & Francis.
- Atta, T. (2015). *Advantages and disadvantages of Vertical axis wind turbine Green Mechanic*. Retrieved May 5, 2015 from <http://www.green-mechanic.com/2013/04/advantages-and-disadvantages-of.html>.
- Burton, T. (2001). *Wind energy handbook*. Chichester New York: J. Wiley.
- Dabiri, J. (2011). Potential order-of-magnitude enhancement of wind farm power density via counter-rotating vertical-axis wind turbine arrays. *Renewable Sustainable Energy*, 3(4), 043-104.
- D'Ambrosio, M., & Medaglia, M. (2010). *Vertical Axis Wind Turbines: History, Technology and Applications* (master's thesis). Halmstad university, Halmstad, Sweden.
- Earnest, J. (2014). *Wind power technology*. New Delhi: PHI Learning.
- Earnest, J. & Wizelius, T. (2011). *Wind power plants and project development*. New Delhi: PHI Learning.
- Eriksson, S. (2008). *Direct driven generators for vertical axis wind turbines* (Unpublished doctoral dissertation). Uppsala university, Uppsala, Sweden.
- Eriksson, S., Bernhoff, H., & Leijon, M. (2008). Evaluation of different turbine concepts for wind power. *Renewable And Sustainable Energy Reviews*, 12(5), 1419-1434.
- French, A. & Ebison, M. (1986). *Introduction to Classical Mechanics*. Dordrecht: Springer Netherlands.

- Gipe, P. (2003). *Wind power*. White River Junction, Vt.: Chelsea Green Pub. Co.
- Gipe, P. (2009). *Wind energy basics: a guide to home and community-scale wind energy system* White River Junction, Vt: Chelsea Green Pub. Co.
- Gosselin, F., De Langre, E., & Machado-Almeida, B. (2010). Drag reduction of flexible plates. *Journal of Fluid Mechanics*, 650, 319-341. doi:10.1017/s0022112009993673.
- Graebel, W. (2001). *Engineering fluid mechanics*. New York: Taylor & Francis.
- Gupta, R., & Biswas, A. (2011). CFD Analysis of flow physics and aerodynamic performance of a combined three-bucket Savonius and three-bladed Darrieus turbine. *International Journal of Green Energy*, 8(2), 209-233.
- Gupta, R., Biswas, A., & Sharma, K. (2008). Comparative study of a three-bucket Savonius rotor with a combined three-bucket Savonius-three-bladed Darrieus rotor. *Renewable Energy*, 33(9), 1974-1981.
- Hau, E. (2006). *Wind turbines fundamentals, technologies, application, economics*. Berlin New York: Springer.
- Hemami, A. (2012). *Wind turbine technology*. Clifton Park, NY: Delmar, Cengage Learning.
- Hutchinson, J. (2005). *Basic Flight Physics*. Retrieved October 5, 2015 from <http://www.ucmp.berkeley.edu/vertebrates/flight/physics.html>.
- Kinzel, M., Mulligan, Q., & Dabiri, J. (2012). Energy exchange in an array of vertical-axis wind turbines. *Journal of Turbulance*, 13, 38-54. doi: 10.1080/14685248.2012.712698.
- Layton, J. (2006). *How Wind Power Works*. Retrieved October 6, 2015 from <http://science.howstuffworks.com/environmental/green-science/wind-power1.htm>.
- Manwell, J., McGowan, J. & Rogers, A. (2009). *Wind energy explained : theory, design and application*. Chichester, U.K: Wiley.
- Morshed, K., Rahman, M., Molina, G., & Ahmed, M. (2013). Wind tunnel testing and numerical simulation on aerodynamic performance of a three-bladed Savonius wind

turbine. *International Journal of Energy and Environmental Engineering*, 4(1), 18.

Priya, S., O'Brien, W., & Tafti, D. (2013). *Small-scale Wind Energy Portable Turbine (SWEPT)* (master's thesis). Blacksburg university, Virginia, United State of America.

Rassoulinejad-Mousavi, M., Jamil, M., & Layeghi, M. (2013). Experimental Study of a Combined Three Bucket H-Rotor with Savonius Wind Turbine. *World Applied Sciences*. World Applied Sciences Journal 28 (2), 205-211.

Ribrant, J., & Bertling, L. (2007). Survey of failures in wind power systems with focus on Swedish wind power plants during 1997-2005. *Institute of Electrical and Electronics Engineers*, 22(1), 167-173.

Rivkin, D. & Silk, L. (2013). *Wind power generation and distribution*. Burlington, MA: Jones & Bartlett Learning.

Rivkin, D. & Silk, L. (2013). *Wind turbine technology and design*. Burlington, MA: Jones & Bartlett Learning.

Road, Hillington, A. (2016). HAWT, Horizontal axis wind turbines from Gaia wind, Their advantages and disadvantages plus the effects of cyclic stress and vibration. Retrieved Octobre 6, 2015 from <http://www.azocleantech.com/article.aspx?ArticleID=191>.

Roberson, J., & Crowe, C. (1997). *Engineering fluid mechanics*. New York: J. Wiley & Sons.

Saha, U., & Rajkumar, M. (2006). On the performance analysis of Savonius rotor with twisted blades. *Renewable Energy*, 31(11), 1776-1788.

Saha, U., Thotla, S., & Maity, D. (2008). Optimum design configuration of Savonius rotor through wind tunnel experiments. *Journal of Wind Engineering And Industrial Aerodynamics*, 96(8-9), 1359-1375.

Sheldahl, R., Feltz, L., & Blackwell, B. (1978). Wind tunnel performance data for two- and three-bucket Savonius rotors. *Journal of Energy*, 2(3), 160-164.

Vogel, S. (1984). Drag and flexibility in sessile organisms. *American Zoologist*, 24(1), 37-44.

Fox, R., McDonald, A. & Pritchard, P. (2002). *Introduction to fluid mechanics*. New York: Wiley.

Wenehenubun, F., Saputra, A., & Sutanto, H. (2014). An experimental study on the performance of Savonius wind turbines related with the number of blades. *Science Direct*, 68, 297–304. doi: 10.1016/j.egypro.2015.03.259.